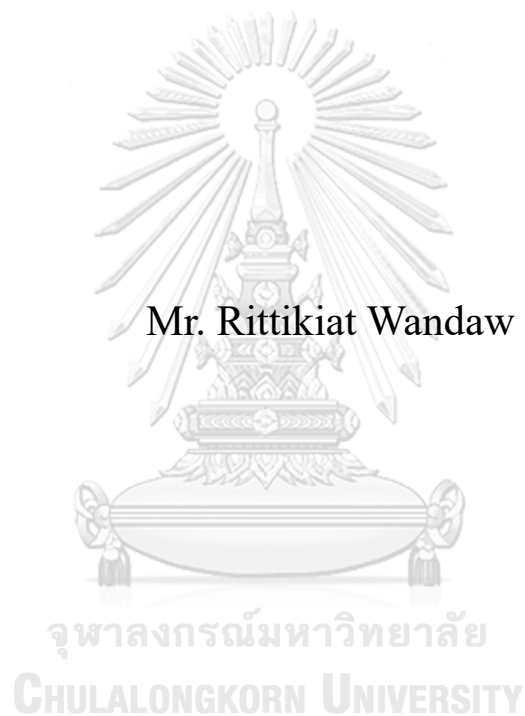


Effect of Dispersion of Carbon Nanotubes on Electrical
Conductivity and Compressive Strength of CNT/Cement
Composite



A Thesis Submitted in Partial Fulfillment of the Requirements
for the Degree of Master of Engineering in Chemical Engineering
Department of Chemical Engineering
Faculty Of Engineering
Chulalongkorn University
Academic Year 2023

อิทธิพลของการกระจายตัวของท่อนาโนคาร์บอนต่อค่าการนำไฟฟ้าและกำลังรับแรงอัดของวัสดุ
ผสมท่อนาโนคาร์บอนและซีเมนต์



วิทยานิพนธ์นี้เป็นส่วนหนึ่งของการศึกษาตามหลักสูตรปริญญาวิศวกรรมศาสตรมหาบัณฑิต
สาขาวิชาวิศวกรรมเคมี ภาควิชาวิศวกรรมเคมี
คณะวิศวกรรมศาสตร์ จุฬาลงกรณ์มหาวิทยาลัย
ปีการศึกษา 2566

Thesis Title	Effect of Dispersion of Carbon Nanotubes on Electrical Conductivity and Compressive Strength of CNT/Cement Composite
By	Mr. Rittikiat Wandaw
Field of Study	Chemical Engineering
Thesis Advisor	Professor TAWATCHAI CHARINPANITKUL, D.Eng.
Thesis Co Advisor	Associate Professor PITCHA JONGVIVATSAKUL, Ph.D.

Accepted by the FACULTY OF ENGINEERING, Chulalongkorn University
in Partial Fulfillment of the Requirement for the Master of Engineering

..... Dean of the FACULTY OF
ENGINEERING
(Professor SUPOT TEACHAVORASINSKUN, D.Eng.)

THESIS COMMITTEE

..... Chairman
(Professor PAISAN KITTISUPAKORN, Ph.D.)
..... Thesis Advisor
(Professor TAWATCHAI CHARINPANITKUL, D.Eng.)
..... Thesis Co-Advisor
(Associate Professor PITCHA JONGVIVATSAKUL,
Ph.D.)
..... Examiner
(Assistant Professor RUNGTHIWA METHAAPANON,
D.Eng.)
..... External Examiner
(Assistant Professor Weerawut Chaiwat, D.Eng.)

จุฬาลงกรณ์มหาวิทยาลัย
CHULALONGKORN UNIVERSITY

ฤทธิเกียรติ วัลย์ดาว : อธิปไตยของการกระจายตัวของท่อนาโนคาร์บอนต่อค่าการนำไฟฟ้าและกำลังรับแรงอัดของวัสดุผสม
ท่อนาโนคาร์บอนและซีเมนต์. (Effect of Dispersion of Carbon Nanotubes on Electrical
Conductivity and Compressive Strength of CNT/Cement Composite) อ.ที่ปรึกษาหลัก :
ศ. ดร.ธวัชชัย ชรินพานิชกุล, อ.ที่ปรึกษาร่วม : รศ. ดร.พิชชา จงจิววิมลสกุล

ท่อนาโนคาร์บอนเป็นวัสดุนาโนที่มีคุณสมบัติโดดเด่นทั้งคุณสมบัติการนำไฟฟ้า ความแข็งแรงเชิงกล และความเสถียรที่สูง คุณสมบัติเหล่านี้ทำให้ท่อนาโนคาร์บอนเหมาะสำหรับการใช้งานที่หลากหลาย โดยเฉพาะอย่างยิ่งการใช้เป็นสารเติมแต่งในการเพิ่มประสิทธิภาพโดยรวม การใช้งานที่โดดเด่นอย่างหนึ่งคือการนำท่อนาโนคาร์บอนมาใช้กับซีเมนต์คอมโพสิตเพื่อปรับปรุงคุณสมบัติเชิงกลและไฟฟ้า อย่างไรก็ตาม คุณสมบัติที่ไม่ชอบน้ำของท่อนาโนคาร์บอนทำให้เกิดปัญหาในการกระจายตัวภายในเนื้อซีเมนต์ที่มีคุณสมบัติที่ชอบน้ำ ดังนั้นจึงมีการพัฒนาวิธีการต่างๆ เพื่อช่วยให้กระจายตัวของท่อนาโนคาร์บอนทั้งในน้ำและในเนื้อของซีเมนต์ ในวิทยานิพนธ์นี้ใช้ไทรทันเอกซ์ 100 ซึ่งเป็นสารลดแรงตึงผิวในการกระจายตัวของท่อนาโนคาร์บอนในน้ำโดยใช้อัตราส่วนต่างๆ (0.5:1, 1:1, 1.5:1 และ 2:1) ในสารแขวนลอยของท่อนาโนคาร์บอน การกระจายตัวของท่อนาโนคาร์บอนในสารแขวนลอยถูกจำแนกโดยใช้เทคนิค UV-vis spectroscopy เพื่อกำหนดอัตราส่วนที่เหมาะสมระหว่าง ไทรทันเอกซ์ 100 และ ท่อนาโนคาร์บอน ต่อจากนั้น มีการนำเจลไอซ์ที่แสดงให้เห็นถึงการกระจายตัวของท่อนาโนคาร์บอนที่มีประสิทธิภาพด้วย ไทรทันเอกซ์ 100 ตามที่ระบุจากผลลัพธ์ที่ได้จากเทคนิค UV-vis spectroscopy และผสมกับซีเมนต์เพื่อสร้างคอมโพสิตระหว่างท่อนาโนคาร์บอนและซีเมนต์ คุณสมบัติของคอมโพสิตเหล่านี้ได้รับการวิเคราะห์โดยการเปลี่ยนอัตราส่วนไทรทันเอกซ์ 100 ต่อ ท่อนาโนคาร์บอน (1:1, 1.5:1 และ 2:1) และปริมาณของท่อนาโนคาร์บอนในอัตราส่วนโดยน้ำหนักของซีเมนต์ (0.1 – 0.4 % โดยน้ำหนักซีเมนต์) คุณสมบัติของคอมโพสิตได้รับการตรวจสอบ ได้แก่ การไหลตัว ความพรุน กำลังรับแรงอัด และการนำไฟฟ้า นอกจากนี้ ลักษณะทางสัณฐานวิทยาและการกระจายตัวของท่อนาโนคาร์บอนภายในคอมโพสิตได้รับการตรวจสอบเพิ่มเติมโดยใช้กล้องจุลทรรศน์อิเล็กตรอนแบบส่องกราด (SEM) จากผลการทดลองในเจลไอซ์ที่มีการเพิ่มปริมาณของไทรทันเอกซ์ 100 ในขณะที่ควบคุมปริมาณท่อนาโนคาร์บอนช่วยเพิ่มการกระจายตัวของท่อนาโนคาร์บอนภายในคอมโพสิตได้อย่างมีนัยสำคัญ นอกจากนี้ การเพิ่มปริมาณ ท่อนาโนคาร์บอนภายใต้สภาวะที่เหมาะสมจะช่วยเพิ่มกำลังรับแรงอัดกำลังรับแรงอัดสูงสุดของคอมโพสิตที่เวลาการบ่ม 28 วันที่มีค่าการกระจายตัวของท่อนาโนคาร์บอนสูงสุดในคอมโพสิต เกิดขึ้นภายใต้เจลไอซ์ที่มี ท่อนาโนคาร์บอน 2 กรัม และ ไทรทันเอกซ์ 100 1 กรัม ซึ่งมีกำลังรับแรงอัดเหนือกว่าเจลไอซ์ควบคุมถึง 21.77% ยิ่งไปกว่านั้น ค่าการนำไฟฟ้าสูงสุดเกิดขึ้นในคอมโพสิตที่มีเจลไอซ์การเติม ท่อนาโนคาร์บอน 4 กรัม และ ไทรทันเอกซ์ 100 1 กรัม ซึ่งถือเป็นเจลไอซ์ที่มีปริมาณ ท่อนาโนคาร์บอน สูงสุดในงานวิจัยนี้ สิ่งนี้แสดงให้เห็นถึงการเพิ่มขึ้นอย่างมากถึง 44.30% เมื่อเทียบกับเจลไอซ์ควบคุมที่ระยะเวลาการบ่ม 28 วัน

จุฬาลงกรณ์มหาวิทยาลัย
CHULALONGKORN UNIVERSITY

สาขาวิชา วิศวกรรมเคมี
ปีการศึกษา 2566

ลายมือชื่อนิติกร
ลายมือชื่อ อ.ที่ปรึกษาหลัก
ลายมือชื่อ อ.ที่ปรึกษาร่วม

6270236721 : MAJOR CHEMICAL ENGINEERING

KEYWORD: Carbon nanotube Cement composite Surfactant Electrical property
Mechanical property

Rittikiat Wandaw : Effect of Dispersion of Carbon Nanotubes on Electrical Conductivity and Compressive Strength of CNT/Cement Composite. Advisor: Prof. TAWATCHAI CHARINPANITKUL, D.Eng. Co-advisor: Assoc. Prof. PITCHA JONGVIVATSAKUL, Ph.D.

Carbon nanotubes (CNTs) are promising nanomaterials due to their exceptional properties, including high electrical, mechanical, and stability characteristics. These advantageous features position CNTs as suitable candidates for diverse applications, particularly in additive formulations designed to enhance overall performance. One notable application is their use in cement composites to improve mechanical and electrical properties. However, the hydrophobic property of CNTs presents challenges for dispersion within the hydrophilic cement matrix. Consequently, methods have been developed to aid CNT dispersion in both water and cement matrices. In this thesis, Triton X-100 employed as a surfactant, was used to disperse CNTs in water using various ratios (0.5:1, 1:1, 1.5:1, and 2:1) in a CNT suspension. The dispersion of CNTs in suspension was characterized using UV-vis spectroscopy to determine the optimal ratio between Triton X and CNTs. Subsequently, conditions demonstrating effective CNT dispersion with Triton X-100, as identified from the UV-vis spectroscopy results, were applied and mixed with cement to form CNT/cement composites. The properties of these composites were analyzed by varying the ratio of Triton X-100 to CNTs (1:1, 1.5:1, and 2:1) and the amount of CNTs in the cement ratio (0.1 – 0.4 wt%). The properties of composite were investigated, including flowability, porosity, compressive strength, and electrical conductivity. Additionally, morphology and dispersion of CNTs within composites were further examined using scanning electron microscopy (SEM). From the results, the condition involving an increase in Triton X-100 while controlling CNT content significantly improved CNT dispersion within the composite. Furthermore, an increase in the CNT content under appropriate conditions enhanced compressive strength. The highest compressive strength at a curing time of 28 days, with the highest CNT dispersion value within the composite, was achieved with 2 g of CNTs and 1 g of Triton X-100 condition. The compressive strength of this condition surpassed the control condition by 21.77%. Moreover, the highest electrical conductivity was achieved in the composite with 4 g of CNTs and 1 g of Triton X-100, marking the highest CNT content condition in this study. This represents a substantial 44.30% improvement compared to the control condition at a curing time of 28 days.

Field of Study: Chemical Engineering
Academic Year: 2023

Student's Signature
Advisor's Signature
Co-advisor's Signature

ACKNOWLEDGEMENTS

Firstly, I would like to express my appreciation to my thesis advisor, Professor Tawatchai Charinpanitkul, from Department of Chemical Engineering, Chulalongkorn University, and my thesis co-advisor, Assoc. Prof. Dr. Pitcha Jongvivatsakul, from Department of Civil Engineering, Chulalongkorn University, for their support, valuable experience, suggestions, and contributions to the completion of my thesis.

Secondly, I would like to thank Dr. Giang T. T. Le for the continuous support and guidance throughout my thesis. Additionally, I am grateful to all members of Prof. Tawatchai's research group for their support, suggestions, and collaboration.

Thirdly, my sincere thanks go to Dr. Peem Nuaklong and Kantipok Hamcumpai from Department of Civil Engineering, Chulalongkorn University, for their helpful advice and support during the experimental phase of my thesis work.

Fourthly, I extend my gratitude to Prof. Paisan Kittisupakorn, Ph.D., as the chairman, Asst. Prof. Rungthiwa Methaapanon, Ph.D., and Asst. Prof. Dr. Weerawut Chaiwat, Ph.D., as the members of the thesis committee, for their valuable comments and suggestions.

Furthermore, I would like to acknowledge the support of the Ratchadapisek Somphot Fund at Chulalongkorn University, CEPT, NANOTEC, NSTDA, and the Ministry of Higher Education, Science, Research, and Innovation, Thailand, through the Research Network of NANOTEC (RNN) program for their financial support of this project.

Lastly, I would like to thank my family, especially my mother, for their support throughout my life.

Rittikiat Wandaw

TABLE OF CONTENTS

	Page
ABSTRACT (THAI)	iii
ABSTRACT (ENGLISH).....	iv
ACKNOWLEDGEMENTS.....	v
TABLE OF CONTENTS	vi
LIST OF TABLES	ix
LIST OF FIGURE.....	x
CHAPTER 1 INTRODUCTION	1
1.1. Motivation.....	1
1.2. Research objective	2
1.3. Scope of this research	2
1.4 Expected benefits	3
CHAPTER 2 Fundamental knowledge.....	1
2.1 Basic knowledge of carbon nanotubes	1
2.1.1 Characteristics of Carbon Nanotubes	1
2.1.2 Methodology for carbon nanotube synthesis.....	2
2.2 Basic knowledge of Cement Composite.....	3
2.2.1 Chemical reactions between the cement and water.....	4
2.2.2 Properties of cement sample.....	6
2.2.2.1 Compressive strength	6
2.2.2.2 Workability	7
2.2.2.3 Electrical conductivity.....	7
2.3 Basic knowledge of surfactant.....	9
2.3.1 Surfactant and type of surfactant.....	9
2.3.2 Triton X-100 surfactant	10
2.4. Methods for CNT Dispersion	11

2.5 Characterization of CNT dispersion	12
2.6 Literature survey	13
2.6.1 The dispersion of CNTs in water	13
2.6.2 Compressive strength of CNT/cement composite	15
2.6.3 Electrical conductivity of CNT/Cement composite	18
CHAPTER 3 RESEARCH METHODOLOGY	19
3.1 Material and chemicals	19
3.2 Preparation and characterization of CNT suspension	20
3.2.1 Preparation of CNT suspension	20
3.2.2 Characterization of CNT suspension	21
3.3 Preparation of CNT/cement composite	22
3.4 Flowability test of CNT/Cement composite paste	23
3.5 Molding and Curing Processes of CNT/Cement Composite Samples	24
3.6 Performance test and analyst technique of CNT/cement composite	26
3.6.1 Compressive strength test	26
3.6.2 Electrical conductivity measurement	27
3.6.3 Bulk density measurement method	28
3.6.4 Microstructure and Morphology	28
3.6.5 Porosity and water absorption	29
3.6.6 CNT dispersion analysis	31
CHAPTER 4	35
RESULTS AND DISCUSSION	35
4.1 Morphology and size distribution of CNTs	35
4.2 Characterization of CNT suspension with Triton X-100	36
4.2.1 Apparent CNT suspension	36
4.2.2 Evaluation of uniform CNT dispersion	38
4.3 Flowability of CNT/Cement composite paste	40
4.4 Characterization of CNT dispersion in CNT/Cement composite	42
4.4.1 Bulk surface property of CNT/Cement composite	42

4.4.2 Porosity and water absorption of CNT/Cement composite.....	46
4.4.3 Microstructure of CNT/Cement composite	49
4.4.4 Dispersion of CNTs in CNT/Cement composite	50
4.4.5 Image processing analysis of CNT dispersion	52
4.4.5.1 Appropriate gridline for CNT dispersion analysis.....	52
4.4.5.2 Analyses of CNT dispersion with different Triton X-100 in CNT/Cement composite	53
4.4.6 Compressive strength and bulk density of CNT/Cement composite.....	55
4.4.7 Effect of curing time on compressive strength of CNT/Cement composite	58
4.4.8 Electrical conductivity of CNT/Cement composite	60
4.4.9 Effect of curing time on electrical conductivity of CNT/Cement composite.....	62
CHAPTER 5	64
CONCLUSIONS AND RECOMMENDATIONS	64
5.1 Conclusions.....	64
5.2 Remaining issues and recommendations for further investigation.....	66
APPENDIX A Size distribution of CNT.....	67
APPENDIX B Flowability of CNT/Cement composite paste	72
APPENDIX C Porosity and water absorption of CNT/Cement composite.....	73
APPENDIX D Compressive strength of CNT/Cement composite.....	76
APPENDIX E Electrical conductivity of CNT/Cement composite.....	81
APPENDIX F SEM image of CNT dispersion in composite	87
APPENDIX G CNT dispersion analysis.....	95
REFERENCES	99
VITA	105

LIST OF TABLES

	Page
Table 1 Chemical composition of clinker	3
Table 2 Chemical constituents of cement	4
Table 3 Properties of Triton X-100 surfactant	11
Table 4 Results of quasi-static compression tests on Portland cement specimens with CNT suspension at one repose week [41]	16
Table 5 Specification and properties of CNTs	20
Table 6 Mixing conditions of CNT suspension	21
Table 7 Mixing conditions of CNT/Cement composite with varied Triton X-100.....	22
Table 8 Mixing conditions of CNT/Cement composite with varied ratio of CNTs-to-Triton X-100	23
Table 9 Grid line condition for dispersion analysis of CNTs	33

LIST OF FIGURE

	Page
Figure 1 (a) Single-walled carbon nanotube (SWCNT) and (b) Multi-walled carbon nanotube (MWCNT) [7]	1
Figure 2 Heat flow and cumulative heat in the first 48 h of hydration [10]	4
Figure 3 Relationship between compressive strength of ordinary Portland cement (OPC) concrete and water to cement ratio [12]	6
Figure 4 Diagram of a surfactant molecule [30]	9
Figure 5 Type of surfactants [30]	9
Figure 6 Chemical structure of Triton X-100 [33]	11
Figure 7 Illustration of surfactant-assisted dispersion of CNTs (a) Cross section of CNT structure, (b) Side view of CNT structure [36]	12
Figure 8 UV-Vis spectrophotometer test results of CNT suspension example [37] ...	13
Figure 9 Stability of CNT suspension after (a) 5 min and (b) 72 h at various surfactant concentrations [39]	14
Figure 10 UV-vis spectra for CNT in water dispersions using Triton X-100 and SDS for different sonication times [40]	14
Figure 11 UV-Vis spectra in CNT suspension at 0.35 wt% of CNTs with 10 mM of TritonX-100 as a function of sonication energy [41]	15
Figure 12 Compressive strength of CNT/cement composite using TritonX-100 and SDS as surfactant with different sonication times [40]	17
Figure 13 Flexural strength of CNT/cement composite using TritonX-100 and SDS as surfactant with different sonication times [40]	17
Figure 14 Ultrasonic bath machine	21
Figure 15 Flow table	24
Figure 16 Cement paste in cube cement mold after preparing	25
Figure 17 cement paste in mold cover with plastic sheet	25
Figure 18 Curing cement samples	25
Figure 19 Compressive strength machine	26
Figure 20 Electrical conductivity measurement using digital multimeter.	27

Figure 21 SEM image of CNT dispersion within composite with gridline (Red line indicates CNTs).....	32
Figure 22 SEM image of CNT dispersion within composite with gridline	32
Figure 23 SEM image of CX-2,1 condition (picture 1) under various grid line conditions (a) 6×6 condition (b) 12×12 condition (c) 18×18 condition (d) 24×24 condition (e) 30×30 condition and (f) 30×30 condition.	34
Figure 24 SEM image of carbon nanotubes (CNTs) with different magnifications (a) 30000 x and (b) 150,000 x	35
Figure 25 Size distribution of CNTs (200 tubes)	36
Figure 26 CNT suspension with different Triton X-100 concentration (a) 0 g (b) 0.5 g (c) 1 g (d) 1.5 g and (e) 2 g of Triton X-100	37
Figure 27 UV-Vis spectra of CNT dispersion in water with different amount of Triton X-100	39
Figure 28 Maximum absorbance of CNT dispersion at 253 nm in water with difference Triton X-100 concentrations	39
Figure 29 Flowability of CNT/Cement composite paste with varied TX-100 concentration.....	41
Figure 30 Flowability of CNT/Cement composite paste with varied CNTs: TX-100 concentration.....	42
Figure 31 SEM image of morphology of CNT/Cement composite (a) control, (b) CX-1,0, (c) CX-0,1	43
Figure 32 SEM image of morphology of CNT/Cement composite (a) CX-1,1, (b) CX-1,1.5, (c) CX-1,2	44
Figure 33 SEM image of morphology of CNT/Cement composite (a) CX-2,1, (b) CX-3,1, (c) CX-4,1	45
Figure 34 Effect of TX-100 concentrations on porosity and water absorption	47
Figure 35 Effect of CNTs: TX-100 concentrations on porosity and water absorption.....	48
Figure 36 SEM images of cement paste after 28 days of curing time (a) 10,000x, (b) 30,000x.....	49
Figure 37 Dispersion of CNTs in composites with varied Triton X-100 conditions (a) CX-1,0, (b) CX-1,1, (c) CX-1,1.5, (d) CX-1,2	50
Figure 38 Dispersion of CNTs in composite with varied ratio CNTs: TX-100 from 2:1 to 4:1 (a) CX-2,1, (b) CX-3,1, and (c) CX-4,1	51

Figure 39 CNT dispersion ratio with CX-2,1 condition picture 1 different number of grid.....	52
Figure 40 CNT dispersion ratio within composite with varied Triton X-100.....	53
Figure 41 CNT dispersion ratio within composite with varied CNT: TX-100.....	54
Figure 42 Effect of TX-100 concentrations on compressive strength and density of composite at curing time of 7 days	56
Figure 43 Effect of CNTs: TX-100 concentration on compressive strength and density of composite at curing time of 7 days.....	58
Figure 44 Effect of curing time on compressive strength of CNT/Cement composite	59
Figure 45 Effect of TX-100 concentrations on electrical conductivity of composite at curing time of 28 days.....	61
Figure 46 Effect of CNTs: TX-100 ratios on electrical conductivity of composite at curing time of 28 days.....	62
Figure 47 Effect of curing time on electrical conductivity of varied Triton X-100 concentrations	63
Figure 48 Effect of curing time on electrical conductivity of varied CNTs: TX-100 ratio conditions.....	63

CHAPTER 1

INTRODUCTION

1.1. Motivation

Carbon nanotubes (CNTs) are a member of carbonaceous nanomaterials, which can be classified as single-walled (SWCNTs) when a superficial cylindrical layer of graphene structure or as multiple-walled (MWCNTs) formed two or more single cylindrical layers with unique properties of high mechanical strength, superior electrical and thermal conductivity. CNTs have been applied in several fields such as functional composites, energy, chemistry, and electronic materials, due to high mechanical properties, thermal conductivity, electrical conductivity, corrosion resistance, and low specific weight [1]. CNTs have been combined with other materials to enhance their properties and applied for specific applications, such as polymer, epoxy, graphene, silica, and clay, indicating the potential of CNTs in numerous fields.

Cementitious materials are raw materials for the production of many construction works due to their cost-effectiveness and high compressive strength. However, cementitious materials are brittle and exhibit low tensile strength. The development of cement-based composites, such as improving their compressive strength and electrical conductivity, has been recently focused [2].

The dispersion of CNTs in the cement matrix is challenging due to the agglomeration of CNTs caused by strong van der Waals forces (VDW), which originate from their polarizable π -electron systems. This phenomenon leads to a tendency for CNTs to agglomerate. This behavior results in decreased mechanical and electrical properties of the cement composite [3].

Various methods could improve the dispersion uniformity of CNTs in a cement matrix. It is necessary to use a high concentration of dispersing agents with the sonication process. The most common dispersing agents are surfactants, which

could improve dispersion uniformity by reducing surface tension of water and adsorption on CNT surface by hydrophobic interactions. The surfactant molecules are adsorbed on the CNT surface for maintaining colloidal stability by the electrostatic repulsion between CNT surface and electrical charges [4].

In this work, a CNT suspension is prepared by dispersing CNTs with varying concentrations of TritonX-100 and characterized using a UV-VIS spectrophotometer. Subsequently, the suspension is mixed with cement paste at different weight ratios of CNTs to cement (0.1 wt%, 0.2 wt%, 0.3 wt%, and 0.4 wt%). The CNT/cement composite samples are then analyzed using a scanning electron microscope (SEM), a universal mechanical testing machine, and a digital multimeter, respectively.

1.2. Research objective

The objective of this research is to investigate the compressive strength, electrical conductivity, and microstructural properties of CNT/cement composites employing surfactants for the dispersion of CNTs in cement, considering various weight ratios of CNTs.

1.3. Scope of this research

The scope of this research is designed to cover four main parts. The effects of the weight ratio of CNTs to cement and the concentration of surfactant for dispersing CNTs are studied.

1.3.1. Study effect of TritonX-100-to-CNTs ratio on CNT dispersion (0.5:1, 1:1, 1.5:1 and 2:1)

1.3.2. Study effect weight ratio of CNTs to cement (0.1 wt%, 0.2 wt%, 0.3 wt%, and 0.4 wt%)

1.3.3. Study the dispersion uniformity of CNTs in cement sample

1.3.4. Study compressive strength and electrical conductivity of CNT/ cement composite after 3, 7, 14, and 28 days

1.4 Expected benefits

1.5.1. Gain knowledge of preparation of CNT/cement composites using surfactants for dispersion of CNTs

1.5.2. Understand behavior and effect of surfactant and CNTs when mixing with cement



CHARTER 2

Fundamental knowledge

2.1 Basic knowledge of carbon nanotubes

Carbon nanotubes (CNTs) are robust materials characterized by tubular structures, nanoscale diameter, and a high length-to-diameter ratio. CNTs can consist of anywhere from one to hundreds of concentric shells. The carbon network of these shells, or graphite sheets, is composed of carbon atoms arranged in a honeycomb pattern [5].

2.1.1 Characteristics of Carbon Nanotubes

CNTs are bonding of carbon in different ways to construct structures with different properties. The sp^2 hybridization of carbon builds a layered construction with weak out-of-plane bonding by the van der Waals force. Carbon nanotubes are classified as single-walled carbon nanotubes (SWCNTs), which are cylinders formed with only one layer of graphite sheet. These commonly have been fabricated in diameters ranging from 0.4 to 2 nm. Multi-walled carbon nanotubes (MWCNTs) are multiple layers of graphite sheets, consequentially increasing diameters of carbon layers [6]. The structure of SWCNTs and MWCNTs is shown in **Fig. 1**.

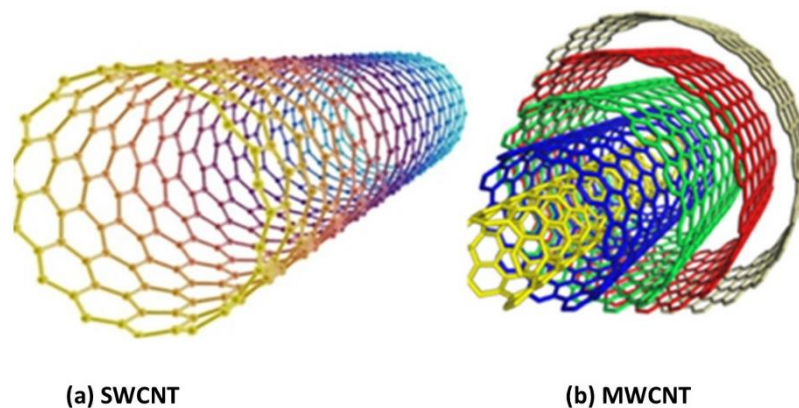


Figure 1 (a) Single-walled carbon nanotube (SWCNT) and (b) Multi-walled carbon nanotube (MWCNT) [7]

2.1.2 Methodology for carbon nanotube synthesis

Several techniques have been developed for synthesis of CNTs, which mainly involve gas-phase processes [2].

- Arc-discharge method

In comparison to other techniques, arc discharge uses higher temperature for synthesis of CNTs with fewer structural defects. This technique uses arc discharge between high-purity electrodes and water-cooled electrodes placed in a chamber filled with He, H₂, or CH₄. The chamber contains a graphite cathode, anode, evaporated carbon molecules, and some amount of metal catalyst particles (Co, Ni, or Fe). The chamber is connected with a direct current. The chamber is pressurized and heated to approximately 4,000 K. Arc is evaporated to form carbon solidifies on the cathode tip. The inner core, cathode soot, and chamber soot, which are dark and soft, yield either single-walled or multi-walled carbon nanotubes and graphene particles.

- Chemical vapor deposition method (CVD)

CVD method can be employed to synthesize CNTs by using hydrocarbon gas as a carbon precursor. The hydrocarbon gas is injected into a quartz tube with catalyst particles on the boat, which is placed inside a furnace under operating temperature of 500-900°C and an inert gas atmosphere. Pyrolysis of precursors would result in supply of carbon atoms. Those carbon atoms would undergo the so-called self-assembly, leading to formation of CNTs.

- Laser ablation method

Laser ablation method using high-power laser vaporization, a quartz tube containing a block of graphite is heated inside a furnace at 1,200 °C under argon

atmosphere. The laser vaporizes the graphite within the quartz. Carbon nanotubes form from condensation of vaporized carbon on the cooler surfaces of the reactor.

CNTs have sp^2 bonds and sp^3 bonds, which are stronger than sp^3 bonds in diamond [1] [2]. Therefore, CNTs have high mechanical strength with Young's modulus of 1.2 TPa and tensile strength of 50–200 GPa [8]. These make CNTs the strongest materials on earth. Additionally, carbon nanotubes (CNTs) exhibit elasticity when subjected to forces, bending, or twisting, with the ability to return to their original shape.

2.2 Basic knowledge of Cement Composite

Cement is a fine powder normally with grey color. The production of cement uses limestone and clay as raw materials. As summarized in **Table 1** and **Table 2**, clinker is agglomerating product of calcium, aluminum, silicon, and other trace compounds, which is employed as raw materials in a general cement production process. In concrete, the mixing of cement with water, sand, and gravel cement acts as adhesive to bind those materials together. Concrete hardens both in the air and underwater and remains in its hardened state once reached [9].

Table 1 Chemical composition of clinker

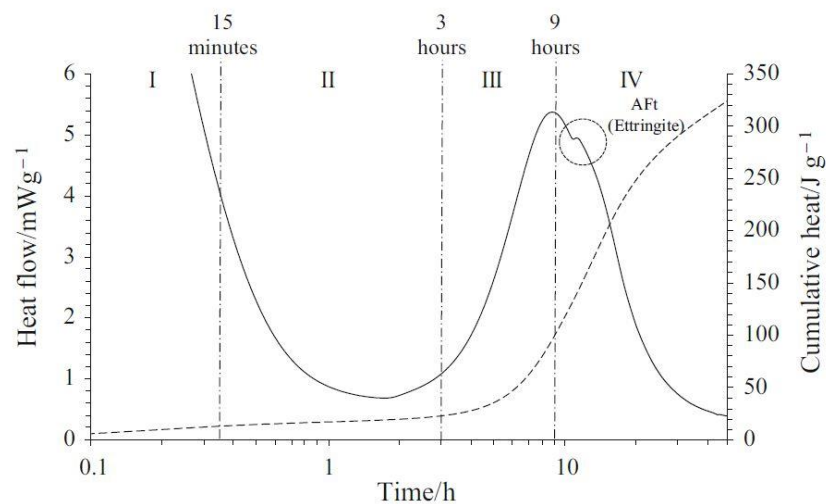
Compound	Formula	Abbreviation	% by weight
Tricalcium aluminate	$Ca_3Al_2O_6$	C_3A	10
Tetracalcium aluminoferrite	$Ca_4Al_2Fe_2O_{10}$	C_4AF	8
Belite or dicalcium silicate	Ca_2SiO_5	C_2S	20
Alite or tricalcium silicate	Ca_3SiO_4	C_3S	55
Sodium oxide	Na_2O	N	≈ 2
Potassium oxide	K_2O	K	
Gypsum	$CaSO_4 \cdot 2H_2O$	CSH_2	5

Table 2 Chemical constituents of cement

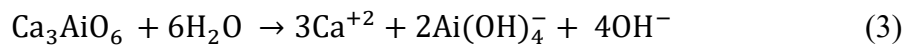
Compound	Formula	Abbreviation
Calcium oxide (lime)	CaO	C
Silicon dioxide (silica)	SiO ₂	S
Aluminum oxide (alumina)	Al ₂ O ₃	A
Iron oxide	Fe ₂ O ₃	F
Water	H ₂ O	H
Sulfate	SO ₃	<u>S</u>

2.2.1 Chemical reactions between the cement and water

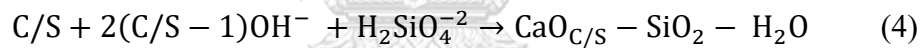
Cement hydration involves many different reactions which occur at the same time. The hydration products bond with sand, gravel particles, and other components to form a solid. A cement reaction mechanism is carried out in 4 states, as shown in **Fig. 2**.

**Figure 2** Heat flow and cumulative heat in the first 48 h of hydration [10]

Stage I: After the water contacts the cement for 15 min, heat occurs due to the neutralization of surface charges of particles and the initial dissolution of cement gypsum, C₃S (Alite), C₂S (Belite), and C₃A following **equations 1,2 and 3** [10].

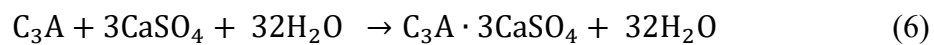


Stage II: When rate of reaction from stage I reaches to a minimum, which is related to a decrease in the dissolution rate of C₃S. Stage II starts after Ca⁺² becomes supersaturated after 3 h of water contact to cement, C-S-H precipitates in anhydrous particles, and portlandite precipitates in the solution following **equations 4 and 5**.

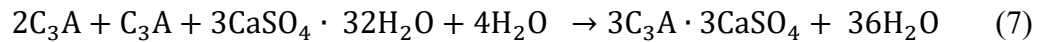


Where C/S is CaO/SiO₂ ratio of C-S-H.

The Ca⁺², OH⁻ and H₂SiO₄⁻² ions are released in initial dissolution reaction. The sulfate is adsorbed on C₃A surface, while the other part is absorbed by C-S-H. After the heat flow peak occurs at 9 h of hydration in Stage III, the reaction rate of C₃S decreases, which is the beginning of Stage IV. The dissolution of C₃A occurs during hydration period. The formation of ettringite occurs following **equation 6**.



After the consumption of sulfate in Stage IV, the rate of reaction increases due to the transformation of ettringite to calcium monosulfoaluminate. The reaction takes place 24 hours following **equation 7**.



2.2.2 Properties of cement sample

Performance and quality of cement samples are evaluated from mechanical properties of cement, which consist of shrinkage, creep, compressive strength, tensile strength, flexural strength, and modulus of elasticity [11].

2.2.2.1 Compressive strength

Compressive strength is the cement sample's most important property, which applied load per cross-section area makes sample failure. Increasing compressive strength is a good performance in construction work. Compressive strength of cement depends on water-to-cement ratio [12], as shown in **Fig. 3**. Additionally, the compressive strength test is calculated using **equation 8** [13].

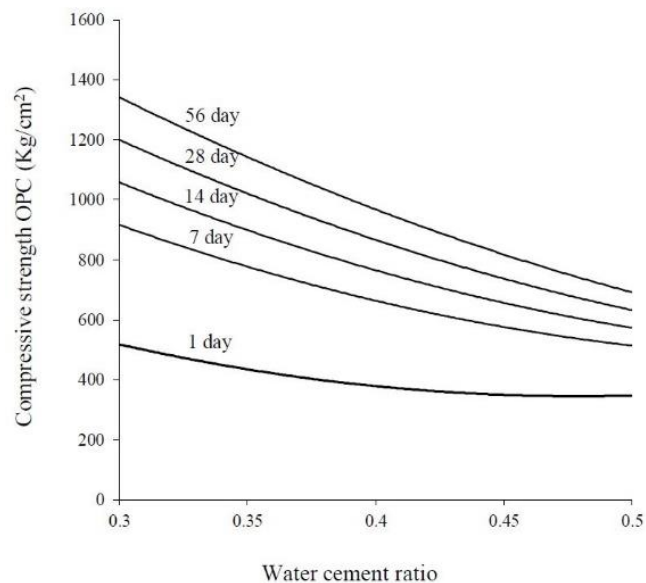


Figure 3 Relationship between compressive strength of ordinary Portland cement (OPC) concrete and water to cement ratio [12]

Compressive strength of cement sample calculation:

$$F = \frac{P}{A} \quad (8)$$

Where:

F = Compressive strength of the sample (MPa)

P = Total maximum load applied to the sample (N)

A = Cross-sectional area of the sample (mm²)

2.2.2.2 Workability

Workability is a property of fresh cement samples and concrete, allowing them to be easily mixed, transported, and compacted with minimum loss of homogeneity and without bleeding and segregation. Workability affects the quality of the concrete samples. Flowability test is a common method to determine consistency of fresh cement paste. It is used to determine the texture and workability to verify the similarity between batches. The flow standard ranges from 105% to 115%, following the ASTM C1437 standard [14].

2.2.2.3 Electrical conductivity

The conductivity of cement samples is related to certain characteristics of cement samples, which are of interest for development in some applications. The electrical conductivity of cement sample is influenced by microstructure of cement, water-to-cement ratio, and curing time of cement sample. The conductivity can convert to electrical resistivity. The resistivity of cement sample is in the range of 10^5 - 10^{12} ohm.mm., which acts as an insulator. However, there are many methods to improve the electrical conductivity of cement samples. One of them is the dispersion of CNTs which have high electrical conductivity [15].

One of the biggest problems in preparing CNT/cement composite materials is the dispersion of CNTs in cement. CNTs can agglomerate in cement due to hydrophobic property and strong van der Waals forces between CNTs [16]. The agglomeration of CNTs in cement leads to many problems in the composite, such as a decrease in mechanical performance as well as electrical and thermal properties, which are promising properties of CNTs in cement composite [17]. However, there are many strategies to help CNT disperse in cement composite. It can be easily divided into physical methods, chemical methods, and a combination of two methods. The physical methods include sonication, mechanical stirring, and ball milling [18], [19], [20]. It was found that ball milling is not effective enough because this method damages the structure of the carbon nanotubes, which results in a decrease in aspect ratio of CNTs, thereby reducing the properties of CNTs [21], [22]. The mechanical stirring, which consists of magnetic stirring and hand stirring, cannot disperse CNTs in water well. On the other hand, ultrasonication is an effective method for dispersion of CNTs through induced cavitation [23], [24], [25]. The chemical methods include modifying the surface of CNTs by adding functionalized groups and a dispersing agent to improve the wettability of CNT surface and induce electrostatic charge between each surface of CNTs. The modification of CNT surface is the addition of polar functional groups to CNT surface, such as hydroxyl (-OH), carboxyl(-COOH), and carbonyl (=O). The polar functional groups on CNT surface can bond and contact to cement composite [26]. The common of dispersing agent is surfactants and superplasticizers [27], [28]. Both have hydrophobic and hydrophilic groups in a structure. Dispersing agents can adsorb on the surface of CNTs and increase of wettability of CNTs, which can separate the individual CNTs in cement composite [29].

2.3 Basic knowledge of surfactant

2.3.1 Surfactant and type of surfactant

Surfactants are a contraction of surface-active agents [30], which are a primary component of cleaning detergents. As schematically shown in **Fig. 4**, surfactant molecule basically consists of a hydrophobic tail and a hydrophilic head. Surfactants can reduce the surface tension between two materials, whether gas and liquid, two liquids, or a liquid and solid. All surfactant molecules have a hydrophilic head (water-soluble) and a hydrophobic tail (oil-soluble). When surfactants are added to water, surfactants gather on the surface of the water and form a layer at the interface, with the hydrophilic heads toward the water and the hydrophobic tails in the air, which results in a decrease in surface tension. Surfactants can be divided into 4 types, which are non-ionic, anionic, cationic, and amphoteric, as shown in **Fig 5**.

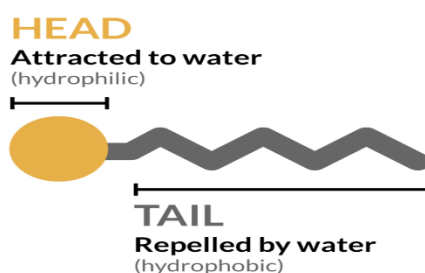


Figure 4 Diagram of a surfactant molecule [30]

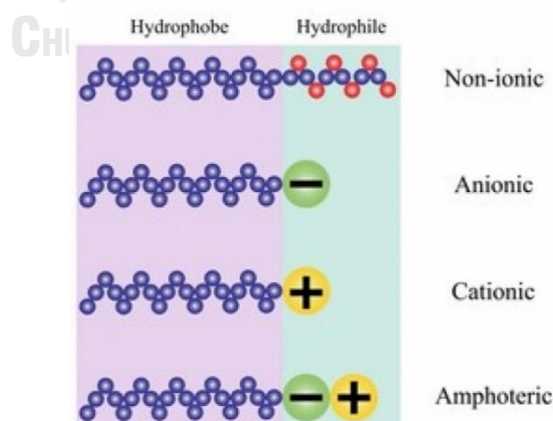


Figure 5 Type of surfactants [30]

- Non-ionic surfactants

Non-ionic surfactants do not have an electrical charge on hydrophilic groups; they are neutral. This type of surfactant can exhibit low foaming properties, making them suitable for use in low-foaming applications.

- Anionic surfactants

Anionic surfactants have a negative charge on hydrophilic groups, which helps the surfactant molecules lift and suspend soils in micelles. Commonly, anionic surfactants are used in soaps and detergents, which can create a lot of foam when mixed. Moreover, anionic surfactants are excellent for lifting and suspending particulate soils.

- Cationic surfactants

Cationic surfactants have a positive charge on hydrophilic groups usually obtained from nitrogen compounds. This surfactant cannot be used with anionic surfactant because a positive charge from cationic surfactants will react with a negative charge from anionic surfactant. That makes surfactant become to ineffective compound.

- Amphoteric surfactants

Amphoteric surfactants have both positive and negative charges on hydrophilic groups. The total charge of this surfactant is zero because they cancel each other out, referred to as zwitterionic.

2.3.2 Triton X-100 surfactant

Triton X-100 (TX-100), (IUPAC name 2-[4-(2,4,4-trimethylpentan-2-yl)phenoxy]ethanol) is a non-ionic surfactant widely used across various fields. Chemical formula of Triton X-100 is $C_{16}H_{26}O_2$. Chemical structure of Triton X-100, shown in **Fig 6**, exhibits both hydrophobic and hydrophilic structures. Hydrophilic structure is polyethoxyl, comprising polyethoxyl chains and hydroxyl groups that facilitate water adsorption. On the other hand, hydrophobic structure is 4-(1,1,3,3-tetramethylbutyl)-phenyl group that can adsorb non-polar molecules such as oil [31]. The properties of Triton X-100 are presented in **Table 3** including water solubility, making it well-suited for dispersing CNTs in water. It possesses a high dispersing

power for CNTs due to its benzene ring structure, which can strongly absorb to the graphitic surface through π - π interaction with CNTs [32].

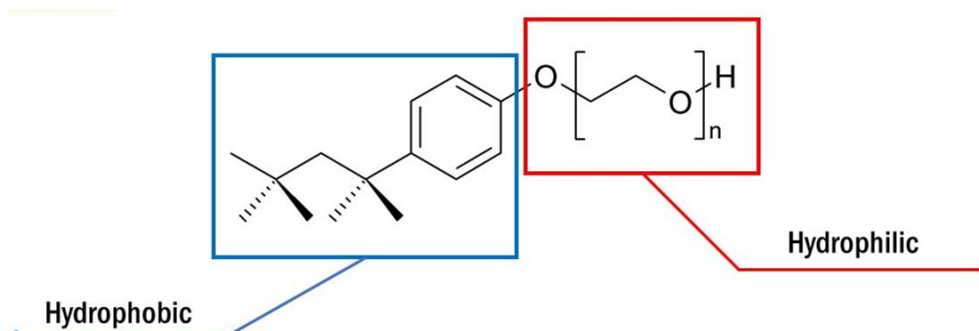


Figure 6 Chemical structure of Triton X-100 [33]

Table 3 Properties of Triton X-100 surfactant

Properties	Triton X-100
Molecular Weight	250.38 g/mol
Color	Colorless to light yellow liquid
pH	6 - 7.5
Density	1.07 g/ml
Solubility	Soluble in water

2.4. Methods for CNT Dispersion

The methods for dispersing CNTs can be broadly classified into two categories: physical methods and chemical methods [1]. A physical method involves the use of mechanical force, such as shear force, to debundle CNT bundles. Sonication is one such physical method that employs ultrasonic waves to separate bundles of CNTs in aqueous solutions [34].

Surfactants can help to dispersion of CNTs in aqueous solution and cement due to the hydrophobic and hydrophilic interaction [35]. When surfactants are introduced into water or cement, the surfactant molecules adsorb on the surface of CNTs using

hydrophobic tail while the hydrophilic head associates with cement and water, as shown in **Fig. 7**. Essentially, this behavior creates a barrier around the surface of CNTs which can reduce van der Waals forces of the individual CNTs.

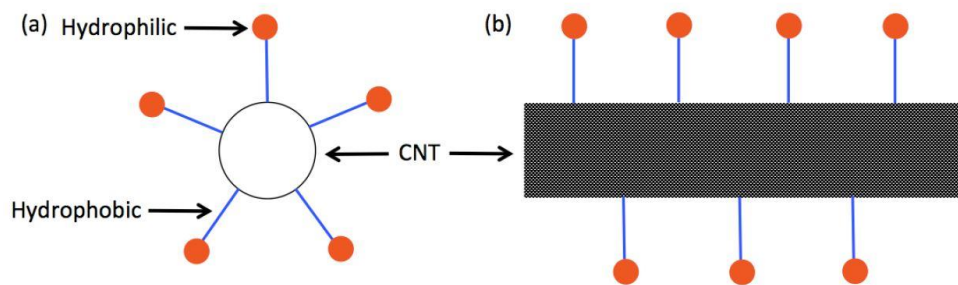


Figure 7 Illustration of surfactant-assisted dispersion of CNTs (a) Cross section of CNT structure, (b) Side view of CNT structure [36]

2.5 Characterization of CNT dispersion

The dispersion of CNTs in water can be investigated by UV-visible spectroscopic analysis [37]. The UV-Vis spectrophotometer determines the uniformity of CNT dispersion in a liquid based on analysis of transmission and absorption of ultraviolet and visible light with different wavelengths. The more absorption wavelengths of CNT suspension, the better the CNT dispersion in the solution. The adsorption peak of CNTs is 250-260 nm [38]. As shown in **Fig. 8**, each CNT suspension had the highest absorbance at a wavelength of 260 nm. The absorbance intensity of the CNT suspension C2 (Redline) is the highest, which indicates the best dispersion of CNT suspension in these results.

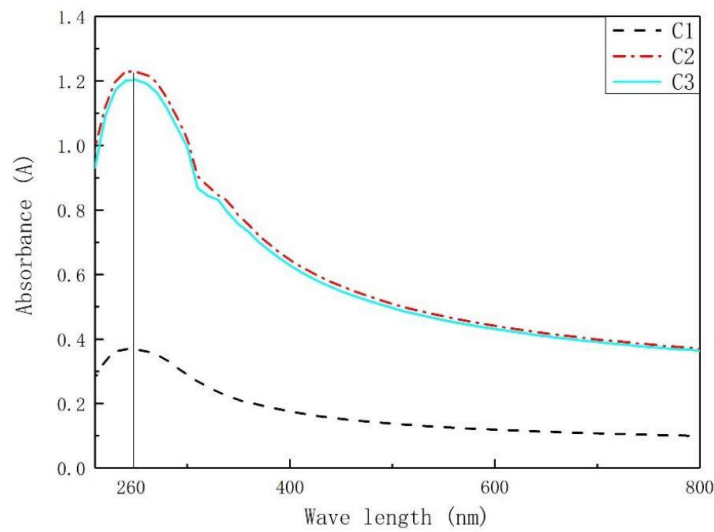


Figure 8 UV-Vis spectrophotometer test results of CNT suspension example [37]

2.6 Literature survey

2.6.1 The dispersion of CNTs in water

Jang et al. [39] studied the influence of surfactant on dispersion of CNTs in water, as shown in **Fig. 9**. 0.1 wt% of CNTs was dispersed in water by using polycarboxylate with concentrations of 0 %, 0.1%, and 0.5% by weight of cement. The results showed CNTs suspension without surfactant aggregated and settled on the bottom of a bottle, indicating the instability of CNTs in water. However, an increase in surfactant in the suspension showed improved dispersion and stability of CNTs in water after 72 h. These results revealed that surfactants could help to improve the dispersion of CNTs in water.

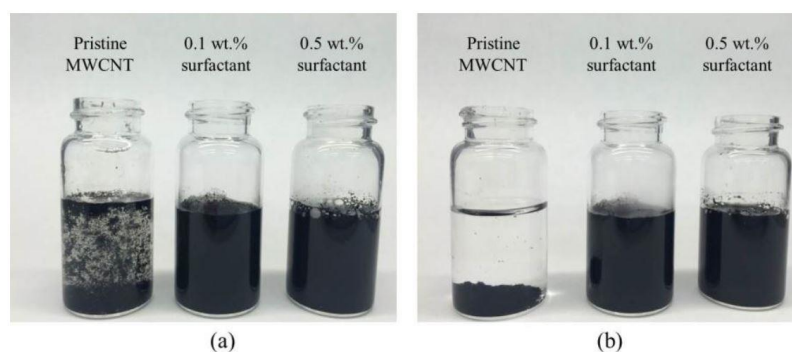


Figure 9 Stability of CNT suspension after (a) 5 min and (b) 72 h at various surfactant concentrations [39]

Elkashef et al. [40] investigated the dispersion of CNTs using different types of surfactants, namely sodium dodecyl sulfate (SDS) and Triton X-100, at a surfactant to CNT ratio of 2.5 and various sonication times ranging from 30 to 90 minutes. Additionally, CNT suspensions with different surfactants were analyzed for the dispersion of CNTs using UV-vis spectroscopy, as shown in **Fig. 10**. The UV-vis spectra of the CNT suspension exhibit higher absorbance in Triton X-100 condition compared to absorbance value of the CNT suspension with SDS. This indicates that Triton X-100 has higher efficiency in dispersing CNTs in suspension compared to SDS. The good dispersion of CNTs with Triton X-100 can be attributed to benzene structure of the hydrophobic part of Triton X-100, providing better adhesion to the surface of CNTs due to π - π interaction.

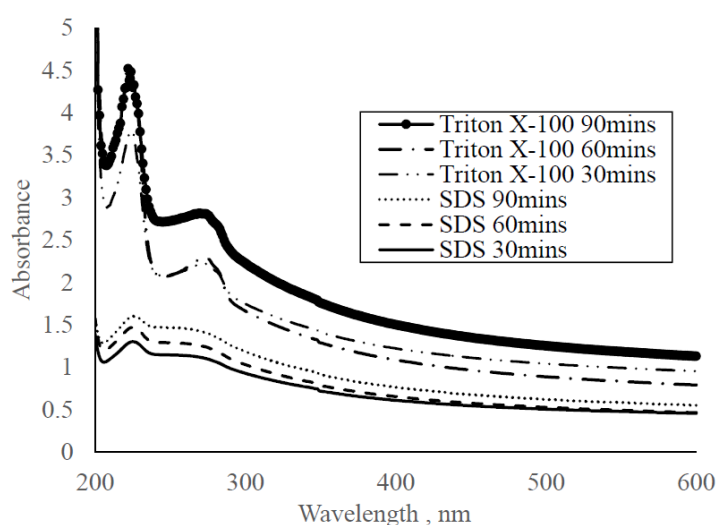


Figure 10 UV-vis spectra for CNT in water dispersions using Triton X-100 and SDS for different sonication times [40]

2.6.2 Compressive strength of CNT/cement composite

Echeverry-Cardona et al. [41] studied the dispersion of CNTs in water using TritonX-100 at different sonication energies. The UV- spectra of CNT suspension at 0.35 wt% of CNTs with 10 mM of TritonX-100 as different sonication energy is shown in **Fig. 11**. The adsorption peak increases with the increase in sonication energy due to the deagglomeration and fragmentation of CNTs. After that, CNT suspension is added to cement for preparation of CNT/cement composite, and the properties of composite are tested, as shown in **Table 4**. The elasticity modulus and compressive strength of the composite increase as sonication energy of CNT suspension and curing time due to dispersion of CNT in cement and the hydration reaction of cement.

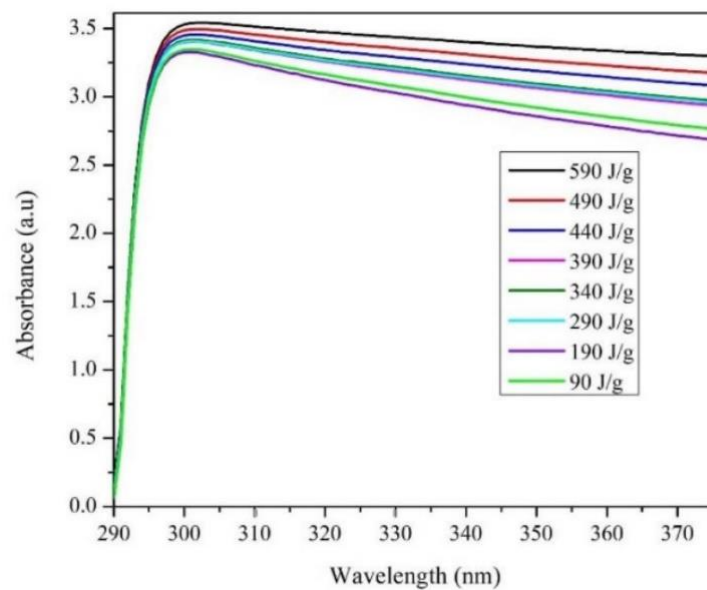


Figure 11 UV-Vis spectra in CNT suspension at 0.35 wt% of CNTs with 10 mM of TritonX-100 as a function of sonication energy [41]

Table 4 Results of quasi-static compression tests on Portland cement specimens with CNT suspension at one repose week [41]

Cement Paste Cylinder		Cement Paste	Cement Paste	Cement Paste	Cement Paste
		+ H ₂ O + TritonTX-100	with a Solution of H ₂ O + TX-100 + MWCNTs Submitted to 190 J/g	with a Solution of H ₂ O + TX-100 + MWCNTs Submitted to 390 J/g	with a Solution of H ₂ O + TX-100 + MWCNTs Submitted to 490 J/g
Curing Time					
7 days	Elasticity Modulus (GPa)	2.36 ± 0.46	2.66 ± 0.11	2.96 ± 0.10	3.51 ± 0.25
	Maximum Strength (MPa)	15.44 ± 0.79	20.49 ± 0.21	22.29 ± 0.17	24.59 ± 0.24
14 days	Elasticity Modulus (GPa)	2.70 ± 0.85	2.75 ± 0.13	3.66 ± 0.27	3.73 ± 0.12
	Maximum Strength (MPa)	16.54 ± 0.68	27.84 ± 0.62	27.10 ± 0.33	28.58 ± 0.37
28 days	Elasticity Modulus (GPa)	2.84 ± 0.97	2.88 ± 0.04	3.89 ± 0.45	5.21 ± 0.11
	Maximum Strength (MPa)	19.54 ± 0.59	32.47 ± 0.45	33.18 ± 0.76	37.85 ± 0.99

Elkashef et al. [40] studied the performance of CNT/cement composite using different surfactants. 0.2 wt% of CNTs are dispersed with Triton X-100 and sodium dodecyl sulfate (SDS) using a surfactant ratio of 2.5 and using 30 and 60 minutes of ultrasonication time. After that, CNT/cement composite is prepared using water/cement/sand ratio of 0.5:1:2.5 for compressive strength and flexural strength tests, as shown in **Fig. 12** and **Fig. 13**. The compressive strength of composite using TritonX-100 increased by 38% as compared to an increase of 20% of SDS at 30 minutes of sonication time. However, the compressive strength at 60-minute condition did not significantly improve. The flexural strength of the composite using TritonX-100 at 30 minutes of sonication increased to 46% and decreased to 33% at 60-minute condition. These results revealed that TritonX-100 is more efficient than SDS for dispersion of CNTs in cement composite.

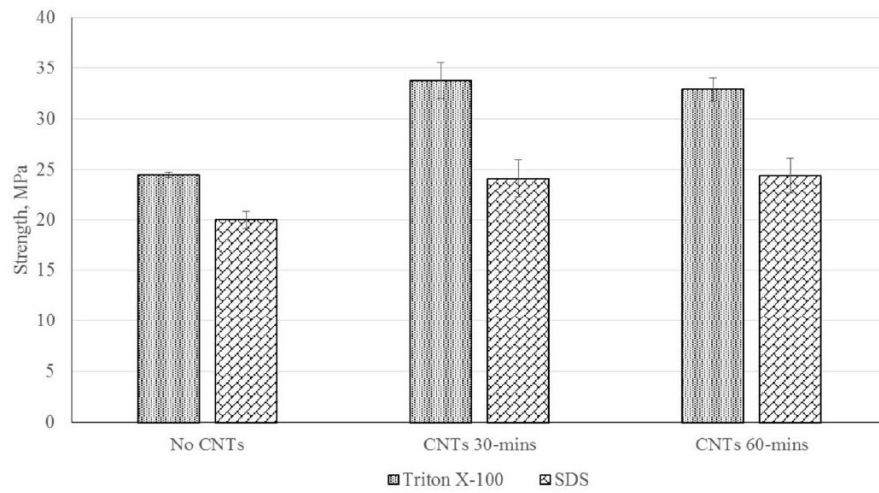


Figure 12 Compressive strength of CNT/cement composite using TritonX-100 and SDS as surfactant with different sonication times [40]

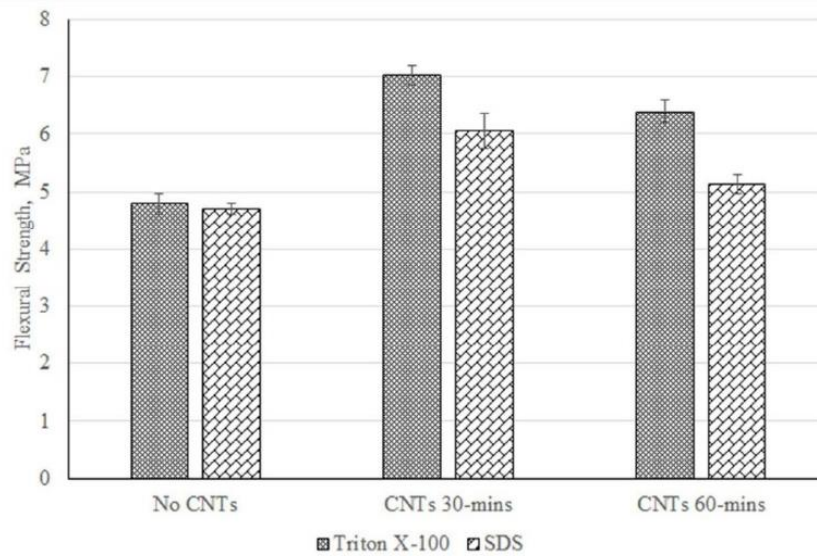


Figure 13 Flexural strength of CNT/cement composite using TritonX-100 and SDS as surfactant with different sonication times [40]

2.6.3 Electrical conductivity of CNT/Cement composite

As summarized, surfactant can help to disperse CNTs in water and cement composite, which TritonX-100 is a suitable surfactant for dispersion of CNTs. Additionally, CNTs with different weight ratios and using surfactant for dispersion can help to improve the strength and electrical conductivity of the composite. From the results, there are still issues about concentration of TritonX-100, which can help to disperse CNTs in cement composite, and the amount of CNTs in cement that can help to improve the strength and conductivity. The two factors mentioned above will be further studied and reported in the next chapter.



CHAPTER 3

RESEARCH METHODOLOGY

In this research, the experimental process can be divided into three main parts.

The first part involves the preparation of the CNTs suspension. This includes dispersing CNTs in water and using surfactant to help for uniform distribution and prevent agglomeration. Various techniques such as sonication and mechanical stirring were also employed to help for well dispersion of CNTs in suspension.

The second part focuses on the preparation of CNT/cement composite, involving the incorporation of CNTs into the cement matrix to create a homogeneous mixture. The mixing process includes mixing the CNT suspension with cement powder using a mechanical mixer following ASTM C305 standards [42].

The final part of the experiment involves testing the prepared CNT/cement composite samples. This includes conducting various tests and measurements to evaluate the properties and performance of the cement composite. These tests include assessing flowability, compressive strength, electrical conductivity, density, and conducting microstructure analysis.

3.1 Material and chemicals

CNTs from Chengdu Organic Chemicals Co. Ltd., China, with specifications as shown in **Table 5** and TritonX-100 from Sigma-Aldrich, were used to prepare CNT suspension. Ordinary Portland cement (type 1) from SCG International Co. Ltd. was used to prepare CNT/cement composite with CNT suspension.

Table 5 Specification and properties of CNTs

Specification	Value
Purity	>95 wt%
Outer diameter	4-8 nm
Length	10-20 μm
Specific surface area	350-550 m^2/g
Color	Black

3.2 Preparation and characterization of CNT suspension

3.2.1 Preparation of CNT suspension

The preparation of CNT suspension involves dispersing CNTs in water using Triton X-100 as a surfactant. The following steps are followed:

1. Preparation of Triton X-100 Solution: Water is mixed with Triton X-100 to create a solution. The proportions of water and Triton X-100 vary based on experimental requirements, with mixing conditions detailed in **Table 6**.
2. Mechanical stirring: Triton X-100 solution is stirred for 10 minutes using a mechanical stirrer. This step helps in achieving a uniform distribution of Triton X-100 in solution.
3. Addition of CNTs and stirring: CNTs are added to Triton X-100 solution and stirred for an additional 10 minutes. Stirring helps in dispersing the CNTs within the solution.
4. Ultrasonication: To ensure a stable suspension of CNTs in suspension, CNT suspension is subjected to ultrasonication for 30 minutes using an ultrasonication (Sonorex Digitec DT156BH, Bandelin, Germany), as shown in **Fig. 14**. Ultrasonication helps to separate any agglomerates or clusters of CNTs, which resulted in a more homogeneous dispersion.
5. Further stirring: After ultrasonication, CNT suspension is stirred again for 10 minutes using a mechanical stirrer. This step ensures continued dispersion of CNTs and helps to achieve a uniform and stable suspension.

Table 6 Mixing conditions of CNT suspension

Case	Name	CNTs (g)	Triton X-100 (g)	Water (g)
1	Control	1	0	400.0
2	CX-1,0.5	1	0.5	399.5
3	CX-1,1	1	1.0	399.0
4	CX-1,1.5	1	1.5	398.5
5	CX-1,2	1	2.0	398.0



จุฬาลงกรณ์มหาวิทยาลัย
CHULALONGKORN UNIVERSITY

Figure 14 Ultrasonic bath machine

3.2.2 Characterization of CNT suspension

CNT suspensions prepared in **Section 3.2** are characterized for the dispersion of CNTs by UV-Vis Spectroscopy in absorption mode spanning 200-800 nm.

3.3 Preparation of CNT/cement composite

CNT/Cement composite is prepared by mixing a CNT suspension with cement powder. The process involves several steps:

1. CNT suspension preparation: CNTs are dispersed in water using Triton X-100 as a surfactant. The procedure is detailed in Section 3.2.1.
2. Mixing CNT suspension with cement powder: CNT suspension is mixed with ordinary Portland cement (type 1) powder. Mixing process follows the ASTM C305 standard [42]. A mechanical mixer is used with a mixing speed of 140 rpm for 30 seconds, which is followed by 285 rpm for 150 seconds.
3. Pouring into Mold: Prepared CNT/Cement composite paste is poured into a cube-shaped mold measuring $50 \times 50 \times 50 \text{ mm}^3$. Then, mold is covered with plastic to protect composite during curing process.
4. Curing: CNT/Cement composite samples are cured for different periods, typically 3, 7, 14, and 28 days. Curing allows composites to gain strength and develop their desired properties. Mixing conditions are shown in **Tables 7 and 8**.

Table 7 Mixing conditions of CNT/Cement composite with varied Triton X-100

Cases	Name	CNTs (g)	Triton X-100 (g)	Water (g)	Cement (g)
1	Control	0	0	400.0	1,000
2	CX-1,0	1	0	400.0	1,000
3	CX-1,1	1	1.0	399.0	1,000
4	CX-1,1.5	1	1.5	398.5	1,000
5	CX-1,2	1	2.0	398.0	1,000

Table 8 Mixing conditions of CNT/Cement composite with varied ratio of CNTs-to-Triton X-100

Cases	Name	CNTs (g)	Triton X-100 (g)	Water (g)	Cement (g)
1	CX-0,1	0	1.0	399.0	1,000
2	CX-1,1	1	1.0	399.0	1,000
3	CX-2,1	2	1.0	399.0	1,000
4	CX-3,1	3	1.0	399.0	1,000
5	CX-4,1	4	1.0	399.0	1,000

3.4 Flowability test of CNT/Cement composite paste

In this part of the research, flowability of CNT/Cement composite paste is determined using the flow table (10" Flow Table, ELE International, United States), as shown in **Fig 15** and following the ASTM C1437 standard [43]. Flow table test is a widely accepted method for evaluating flow characteristics of cementitious materials. Test steps are as follows:

1. The cement composite paste is placed in a mold to a thickness of approximately 25 mm and compacted by tamping it 20 times with a tamper.
2. Then, cement paste is filled and tamped again as the first layer.
3. The top surface of cement paste is smoothed out to create a flat and uniform surface.
4. Mold is lifted from cement paste, and then left cement paste on table for 1 minute.
5. After 1 minute, mold is immediately dropped onto the table 25 times within 15 seconds.
6. The diameter of cement paste spread on flow table is measured along four lines on top surface using a vernier caliper.

The measured diameters are recorded for each line and used in calculation method as follows in **equation 9**.

Flowability of CNT/Cement composite paste calculation :

$$Flowability = \frac{D_{avg} - D_0}{D_0} \times 100 \quad (9)$$

Where,

D_{avg} : Average base diameter

D_0 : Original base diameter (10.15 cm)



จุฬาลงกรณ์มหาวิทยาลัย
CHULALONGKORN UNIVERSITY
Figure 15 Flow table

3.5 Molding and Curing Processes of CNT/Cement Composite Samples

CNT/cement composite with a designated weight ratio of CNTs was poured into a mold with a dimension of $50 \times 50 \times 50 \text{ mm}^3$, as shown in **Fig. 16**, and covered by a plastic sheet for one day, as shown in **Fig.17**. After that, cement samples were cured within a standard time period of 3, 7, 14, and 28 days. Curing cement samples are shown in **Fig.18**.



Figure 16 Cement paste in cube cement mold after preparing



Figure 17 cement paste in mold cover with plastic sheet



Figure 18 Curing cement samples

3.6 Performance test and analyst technique of CNT/cement composite

After being cured for 3, 7, 14, and 28 days, CNT/cement composite samples were analyzed to evaluate their compressive strength, electrical conductivity, and microstructure properties. These analyses provide valuable insights into the mechanical, electrical, and structural characteristics of composite samples.

3.6.1 Compressive strength test

The compressive strength of CNT/cement composite samples was investigated after curing for 3, 7, 14, and 28 days. Composite samples were prepared by removing plastic wrap and then subjected to compression testing using a compressive machine (TMC 3000 MM, Test Material Company Limited, Thailand), following the ASTM C109 standard [44], as shown in **Fig 19**.

The ASTM C109 standard requires samples to have sized of 50 mm x 50 mm x 50 mm. Prior to testing, weight of each sample was measured. Samples were placed and aligned in center of compressive machine. A continuous load was applied at a constant rate until specimen failed, and maximum load at failure was recorded. To ensure reliable and accurate data, 3 samples from each condition were analyzed, and average values of compressive strength measurements were reported.



Figure 19 Compressive strength machine

3.6.2 Electrical conductivity measurement

CNT/cement composite samples were measured electrical property by a digital multimeter (HT118A, HABOTEST, China), as shown in **Fig. 20**. Electrical resistance was assessed through the 2-point probes method [45]. Probes of digital multimeter were connected to cement electrodes, and resistance mode (R) was selected for measurement. Subsequently, electrical resistance value obtained from the cement sample was calculated to determine electrical conductivity value using **equation 10**. To compensate for any measurement deviations, three samples from each condition were analyzed, and average values of the measurements were reported.

Electrical conductivity of CNT/Cement composite calculation equation:

$$\sigma = \frac{L}{R \times A} \quad (10)$$

Where,

σ : Electrical conductivity (S/m)

L: Length between the electrode (2×10^{-2} m)

R: Electrical resistance (Ω)

A: Contact area between the electrode and cement sample (7.5×10^{-4} m²)



Figure 20 Electrical conductivity measurement using digital multimeter.

3.6.3 Bulk density measurement method

Weight of each CNT/cement composite which is cured for 3, 7, 14, and 28 days, is measured using a digital weigh scale (VIBRA AJH 2200CE, SHINKO DENSHI CO., LTD, Japan). Samples are weighed to determine mass at different curing durations.

Additionally, three dimensions (length, width, and height) of cube-shaped samples are measured using a vernier caliper. These measurements are taken to calculate the volume of each sample. Volume is calculated by multiplying length, width, and height values.

Density is calculated following **equation 11**. Additionally, three samples of each condition are calculated and averaged values of the measurements are reported. This approach helps to minimize errors and ensure reliability of density calculations.

Bulk density of CNT/Cement composite calculation equation

$$D = \frac{M}{V} \quad (11)$$

Where,

D: Bulk density of CNT/Cement composite sample (g/cm^3)

M: Mass of CNT/Cement composite sample (g)

V: Volume of CNT/Cement composite sample (cm^3)

3.6.4 Microstructure and Morphology

The scanning electron microscope (JSM-7610F, JEOL, Japan) is utilized to examine microstructure and morphology of CNT/cement composite samples, as well as uniform dispersion of CNTs within cement composite. To determine suitable cement samples for investigating distribution of CNTs in cement composite, conductivity testing is performed on cement samples. Electrical conductivity values of the selected samples are compared to the average range for each condition. Samples that fall within the average range are chosen for further investigation using SEM.

Once the appropriate samples are selected, samples are crushed into smaller pieces and measured approximately 5 mm x 5 mm x 2 mm using a hammer. These smaller sections are subjected to SEM analysis to confirm distribution of CNTs within composite. Individual sections obtained from each condition of cement composite sample are examined using SEM, which allows for a detailed assessment of dispersion of CNTs throughout cement composite.

By employing SEM, microstructure, morphology, and dispersion uniformity of CNTs in CNT/cement composite samples can be visually evaluated, providing valuable insights into structural characteristics and effectiveness of CNT dispersion within the matrix.

3.6.5 Porosity and water absorption

The standard test method for density, absorption, and voids in concrete, as outlined in ASTM C642 [46], is employed to measure porosity and water absorption of CNT/Cement composite samples. The procedure involves the following steps:

1. Preparation and curing of composite sample: CNT/Cement composite samples are prepared, accorded to the desired specifications, and cured for a period of 28 days.
2. Weighing samples: Cured cement samples are weighed to determine their initial mass.
3. Drying sample: Composite samples are placed in an oven (NL 1017 X / 008, NL Scientific Instruments Sdn. Bhd., Malaysia) which is set at 100°C for 2 days to remove water and moisture. After drying, the weight of samples is measured and recorded as *Mass A*.
4. Measurement after immersion: Dried cement samples are immersed in water for 2 days. After immersion, their weight is measured and recorded as *Mass B* to assess water absorption.
5. Boiling sample: Composite samples are boiled in a water bath (WNB 45, Memmert, Germany) at 95°C for 5 hours. After boiling, samples are allowed to cool for at least 14 hours.

6. Weight measurements: Weight of the samples is measured again, noted as *Mass C*. Additionally, samples are suspended with wire in water, and their weight in water is measured, noted as *Mass D*. These measurements contribute to the calculation of apparent density and permeable voids.

By following this ASTM standard test method, it is possible to accurately determine porosity and water absorption characteristics of CNT/Cement composite samples. The porosity and water absorption of cement sample are calculated following **equations 12 and 13**.

Porosity of CNT/Cement composite calculation equation:

$$\text{Porosity (volume of permeable pore space), (\%)} = \frac{\text{Mass C} - \text{Mass A}}{\text{Mass C} - \text{Mass D}} \times 100 \quad (12)$$

Water absorption of CNT/Cement composite calculation equation:

$$\text{Water absorption after immersion and boiling, (\%)} = \frac{\text{Mass C} - \text{Mass A}}{\text{Mass A}} \times 100 \quad (13)$$

Where,

Mass A: Mass of oven-dried sample in air (g)

Mass C: Mass of surface-dry sample in air after immersion and boiling (g)

Mass D: Apparent mass of sample in water after immersion and boiling (g)

3.6.6 CNT dispersion analysis

Dispersion analysis of CNTs from SEM images is performed using a grid method, which counts areas with both individual and agglomerated CNTs. The procedure is outlined as follows.

1. Creation of grid lines on SEM image: Grid lines are meticulously drawn on the SEM image, as shown in **Fig. 21**.
2. Counting cells: Following placement of gridlines, each grid cell in SEM image underwent analysis and counting, as shown in **Fig. 22**.
 - If a grid cell contains only one tube of CNTs, it is categorized as an individual CNT (Yellow color grid).
 - Conversely, if a grid cell contains more than one tube of CNTs, it is classified as agglomerated CNTs (Red color grid).
3. Calculation of individual and agglomerated cells: The counts of individual cells with one tube of CNTs and agglomerated CNTs are calculated. The dispersion of CNTs is quantified using **equation 14**.

This method facilitated a comprehensive analysis of CNT dispersion from SEM images, which provided insights into distribution of individual and agglomerated CNTs under diverse conditions.

The dispersion value obtained from CNT dispersion equation can be interpreted as follows: if the dispersion value is higher than 0 or between 0 and 1, it indicates that the number of cells consisting of individual CNTs is higher than the number of cells consisting of agglomerated cells, which defined good dispersion of CNTs within composite in this condition. Conversely, if the dispersion value is lower than 0 or between 0 and -1, it indicates that the number of cells containing agglomerated CNTs is higher than dispersion cells, which means that CNTs tended to agglomerate within composite in this condition. The dispersion values of each condition are compared to examine the trend of dispersion or agglomeration of CNTs within composite.

Additionally, each condition of CNT/Cement composite is systematically analyzed, and the averaged CNT dispersion value is derived from the analysis of five pictures.

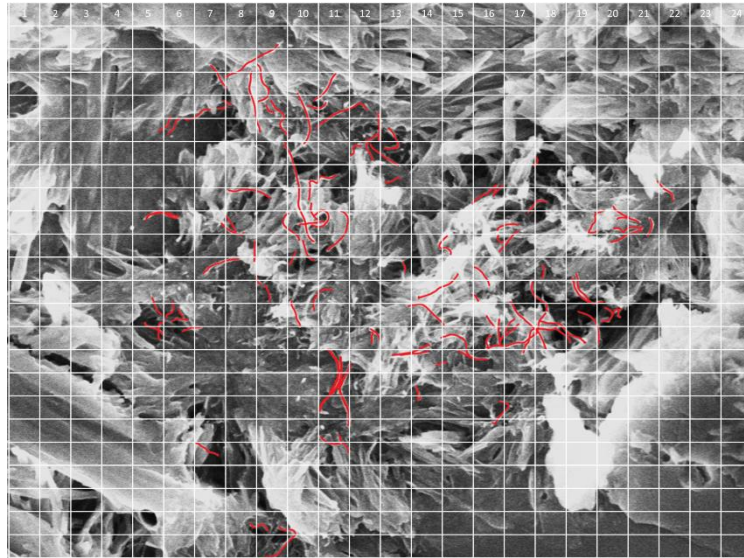


Figure 21 SEM image of CNT dispersion within composite with gridline (Red line indicates CNTs)

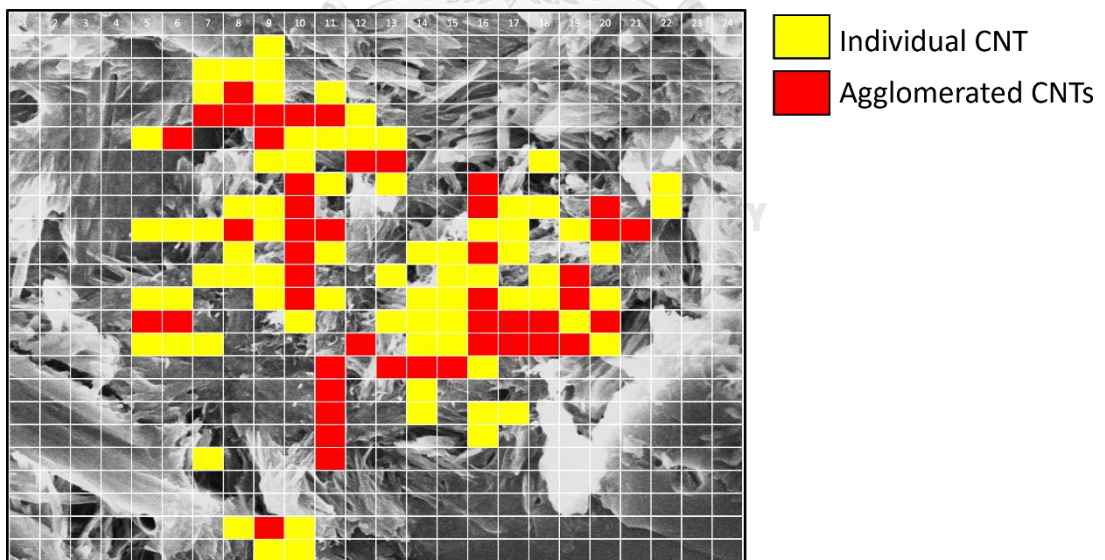


Figure 22 SEM image of CNT dispersion within composite with gridline

CNT dispersion analysis calculation equation:

$$CNT \text{ dispersion ratio} = \frac{\text{Individual CNT-Agglomerated CNTs}}{\text{Total cells}} \quad (14)$$

Where,

Individual CNT: Cells containing one CNT tube each.

Agglomerated CNTs: Cells containing more than one tube of CNTs each.

Total cells: Total number of cells in the picture.

Before using the grid method to analyze CNT dispersion, the number of grid lines is systematically varied to establish appropriate grid conditions for SEM images, which aims to minimize discrepancies in dispersion values. The SEM image of the CX-2,1 condition (picture 1) is selected for analysis to determine the suitable gridline. CNT dispersion ratio analysis is conducted on the SEM image of CNT/Cement composite CX-2,1 condition (picture 1) using different grid line conditions, as detailed in **Table 9** and **Fig. 23(a-f)**.

Table 9 Grid line condition for dispersion analysis of CNTs

Gridline condition	Total cells
6 × 6	36
12 × 12	144
18 × 18	324
24 × 24	576
30 × 30	900
36 × 36	1,296

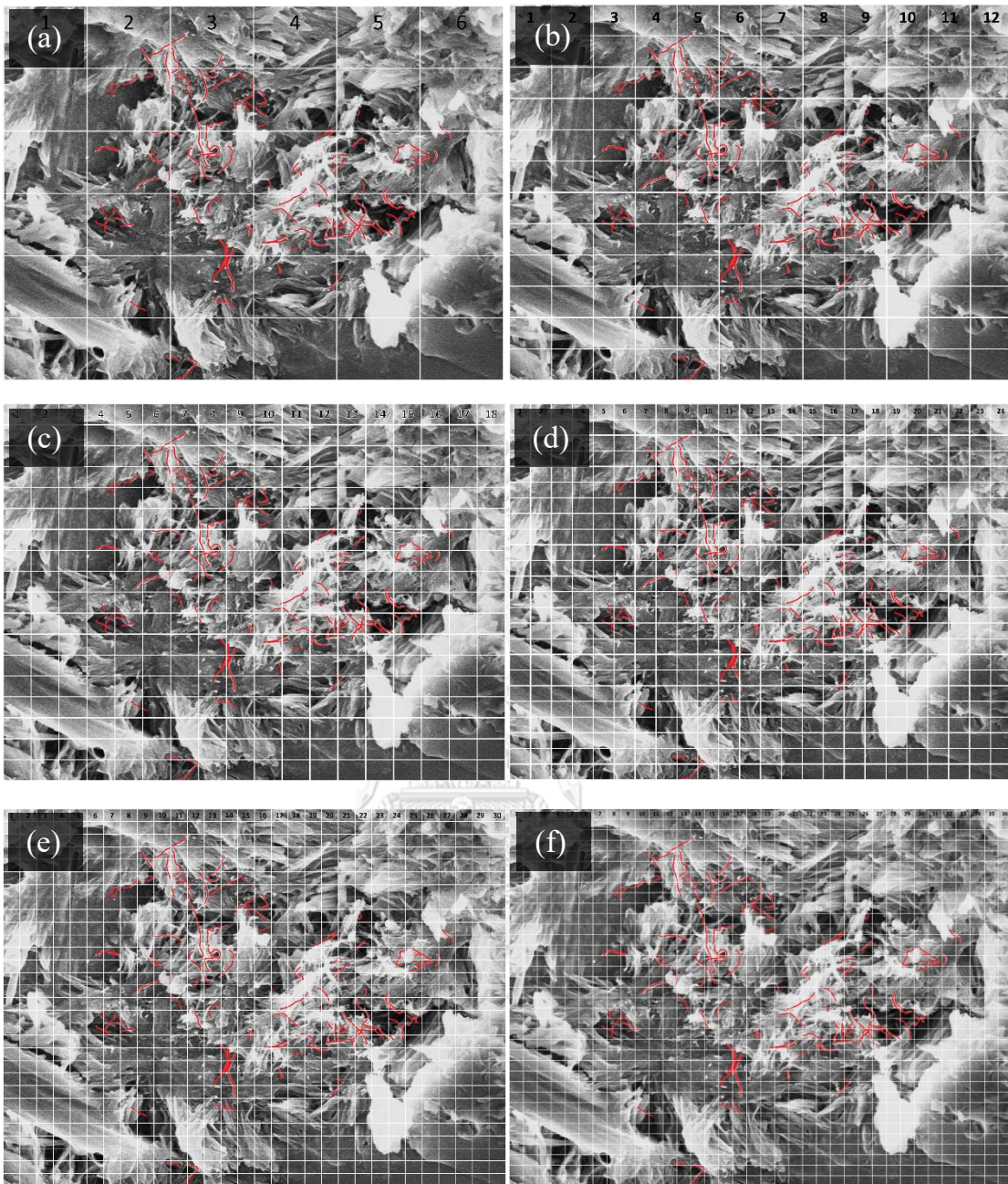


Figure 23 SEM image of CX-2,1 condition (picture 1) under various grid line conditions (a) 6×6 condition (b) 12×12 condition (c) 18×18 condition (d) 24×24 condition (e) 30×30 condition and (f) 30×30 condition.

CHAPTER 4

RESULTS AND DISCUSSION

This research study primarily focuses on preparation of CNT suspension in water with the presence of Triton X-100 as surfactant. Uniformity of CNT suspension was examined by varying ratios of CNTs and Triton X-100. Then, the well-dispersed CNT suspension was incorporated with cement paste for preparation of CNT/Cement composite by incorporating Triton X-100 as a surfactant and varying amounts of CNTs. Several aspects of composite are characterized and analyzed, which include morphology, size distribution of CNTs, dispersion efficiency of CNTs in CNT suspension, flowability, porosity and water absorption, compressive strength, and electrical conductivity.

4.1 Morphology and size distribution of CNTs

Morphology analysis of CNTs was conducted using Field Emission Scanning Electron Microscopy (FESEM), as shown in **Fig 24(a-b)**. SEM image displayed a distribution of fibrous tubular structures, which represented CNTs. The ImageJ software was used for the analysis of the size distribution of CNTs.

From the SEM images, a total of 200 CNT tubes were analyzed for size distribution. The measured diameters of CNTs were recorded and used to calculate average diameter, which revealed an average diameter of 9.1 ± 1.7 nm, as shown in **Fig 25**. The diameter of each CNT is shown in **Appendix A in Table A1**.

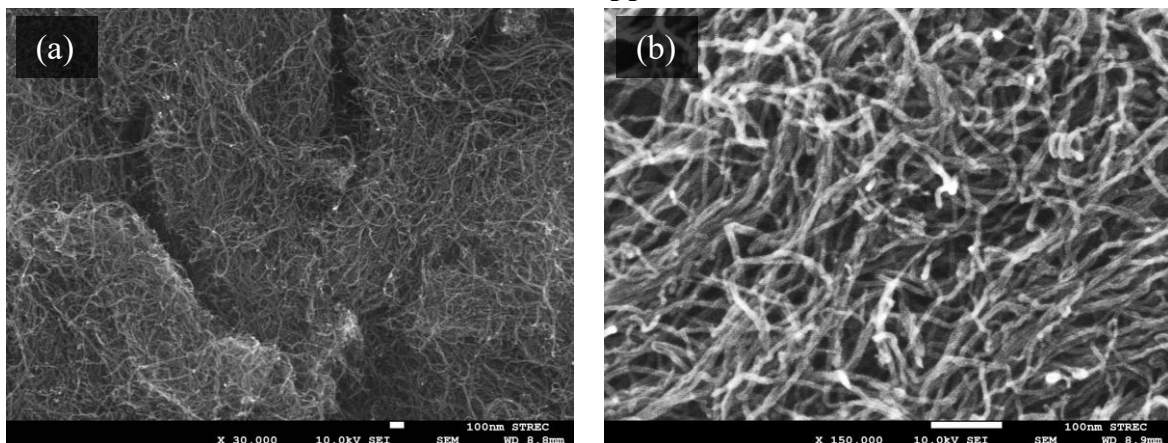


Figure 24 SEM image of carbon nanotubes (CNTs) with different magnifications (a) 30000 x and (b) 150,000 x

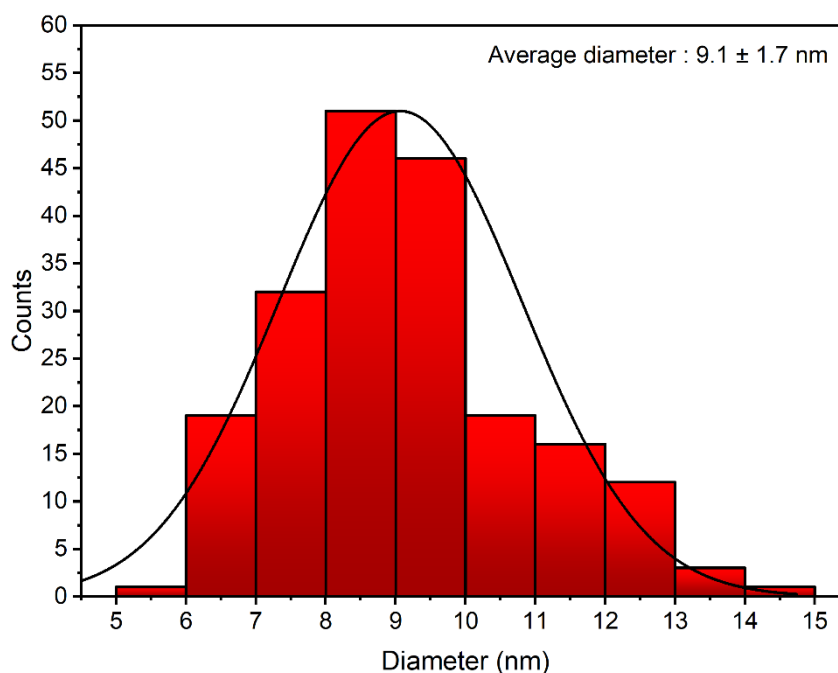


Figure 25 Size distribution of CNTs (200 tubes)

4.2 Characterization of CNT suspension with Triton X-100

4.2.1 Apparent CNT suspension

CNT suspensions were prepared by dispersing CNTs in water using different concentrations of Triton X-100, as shown in **Fig. 26 (a-e)**. The CNT suspension without Triton X-100, after preparation, exhibited clear separation, with CNTs sedimenting and agglomerating at the bottom of the container, as shown in **Fig. 26 (a)**. However, the addition of Triton X-100 at concentrations ranging from 0.5 g to 2 g resulted in suspensions with black color, indicating better dispersion of CNTs, as shown in **Fig. 26 (b-e)**. The suspension with 0.5 g of Triton X-100 displayed a dark color with agglomerated CNTs at the bottom of the container, suggesting low dispersion. On the other hand, CNT suspensions with increased amounts of Triton X-100 (1 g, 1.5 g, and 2 g) exhibited a black color, indicating good dispersion of CNTs based on their physical appearance [47].

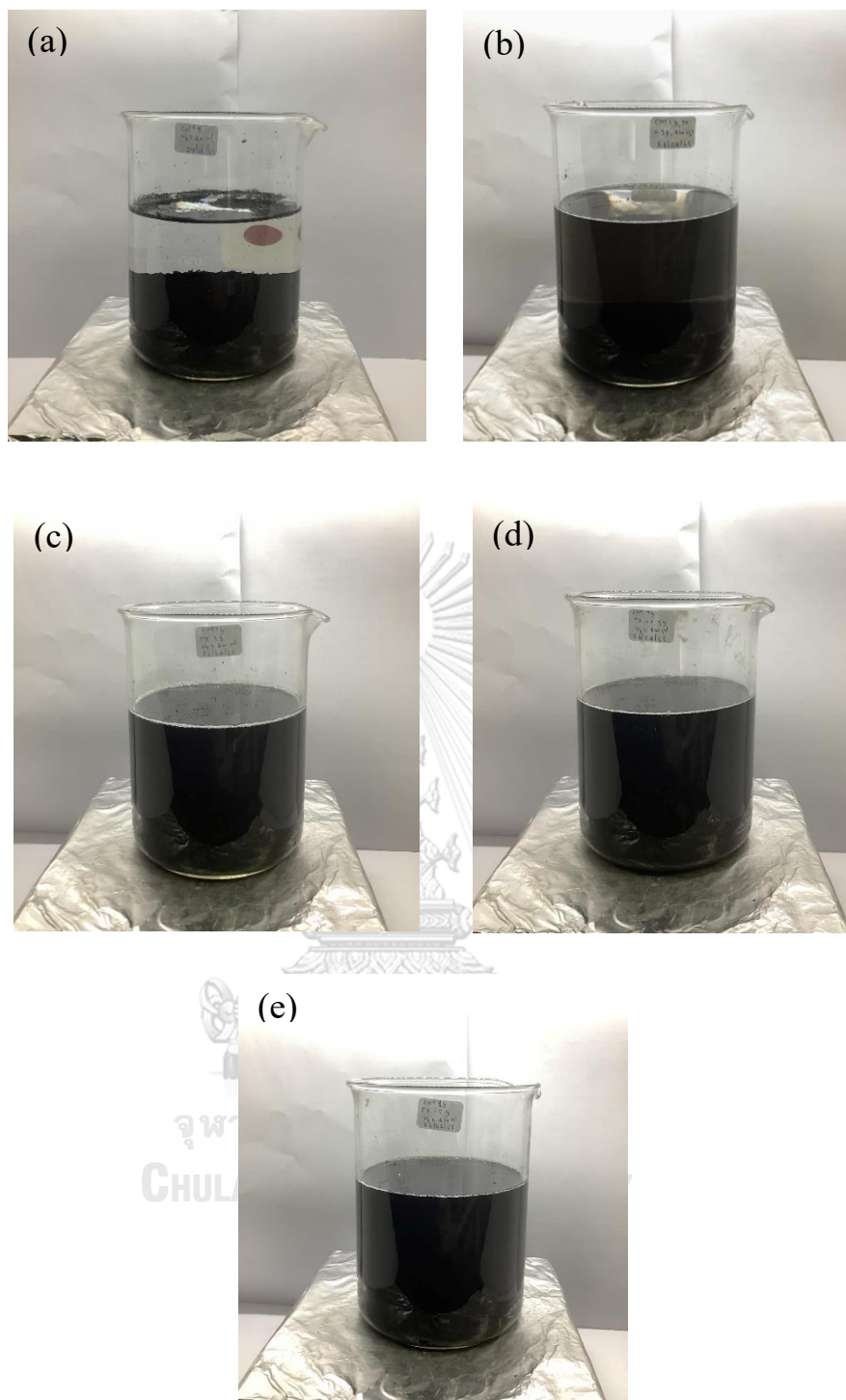


Figure 26 CNT suspension with different Triton X-100 concentration
(a) 0 g (b) 0.5 g (c) 1 g (d) 1.5 g and (e) 2 g of Triton X-100

4.2.2 Evaluation of uniform CNT dispersion

Quality analysis of CNT dispersion in suspension can be analyzed by using UV-vis spectroscopy. UV-vis spectroscopy is a method that determines dispersion of CNTs in a suspension by passing light with different wavelengths through the CNT suspension. UV-spectra of CNT suspension with different amounts of Triton X-100 is shown in **Fig. 27**. CNT suspension was analyzed for dispersion in wavelength range of 200 nm to 800 nm. Maximum absorption peak of CNTs typically occurs around 250-260 nm [37], and the intensity of this peak indicates quality of dispersion. Moreover, addition of Triton X-100 at different concentrations (0.5 g, 1 g, 1.5 g, and 2 g) to suspension led to an increase in intensity of absorbance peak at 253 nm as shown in **Fig. 28**. An increase in absorbance peak upon addition of Triton X-100 suggested that Triton X-100 contributed to better separation of individual CNTs in suspension. This leads to an increase in light absorption, which resulted in improved dispersion of CNTs in suspension [48] [49]. Notably, in conditions with 1 g, 1.5g, and 2 g of Triton X-100, the maximum adsorption peak was significantly higher compared to 0.5 g, which suggested better dispersion of CNTs. These UV-vis spectroscopy results were consistent with visual observation, which appeared black color suspension throughout entire container. Therefore, CNT/Cement composite will be prepared in the next step using conditions of adding 1 g, 1.5 g, and 2 g of Triton X-100.

Based on the abovementioned results, the condition of using 1 g of CNTs dispersed in de-ionized water with variations of 1 g, 1.5 g, and 2 g of Triton X-100 was used for preparing CNT/Cement composite for examining properties of resultant CNT/Cement composites.

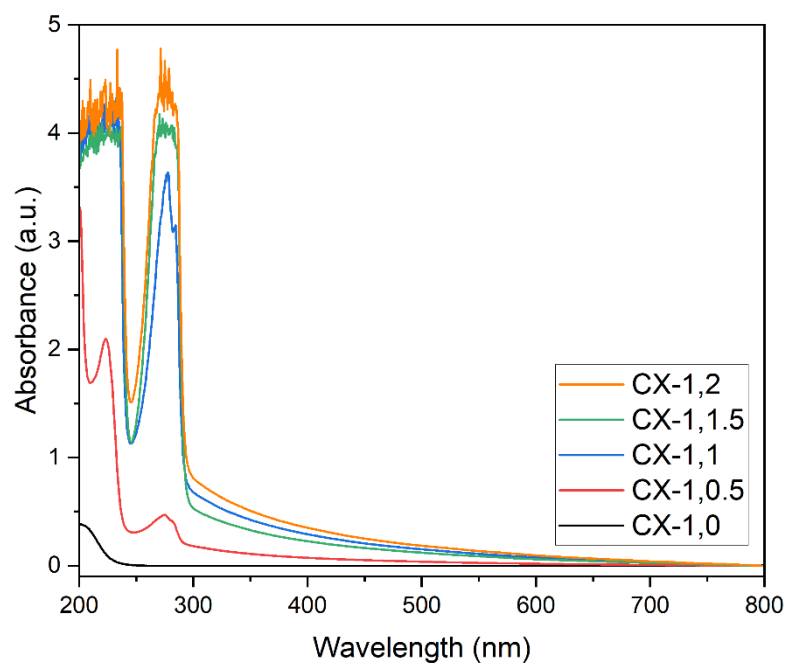


Figure 27 UV-Vis spectra of CNT dispersion in water with different amount of Triton X-100

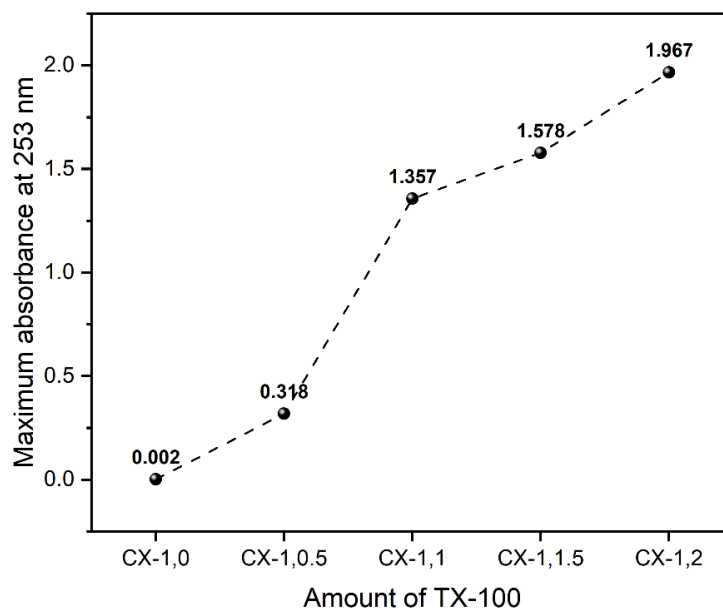


Figure 28 Maximum absorbance of CNT dispersion at 253 nm in water with difference Triton X-100 concentrations

4.3 Flowability of CNT/Cement composite paste

Flowability of CNT/Cement composite paste was an important parameter that determined fluidity and viscosity of cement paste. Flowability results of composite paste with different Triton X-100 concentrations are shown in **Fig. 29**. In control condition with a water-to-cement ratio (w/c) of 0.4, flowability was 106.12%.

However, addition of CNTs to the cement paste typically decreased the flowability to 90.55% in the 1 g of CNTs and without TX-100 condition (CX-1,0), which was lower than control condition. The presence of CNTs affected rheological properties of composite paste and resulted in a higher viscosity.

In contrast, the addition of Triton X-100 at different concentrations (1g, 1.5g, and 2g) increased flowability of composite paste. Flowability values for these conditions are measured to be 112.60%, 121.02%, and 123.90%, respectively, which was higher than control condition. An increase in flowability of composite with addition of Triton X-100 can be explained by absorption of Triton X-100 molecules on cement grains. This absorption helps enhance wettability of cement grains through hydrophilic head of the Triton X-100 molecule, which resulted in improved flowability of cement composite [50].

Furthermore, flowability of composite paste was further investigated by adding different amounts of CNTs from 0 g to 4g while keeping TX-100 concentration constant at 1g, as shown in **Fig. 30**. Flowability of composite with 1 g of TX-100 and without CNTs (CX-0,1) was 125.65%, which was higher than control condition. However, flowability decreased as the amount of CNTs increased from 1 g to 4 g, from 112.60% in 1 g CNTs condition (CX-1,1) to 88.70% in 4 g CNTs condition (CX-4,1)

In summary, these results suggested that an increase in concentration of CNTs relative to Triton X-100 can have a negative impact on flowability of composite paste. The higher concentration of CNTs led to an increase in viscosity and a decrease in flowability of composite paste. The compressive strength data of each condition is shown in **Appendix B** in **Table B1-B2**.

The decrease in flowability when CNTs were increased can be explained by the high surface area and elongated tubular structure of CNTs. The presence of CNTs in composite paste led to entanglement and agglomeration with surrounding cement paste, which resisted flow and increased viscosity of cement paste [51].

The standard for flowability of cement composite paste, according to ASTM C109, ranges from 105% to 115% [44]. This range indicates that control, CX-1,1, and CX-2,1 conditions were within the standard ranges, which indicated appropriate transportation and placement applied to the mold, which made them suitable for use in construction work [52].

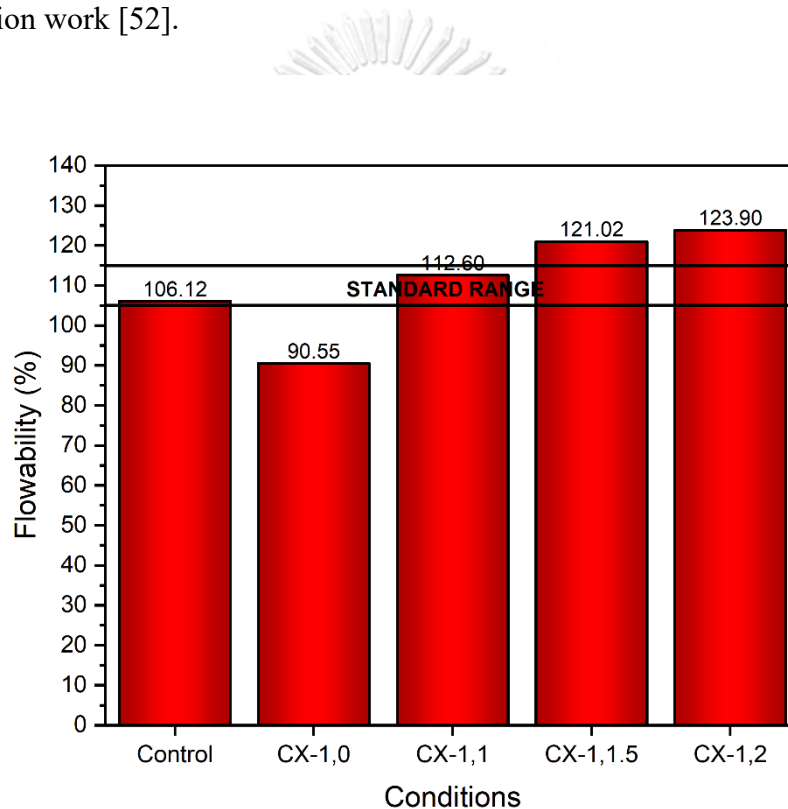


Figure 29 Flowability of CNT/Cement composite paste with varied TX-100 concentration

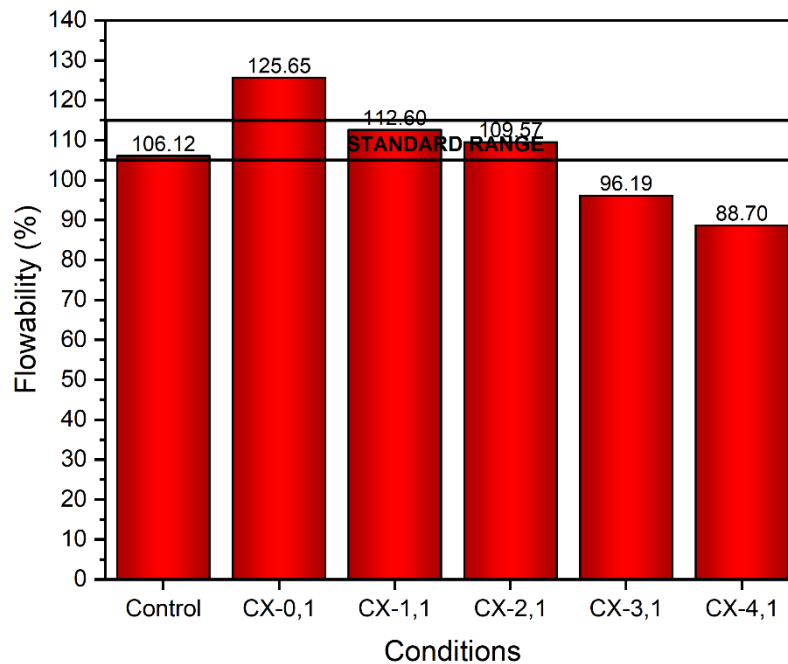


Figure 30 Flowability of CNT/Cement composite paste with varied CNTs: TX-100 concentration

4.4 Characterization of CNT dispersion in CNT/Cement composite

4.4.1 Bulk surface property of CNT/Cement composite

Bulk surface property of CNT/Cement composite with addition of CNTs and Triton X-100 under different conditions is shown in **Fig. 31(a-c)**. Surface characteristics of the composites were analyzed using SEM. In the control conditions, the composite surface, which resulted from mixture of water and cement powder, exhibited a smooth surface, as shown in **Fig. 31(a)**. Similarly, composite condition with addition of 1g CNTs (CX-1,0) exhibited smooth surface characteristics similar to the control conditions, as shown in **Fig. 31(b)**. In contrast, addition of Triton X-100 within solution and mixed with cement to composite resulted in porous surface, which can be attributed to air bubbles that formed during the mixing period, as shown in **Fig. 31(c)**. Appearance of pores on surface of the composite under Triton X-100 condition was caused by addition of Triton X-100 to water. This addition led to a decrease in surface tension, which can be measured by Zeta potential [50]. A decrease in surface

tension allowed air molecules to easily penetrate liquid. When Triton X-100 solution is mixed with cement powder to form cement paste, air molecules easily penetrate cement paste due to low surface tension, which led to formation of bubbles. These air bubbles within cement paste transformed into pores as cement underwent hydration process and solidified [53].

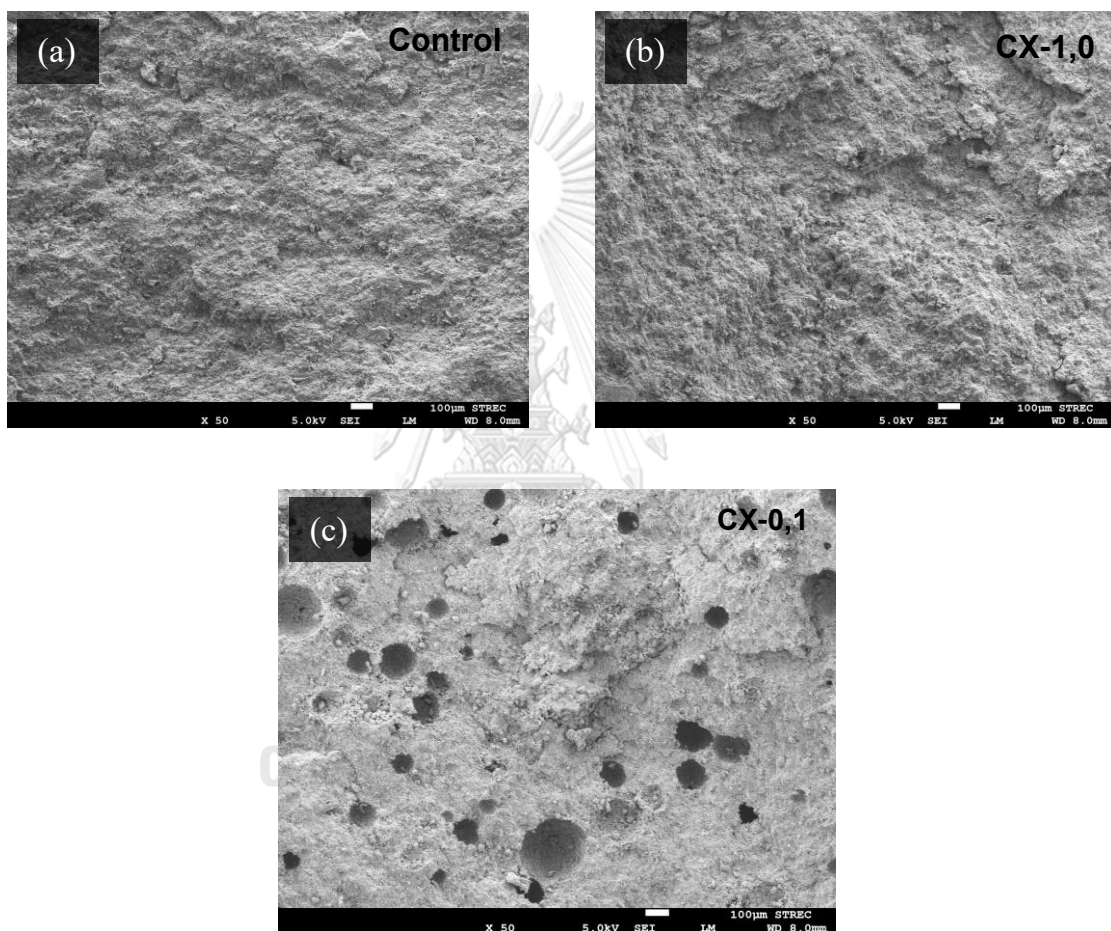


Figure 31 SEM image of morphology of CNT/Cement composite (a) control, (b) CX-1,0, (c) CX-0,1

Surface morphology of CNT/cement composite with 1g of CNTs and varying amounts of Triton X-100 is shown in **Fig. 32(a-c)**. CNT/Cement composite samples with addition of Triton X-100 conditions led to formation of porous surface in composite. Moreover, from naked-eye observation, an increase in the amount of Triton X-100 led to a higher porosity area of the composite. An increase in amount of Triton X-100 for dispersion of CNTs in suspension resulted in a decrease in surface tension. When mixed with cement to form cement paste, this led to more accessible penetration of air into cement paste, which formed bubbles that transformed into more pores after cement hydration process [53].

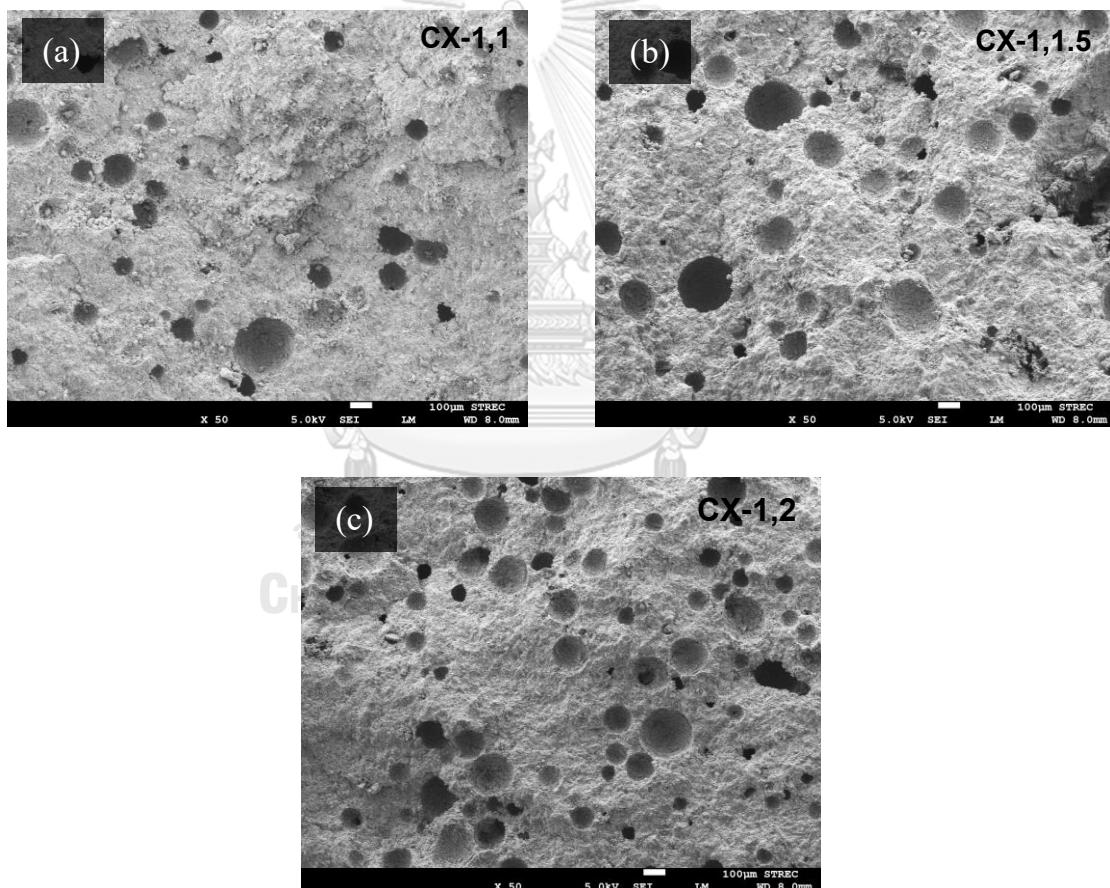


Figure 32 SEM image of morphology of CNT/Cement composite (a) CX-1,1, (b) CX-1,1.5, (c) CX-1,2

The morphology of CNT/Cement composite with addition of CNTs and a fixed amount of Triton X-100 at 1 g is shown in **Fig. 33(a-c)**. An increase in amount of CNTs in composite resulted in a decrease in porosity of composite. An increase in amount of CNTs in composite led to a decrease in porosity of composite. This can be attributed to absorption of Triton X-100 through addition of CNTs in suspension, which reduced the remaining Triton X-100 molecules in water phase. A decrease in Triton X-100 molecules in water resulted in an increased surface tension of suspension, which led air difficult to penetrate in cement paste and forming pores after hydration process.

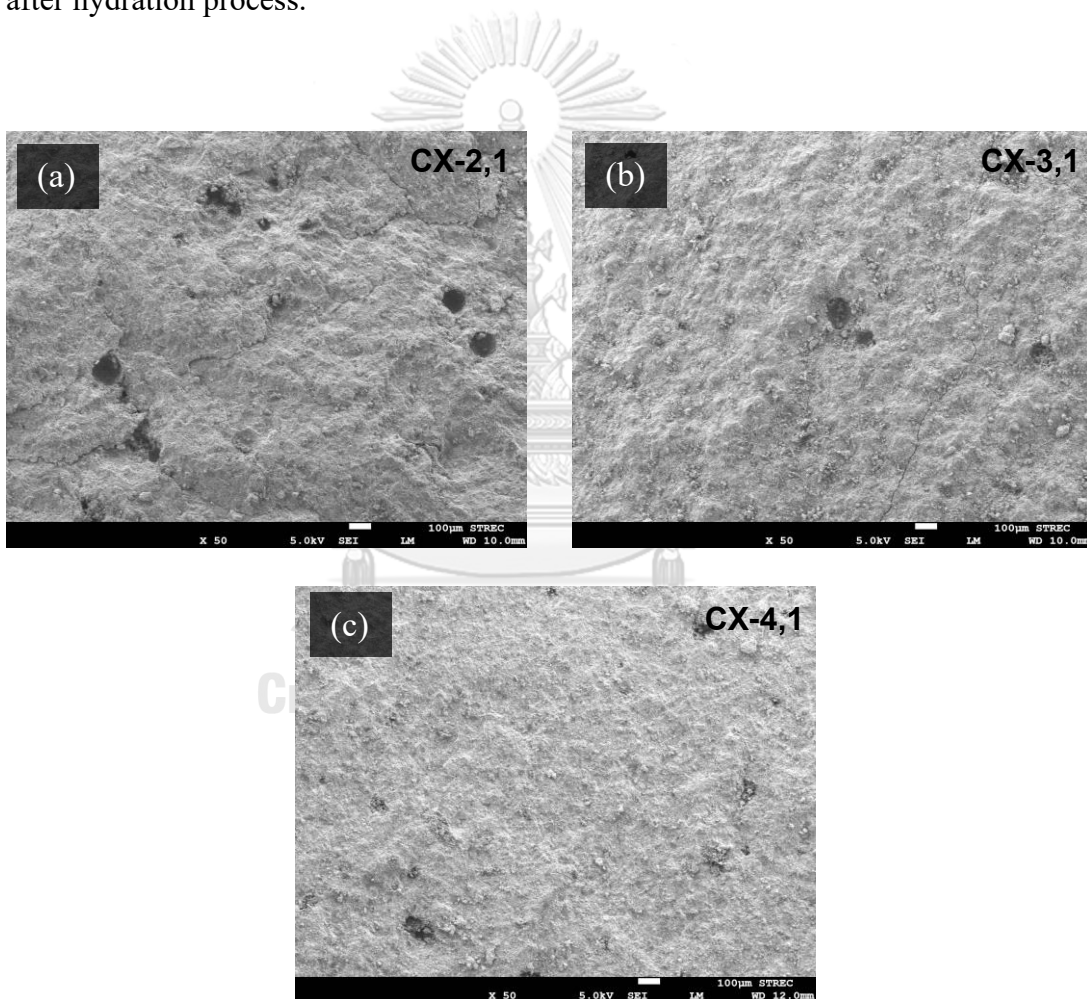


Figure 33 SEM image of morphology of CNT/Cement composite (a) CX-2,1, (b) CX-3,1, (c) CX-4,1

4.4.2 Porosity and water absorption of CNT/Cement composite

Porosity or volume of permeable voids of CNT/Cement composite was determined following ASTM C642 standard test method [46]. Porosity was determined by measuring water absorption of the composite, which represented amount of water that could be absorbed into composite structure. Porosity was calculated using water absorption data according to equation provided in ASTM C642. (**equations 12 and 13**). Results of porosity and water absorption of CNT/Cement composite for different Triton X-100 and CNT conditions are shown in **Figs. 34-35**.

Porosity and water absorption of CNT/Cement composite with varied TX-100 concentrations are shown in **Fig. 34**. Porosity and water absorption of control conditions were measured to be $32.11 \pm 0.36\%$ and $18.56 \pm 0.29\%$, respectively. However, condition with addition of CNTs without Triton X-100 (CX-1,0) resulted in an increase in porosity and water absorption to $32.47 \pm 0.60\%$ and $19.36 \pm 0.36\%$, respectively. In addition, condition with addition of 1g of CNTs with 1g of Triton X-100 (CX-1,1) resulted in an increase in porosity and water absorption to $32.81 \pm 0.19\%$ and $20.88 \pm 0.28\%$, respectively. Similarly, conditions with an increase in amount of Triton X-100 to 1.5 g and 2 g conditions (CX-1,1.5 and CX-1,2) resulted in an increase in porosity and water absorption. An increase in porosity and water absorption in condition of CNT addition was caused by self-aggregation of CNTs within composite [54]. Similar to porosity area observed in SEM results, an increase in porosity and water absorption with addition of Triton X-100 condition can be attributed to presence of remaining Triton X-100 molecules in suspension due to absorption of CNTs. This presence of Triton X-100 contributed to formation and an increase in bubble formation during the mixing period, which ultimately transformed into porosity after hydration process [53].

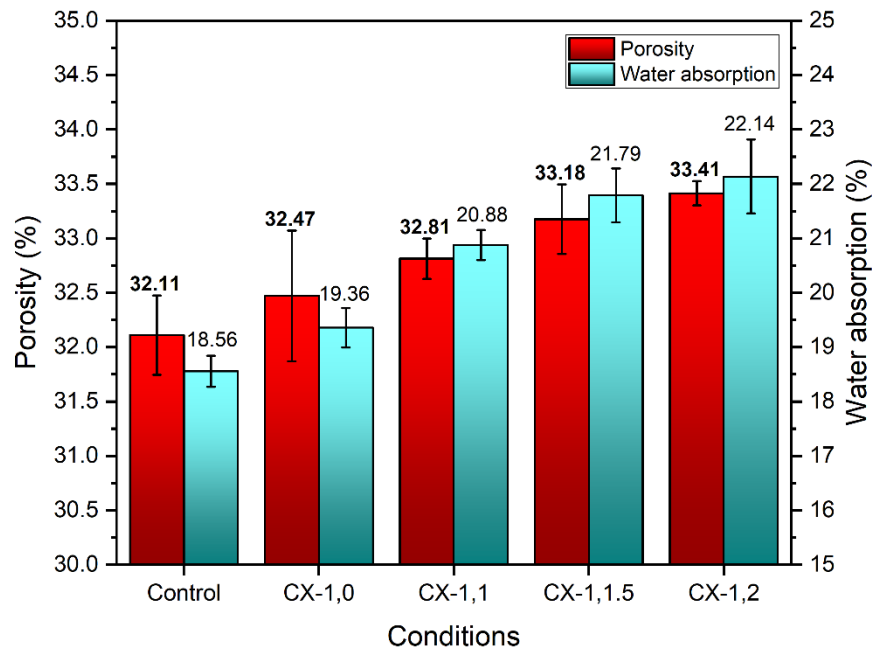


Figure 34 Effect of TX-100 concentrations on porosity and water absorption

Porosity and water absorption of addition of CNTs ranging from 0 g to 4 g, with a fixed amount of Triton X-100 at 1 g, are shown in **Fig. 35**. Addition of Triton X-100 (CX-0,1) also led to increased porosity and water absorption, which measured $33.54 \pm 0.46\%$ and $21.64 \pm 0.51\%$, respectively. These bubbles create voids or empty spaces within the composite, which allows water to penetrate and be absorbed into porous structure. As a result, porosity of CNT/Cement composite increased. However, an increase in amount of CNTs in composite led to decreased porosity and water absorption. Specifically, porosity and water absorption decreased from $32.81 \pm 0.19\%$ and $20.88 \pm 0.28\%$ in 1 g CNT condition (CX-1,1) to $32.44 \pm 0.74\%$ and $19.08 \pm 0.64\%$ in 4 g CNT condition (CX-4,1). These results can be explained similarly to porosity observed in condition with adding 1 g of CNTs with addition of Triton X-100 (CX-1,1). An increase in CNTs led to absorption of more Triton X-100 molecules, which resulted in a decrease in concentration of Triton X-100 in suspension. Consequently, formation of bubbles during mixing period was reduced. The porosity

and water absorption data of each condition are shown in **Appendix C** in **Table C1-C2**.

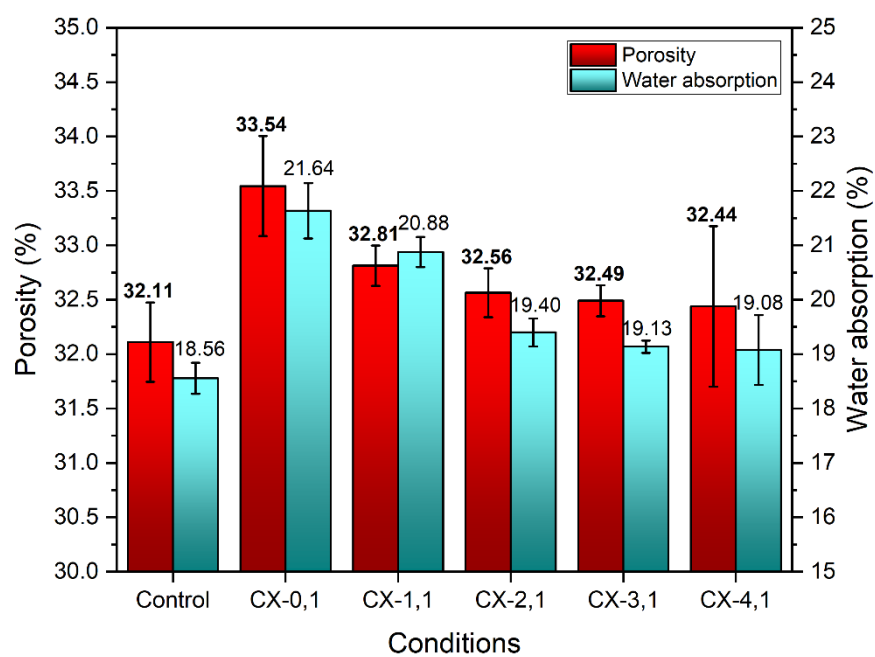


Figure 35 Effect of CNTs: TX-100 concentrations on porosity and water absorption

4.4.3 Microstructure of CNT/Cement composite

Microstructures of bare cement specimen without CNTs after curing for 28 days are shown in **Fig. 36 (a-b)**. The microstructures of typical cement specimen revealed different types of cement hydration products that formed after mixing cement with water and undergoing curing process. Hexagonal plate structures indicate portlandite or calcium hydroxide ($\text{Ca}(\text{OH})_2$), which was a result of the hydration reaction. Additionally, other cement hydration products are present. Needle crystal structures indicated ettringite or calcium aluminate ($3\text{CaO}\cdot\text{Al}_2\text{O}_3$). Additionally, short fibers or needles indicated calcium silicate hydrate ($\text{CaO}\cdot\text{SiO}_2\cdot\text{H}_2\text{O}$) [55].

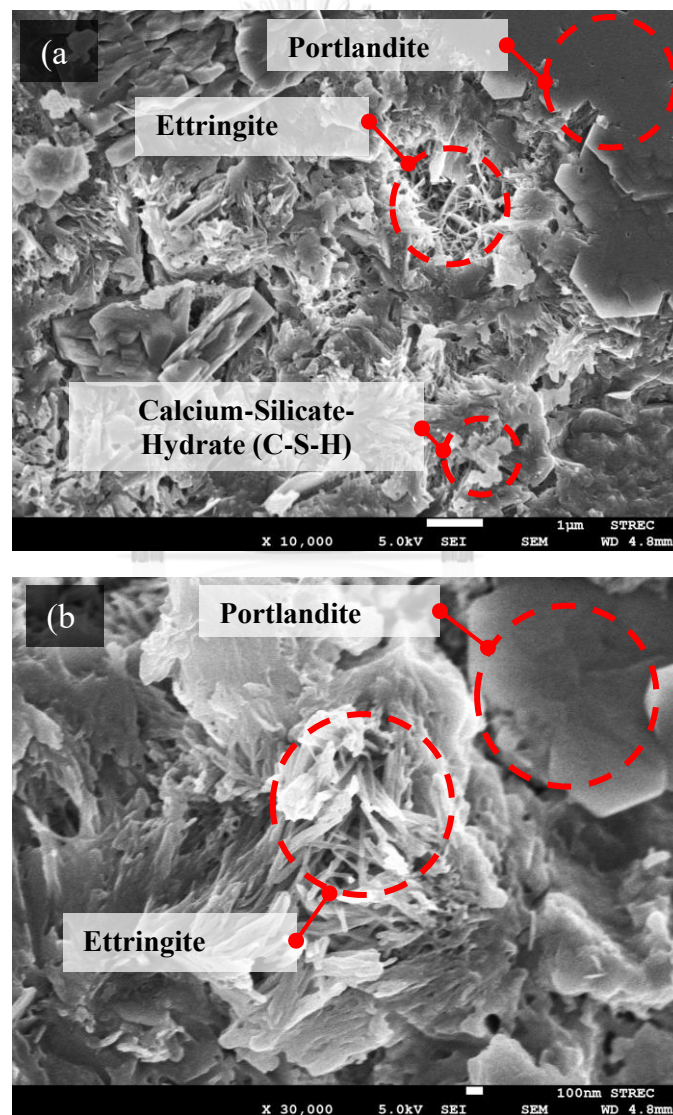


Figure 36 SEM images of cement paste after 28 days of curing time
(a) 10,000x, (b) 30,000x

4.4.4 Dispersion of CNTs in CNT/Cement composite

Dispersion of CNTs in CNT/Cement composite with different Triton X-100 concentrations is shown in **Fig 37(a-d)**. Through naked-eye observation, in case of 1 g of CNTs without Triton X-100 (CX-1,0) condition, CNTs exhibited agglomeration and bundling within composite due to hydrophobic properties of CNTs [56]. Agglomerated CNTs can be observed, as shown in **Fig 37(a)**. However, composite condition with addition of Triton X-100 at concentrations of 1 g, 1.5 g, and 2 g, CNTs in composite exhibited improved dispersion and less agglomeration, which compared to without Triton X-100 condition, as shown in **Fig 37(b-d)**. This indicates that Triton X-100 contributes to dispersion of CNTs within composite matrix, which led to more uniform distribution of CNTs. Additionally, SEM images of CNT dispersion within in composite in 5 different areas of each condition are presented in **Appendix F**.

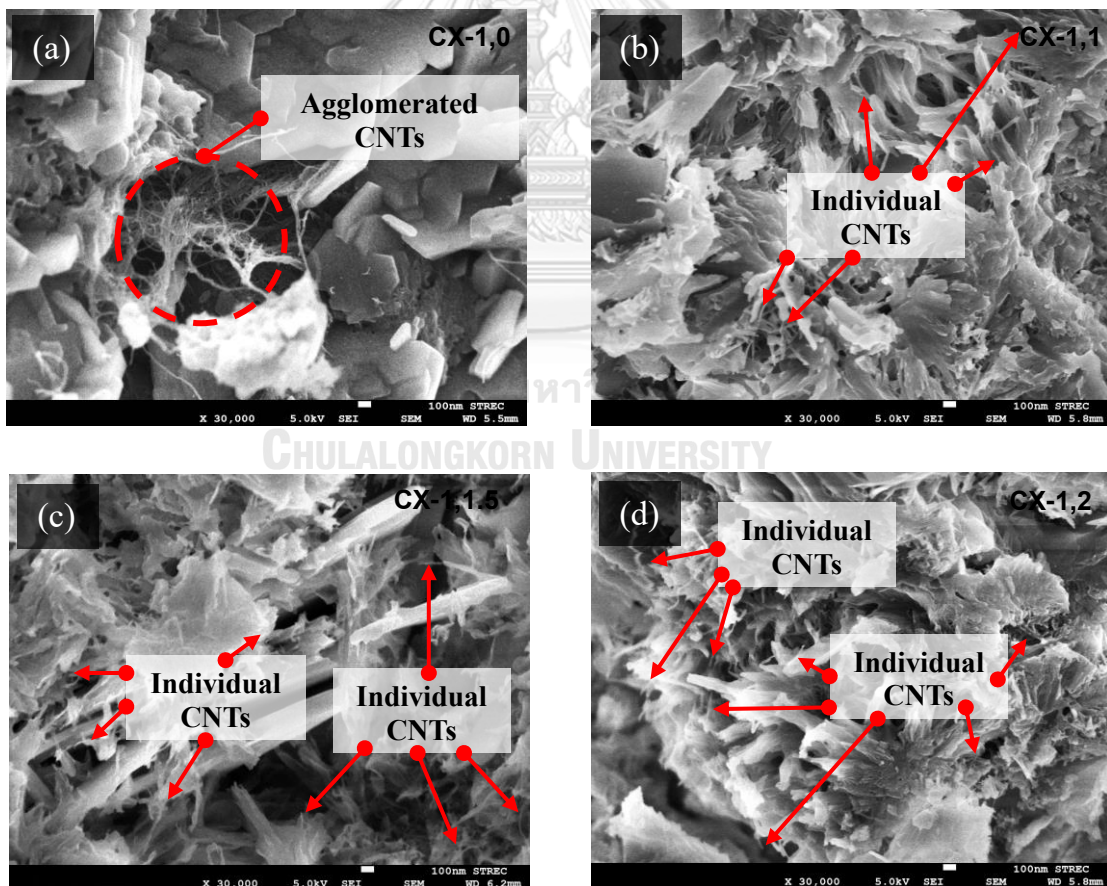


Figure 37 Dispersion of CNTs in composites with varied Triton X-100 conditions

(a) CX-1,0, (b) CX-1,1, (c) CX-1,1.5, (d) CX-1,2

The dispersion of CNTs with the addition of CNTs ranging from 2 g to 4 g, using a fixed amount of Triton X-100 at 1 g, is shown in **Fig 38(a-c)**. An increase in the amount of CNTs to 2 g in condition CX-2,1 showed the dispersion of individual CNTs, as shown in **Fig 38(a)**. However, adding higher amounts of CNTs (3 g and 4 g) in conditions CX-3,1 and CX-4,1 resulted in increased agglomeration and lower dispersion of CNTs, as shown in **Fig 38(b-c)**. These results can be explained by an insufficient amount of Triton X-100 to absorb each individual CNT, which is responsible for dispersing CNTs. Consequently, when higher amounts of CNTs were added with a fixed amount of Triton X-100, CNTs tended to agglomerate instead of being well dispersed. The limited availability of Triton X-100 molecules hindered their ability to disperse CNTs effectively, leading to agglomeration.

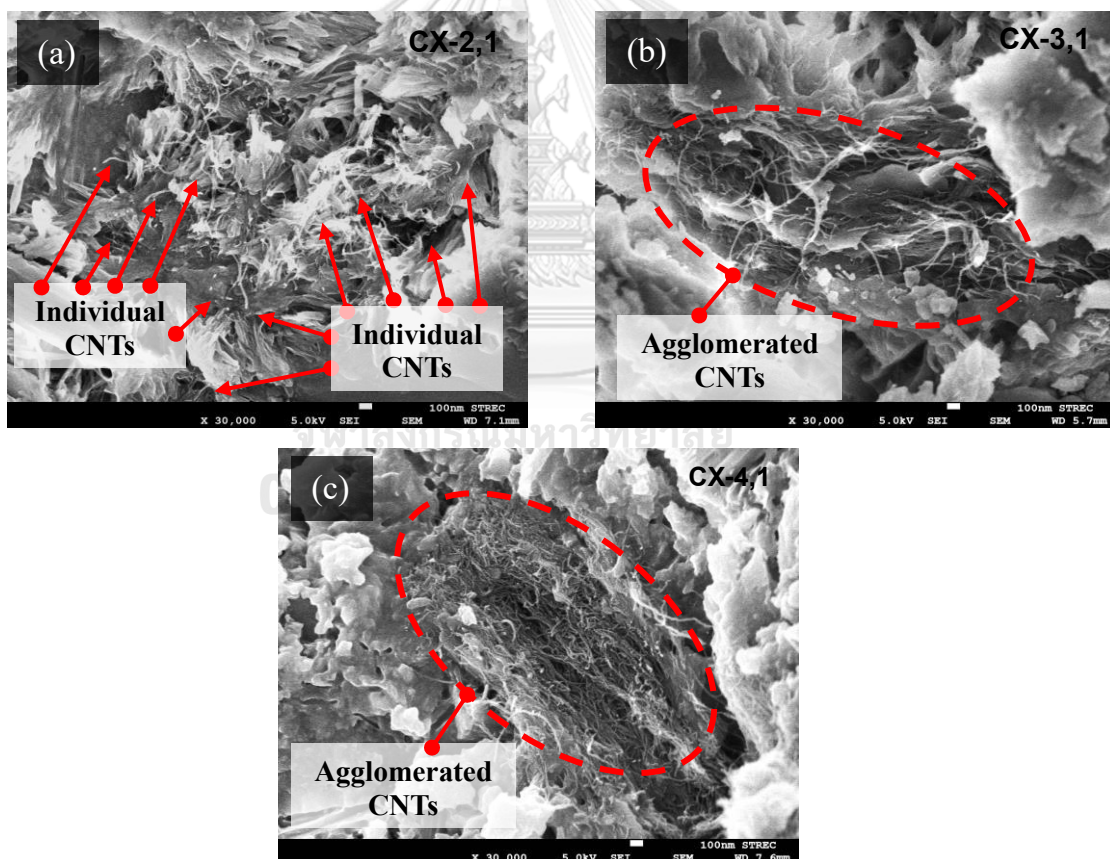


Figure 38 Dispersion of CNTs in composite with varied ratio CNTs: TX-100 from 2:1 to 4:1 (a) CX-2,1, (b) CX-3,1, and (c) CX-4,1

4.4.5 Image processing analysis of CNT dispersion

4.4.5.1 Appropriate gridline for CNT dispersion analysis

Analysis of CNT dispersion was conducted using gridlines with SEM images [57]. SEM image of CNT dispersion in the CX-2,1 condition was selected to find a suitable gridline for analyzing CNT dispersion. The results of CNT dispersion for CX-2,1 condition picture 1 at different grid conditions are shown in **Fig. 39**. CNT dispersion value for 6×6 grid lines was -0.333, which indicated CNT tended to agglomerate within composite. However, with an increase in grid line conditions, dispersion value also increased rapidly and gradually stabilized at the 24×24 condition, which reached a value of 0.047. Subsequently, dispersion values remained constant at 0.049 in the 30×30 condition and 36×36 condition.

Based on these results, the 24×24 grid line condition, which indicated the first stable value for CNT dispersion, was chosen for further analysis of CNT dispersion under different conditions.

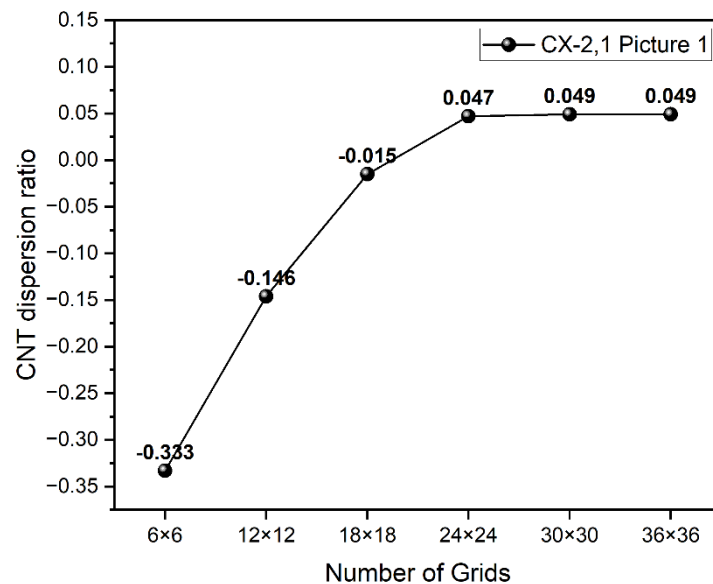


Figure 39 CNT dispersion ratio with CX-2,1 condition picture 1 different number of grid.

4.4.5.2 Analyses of CNT dispersion with different Triton X-100 in CNT/Cement composite

After selecting a 24×24 grid line condition for CNT dispersion analysis, analysis of CNT dispersion from SEM image was further analyzed with other experimental cases. For each condition, CNT dispersion was analyzed from 5 pictures, which were selected from 5 different areas and then calculated and averaged values. The dispersion results of each picture are presented in **Appendix G**.

CNT dispersion ratio values under various TX-100 conditions, which included 0 g, 1 g, 1.5 g, and 2 g, with 1 g of CNTs, are presented in **Fig. 40**. Dispersion value of CX-1,0 (without TX-100) was -0.329 ± 0.260 , which indicated significant CNT agglomeration within composite, with more agglomerated CNT cells than dispersion cells. However, dispersion value increased with addition of Triton X-100, which reached 0.027 ± 0.018 , 0.024 ± 0.01 , and 0.044 ± 0.034 in CX-1,1, CX-1,1.5, and CX-1,2 condition respectively. This increase in dispersion value suggested better dispersion of CNTs within composite with addition of Triton X-100, where a dispersion value greater than 0 implied that the number of individual CNT cells within composite was higher than agglomerated CNT cells.

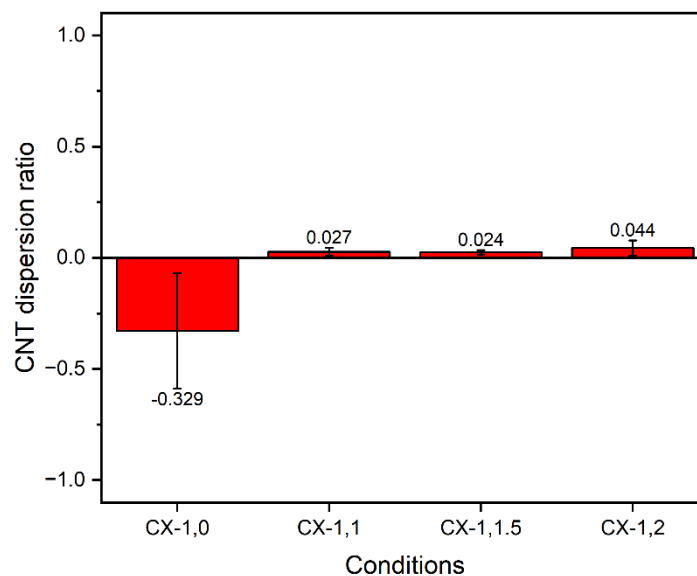


Figure 40 CNT dispersion ratio within composite with varied Triton X-100

CNT dispersion values in composites with varying CNT: Triton X-100 ratios from 1:1 to 4:1 are shown in **Fig. 41**. As the amount of CNTs increased, dispersion values showed notable changes. In the case of CX-2,1 condition, dispersion value was 0.073 ± 0.026 , which was higher than that of the CX-1,1 condition. This indicated better dispersion of CNTs and a higher amount of individual CNTs compared to CX-1,1. However, when the amount of CNTs was increased to 3 g and 4 g in CX-3,1 and CX-4,1 conditions, dispersion values decreased to -0.461 ± 0.244 and -0.519 ± 0.215 , respectively. This decrease in dispersion value to lower than 0 resulted from the high amounts of CNTs that agglomerated within composite, which lacked Triton X-100 necessary for dispersion of CNTs in composite.

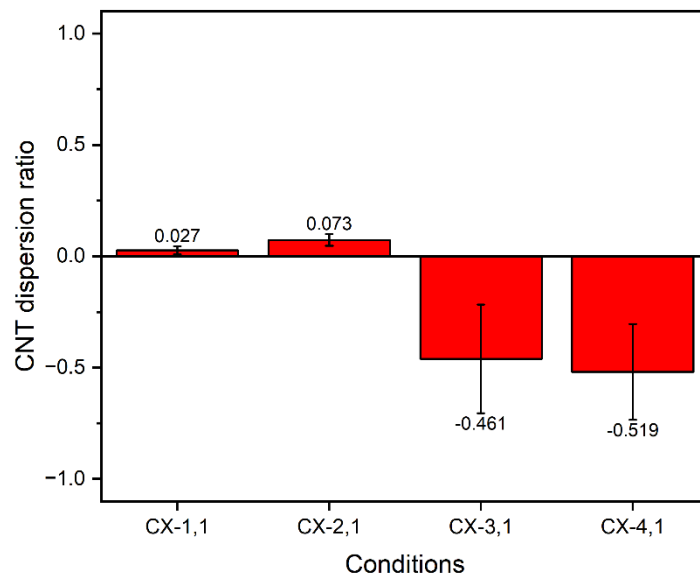


Figure 41 CNT dispersion ratio within composite with varied CNT: TX-100

4.4.6 Compressive strength and bulk density of CNT/Cement composite

Compressive strength and bulk density of CNT/Cement composite were evaluated with varied Triton X-100 concentrations and varied ratios of CNTs-to-Triton X-100 at a curing time of 7 days. Measurements were conducted on three samples for each condition, which followed the ASTM C109 standard [44]. The average values obtained from these measurements are presented in **Figs. 42-43**.

Compressive strength and bulk density of CNT/Cement composite with varied amounts of Triton X-100 at a curing time of 7 days are shown in **Fig. 42**. In control conditions, compressive strength and bulk density of CNT/Cement composite were measured to be 44.13 ± 2.64 MPa and 1.95 ± 0.01 g/cm³, respectively. However, condition with addition of 1 g of CNTs without Triton X-100 (CX-1,0) resulted in a decrease in both compressive strength and bulk density to 43.72 ± 5.43 MPa and 1.91 ± 0.02 g/cm³, respectively. This decrease can be attributed to agglomeration of CNTs within composite structure, which led to an increase in porosity and a decrease in density [54]. However, agglomeration of CNTs within composite resulted in inability to distribute force, and cracks started from agglomerate area, which reduced compressive strength of composite [58, 59].

However, in condition where 1 g of CNTs was added with 1 g of Triton X-100 (CX-1,1), compressive strength and bulk density decreased to 38.95 ± 0.93 MPa and 1.79 ± 0.02 g/cm³, respectively. These results can be explained by an increase in porosity attributed to addition of Triton X-100 to dispersion of CNTs in suspension. A decrease in surface tension facilitated entry of air, which led to formation of pores and resulted in a decrease in density of composite [50]. Additionally, presence of pores within composite led to a decrease in compressive strength [59].

Similarly, when Triton X-100 was increased to 1.5 g and 2 g in CX-1,1.5 and CX-1,2 conditions, compressive strength and bulk density decreased to 33.78 ± 0.71 MPa and 1.70 ± 0.03 g/cm³, and 28.27 ± 8.73 MPa and 1.63 ± 0.04 g/cm³, respectively. This decrease in compressive strength and density with an increase in amount of Triton X-100 can be attributed to an increase in porosity of composite. The higher amount of Triton X-100 led to increased void spaces within composite, which resulted in a reduction in bulk density and structural integrity. Consequently,

composite became more susceptible to failure under compressive loads, which led to a decrease in compressive strength.

Overall, results of this study showed that Triton X-100 had a significant influence on compressive strength of CNT/Cement composite. CX-1,1 condition, where 1 g of CNTs was added with 1 g of Triton X-100, exhibited improved dispersion of CNTs and the lowest porosity compared to other Triton X-100 conditions, which increased compressive strength.

Based on these findings, the CX-1,1 condition was selected as the baseline condition for varying ratios between CNTs and Triton X-100 in the subsequent conditions. This decision was based on the observed enhancements in CNT dispersion and porosity in the CX-1,1 condition, contributing to the improved compressive strength of the composite.

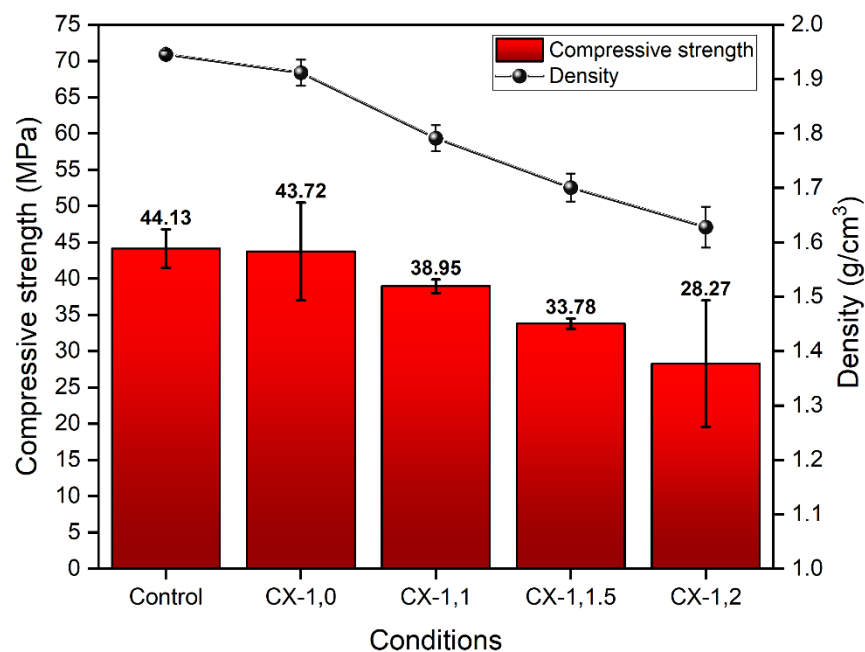


Figure 42 Effect of TX-100 concentrations on compressive strength and density of composite at curing time of 7 days

After evaluating different Triton X-100 conditions, CX-1,1 condition was selected as base condition for investigating effect of adding CNTs on compressive strength. Compressive strength of CNT/Cement composite was examined using different CNTs: Triton X-100 ratios ranging from 0:1 to 4:1, and results are presented in **Fig 43**. In condition with addition of Triton X-100 (CX-0,1) also led to a decrease in compressive strength and bulk density to 34.67 ± 4.05 MPa and 1.72 ± 0.04 g/cm³. This decrease can be explained by an increase in porosity of composite that occurred during mixing process with Triton X-100 [60].

However, in condition with an increase in amount of CNTs from 1 g to 2 g (CX-2,1) in CNT/Cement composite resulted in an increase in both compressive strength and bulk density. Compressive strength was measured to be 46.35 ± 1.8 MPa, which was higher than control condition by 5.04% and higher than CX-1,1 condition by 19.00%. Additionally, bulk density of CX-2,1 condition was measured to be 1.93 ± 0.00 g/cm³, which was higher than CX-1,1 condition. These results were consistent with SEM images and porosity results, which showed a decrease in porosity with an increase in CNT content. Furthermore, SEM image of CX-2,1 condition demonstrated a good dispersion of CNTs within composite structure. Therefore, improved compressive strength and bulk density in CX-2,1 condition can be attributed to reduced porosity and effective dispersion of CNTs [59, 60].

On the other hand, when amount of CNTs was further increased to 3 g and 4 g (CX-3,1 and CX-4,1), a decrease in compressive strength and bulk density was observed. Compressive strength values were measured to be 42.94 ± 1.45 MPa and 39.43 ± 0.93 MPa, respectively. This decrease in compressive strength can be explained by agglomeration of CNTs, which was observed in SEM images and resulted in a disorder in composite structure. Consequently, the higher content of CNTs led to a decrease in compressive strength of composite [60].

In summary, an increase in CNT content up to 2 g (CX-2,1) resulted in improved compressive strength and bulk density of CNT/Cement composite. This improvement can be attributed to the reduction in porosity and effective dispersion of CNTs of composite material. However, further increases in CNT content (3 g and 4 g)

led to a decrease in compressive strength due to agglomeration of CNTs, which resulted in structural disorder within composite [58, 61-63].

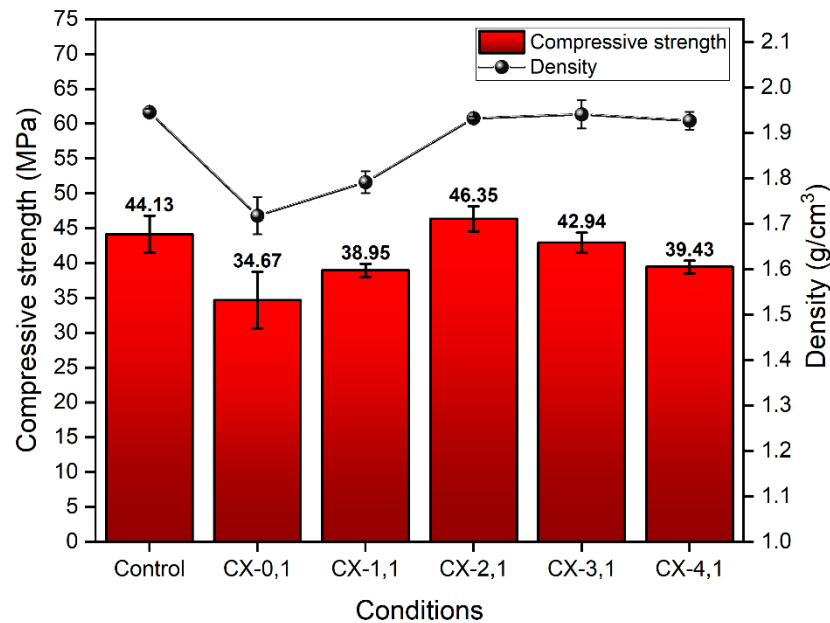


Figure 43 Effect of CNTs: TX-100 concentration on compressive strength and density of composite at curing time of 7 days

4.4.7 Effect of curing time on compressive strength of CNT/Cement composite

To investigate the effect of hydration reaction duration on compressive strength, compressive strength of CNT/Cement composite was measured at different curing times. Compressive strength results of CNT/Cement composite at different curing times, which included 3 days, 7 days, 14 days, and 28 days, are shown in **Fig. 44**.

Compressive results showed that compressive strength consistently increased with longer curing times, which can be attributed to the gradual hydration reaction that occurred between cement and water over time. During hydration, water molecules reacted with cement powder, which led to the formation of various hydration products such as calcium silicate hydrate (C-S-H) gel, calcium hydroxide (CH), and ettringite.

The formation of hydration products contributed to the development of strength in composite. C-S-H gel was the primary binder in cement paste and responsible for enhancing mechanical properties, which included compressive strength. As hydration reaction progressed, C-S-H gel formed a dense and interconnected network, which enhanced strength of composite [64].

Furthermore, formation of calcium hydroxide and ettringite crystals also contributed to improve strength. Calcium hydroxide provided additional bonding and contributed to an increase in strength of composite. Ettringite crystals, which formed by reaction of calcium aluminate compounds with sulfate ions, contributed to strength properties of composite [65].

From all conditions, CX-2,1 demonstrated the highest compressive strength value at a curing time of 28 days, which was 63.69 ± 1.48 MPa. This value was significantly higher than compressive strength of control condition by 21.77 %, which was 52.30 ± 3.49 MPa. Triton X-100 contributed to effective dispersion of CNTs, which led to enhanced compressive strength in composite. The compressive strength and bulk density data of each condition are shown in **Appendix D** in **Table D1-D9**.

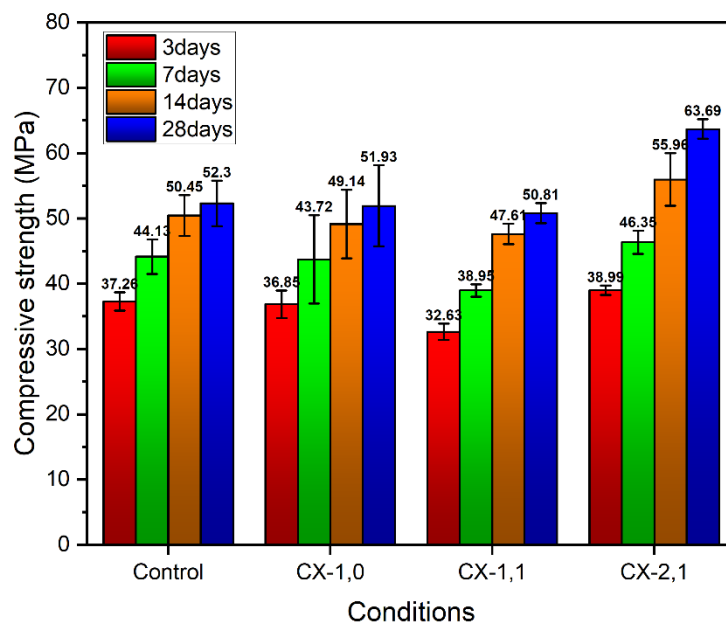


Figure 44 Effect of curing time on compressive strength of CNT/Cement composite

4.4.8 Electrical conductivity of CNT/Cement composite

Electrical conductivity of CNT/Cement composite was measured using a digital multimeter to determine the resistivity. Resistivity values were converted to conductivity values. For each condition, three samples were measured, and averaged values were reported. Average conductivity values of CNT/Cement composite with different conditions at a curing time of 28 days are presented in **Figs. 45-46**.

Electrical conductivity of CNT/Cement composite with varied amounts of Triton X-100 is shown in **Fig. 45**. In control condition, electrical conductivity value was measured to be $529.13 \pm 13.75 \mu\text{S/m}$. However, addition of 1g of CNTs (CX-1,0) resulted in an increased electrical conductivity to $687.48 \pm 27.72 \mu\text{S/m}$, which was 29.93% higher than control condition. This increase in conductivity can be attributed to unique structure and arrangement of carbon atoms in CNTs, which exhibited high electron mobility and allowed efficient transport of electric charges [45].

On the other hand, when 1g of CNTs and 1g of Triton X-100 were added (CX-1,1), the conductivity value increased to $670.56 \pm 35.84 \mu\text{S/m}$, which was 26.73% higher than control condition but still lower than CX-1,0 condition. These results indicated that the addition of CNTs contributed to an increase in conductivity. However, conductivity was still lower than in CX-1,0 condition due to an increase in porosity, which hindered conductive pathway [66].

Furthermore, when amount of Triton X-100 was increased to 1.5g and 2g (CX-1,1.5 and CX-1,2), conductivity values were $657.08 \pm 31.48 \mu\text{S/m}$ and $627.04 \pm 38.25 \mu\text{S/m}$, respectively, which were lower than CX-1,0 and CX-1,1. A decrease in conductivity in CX-1,1.5 and CX-1,2 conditions can be attributed to an increase in porosity in composite. A decrease in electrical conductivity within composite, due to addition of Triton X-100 in suspension can be explained by presence of pores. This presence led to a reduction in uniformity of CNTs within composite, which tended towards agglomeration. Additionally, the presence of voids acted as a barrier for electron transport, which made it difficult for electrons to move within composite. This ultimately resulted in a reduction in electrical conductivity [66, 67].

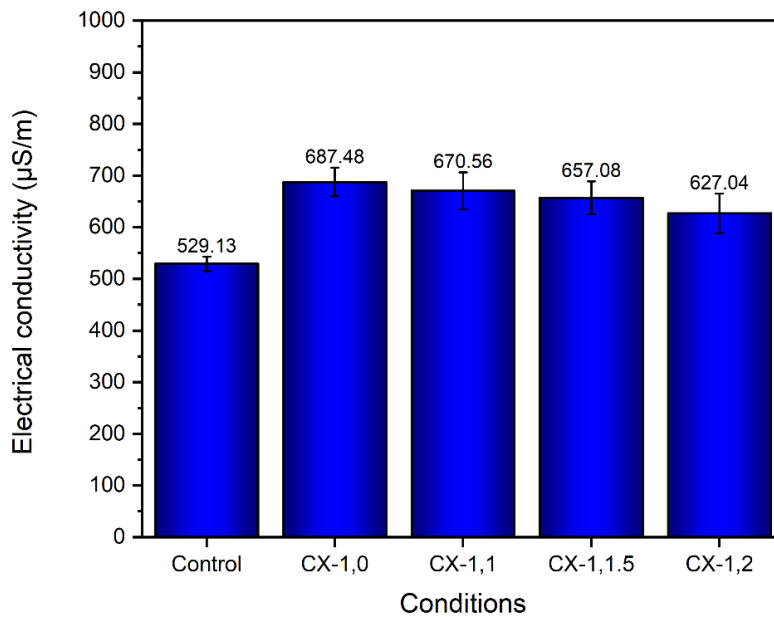


Figure 45 Effect of TX-100 concentrations on electrical conductivity of composite at curing time of 28 days

Electrical conductivity of CNT/Cement composite with varied ratios between CNTs to Triton X-100 is shown in **Fig. 46**. Addition of 1g of Triton X-100 (CX-0,1) led to a decrease in electrical conductivity to $515.56 \pm 24.32 \mu\text{S/m}$, which was 2.63% lower than control condition. This decrease in conductivity in the CX-0,1 condition can be explained by an increase in air voids during mixing process, which was observed in porosity results. Similarly, with the addition of Triton X-100, the presence of air voids within composite disrupted continuity of electron flow, which resulted in a decrease in electrical conductivity. Thus, electrical conductivity was reduced in CX-0,1 condition [67].

When the amount of CNTs was increased from 0 g to 4 g while keeping Triton X-100 at 1 g (CX-4,1 condition), electrical conductivity increased to $763.56 \pm 17.60 \mu\text{S/m}$, which was 44.30% higher than control condition. This increase in conductivity can be attributed to presence of a higher number of conductive pathways from addition of CNTs, which allowed transport of electric charges within composite [68, 69].

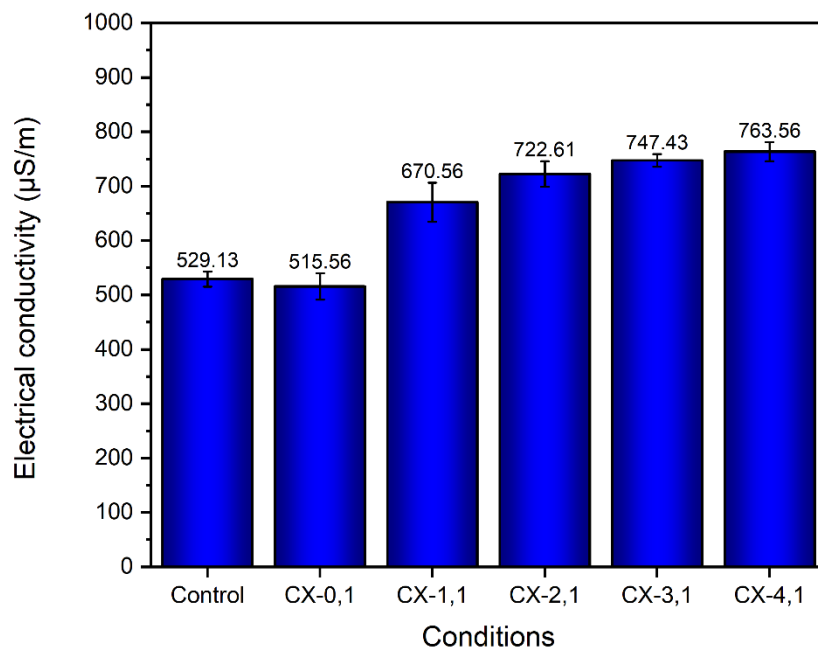


Figure 46 Effect of CNTs: TX-100 ratios on electrical conductivity of composite at curing time of 28 days

4.4.9 Effect of curing time on electrical conductivity of CNT/Cement composite

When CNT/Cement composite samples were cured for 3, 7, 14, and 28 days, electrical conductivity was changed with different curing times, as shown in **Figs. 47-48**. Electrical conductivity of CNT/Cement composite samples decreased with an increase in curing time from 3, 7, 14, to 28 days. This decrease in electrical conductivity can be explained by hydration reaction that occurred during curing process. Water reacts with cement composition to form reaction products. These reaction products typically have lower electrical conductivity than water.

Additionally, the loss of water during the curing process further contributed to a decrease in electrical conductivity. During hydration process and water evaporating, amount of water decreased, which led to a decrease in electrical conductivity [70]. This water loss resulted in a denser composite structure that reduced water filled in pores, which restricted the movement of electric charges and decreased conductivity. Therefore, longer curing time resulted in lower electrical conductivity of CNT/Cement composite due to both hydration reaction and water loss during the

curing process [71, 72]. The electrical conductivity data of each condition is shown in **Appendix E in Table E1-E9**.

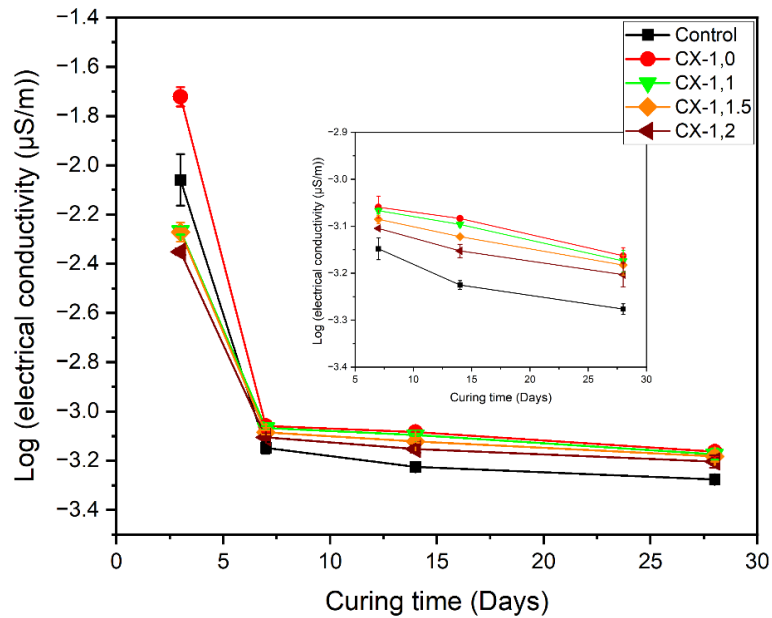


Figure 47 Effect of curing time on electrical conductivity of varied Triton X-100 concentrations

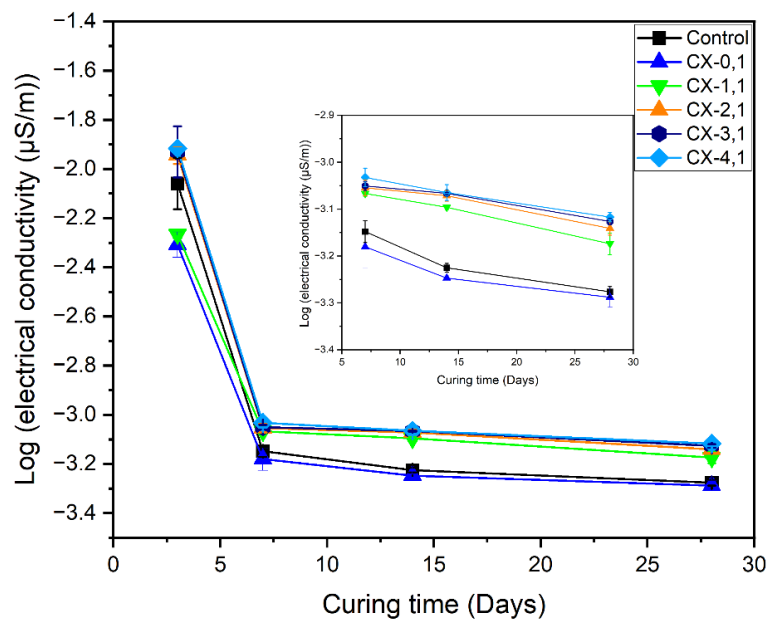


Figure 48 Effect of curing time on electrical conductivity of varied CNTs: TX-100 ratio conditions

CHAPTER 5

CONCLUSIONS AND RECOMMENDATIONS

5.1 Conclusions

Based on the experimental results, the following conclusions can be made.

- (1) An increase in the amount of Triton X-100 to 2 g with 1 g of CNTs was found to be an optimal value for enhancing CNT dispersion in water. This was evident from both the physical appearance and UV-vis spectra results, demonstrating the effectiveness of Triton X-100 in ensuring the proper dispersion of CNTs in suspension.
- (2) The addition of Triton X-100 enhanced the flowability of the composite paste. However, cement composite pastes with the addition of Triton X-100 exhibited bubble formation due to a reduction in surface tension, allowing air to easily penetrate and become entrapped within the composite paste. On the other hand, the addition of CNTs to the cement composite paste resulted in a reduction in the flow value due to the entanglement of CNTs with the surrounding cement paste. Flowability values of the composite paste under control, CX-1,1, and CX-2,1 conditions, which were 106.12%, 112.60%, and 109.57%, respectively, were within the standard range according to ASTM C109. These conditions can still be considered suitable for use in construction work.
- (3) The porosity of the composite increased with the addition of Triton X-100, resulting from air bubbles during the mixing period. However, the porosity of the composite decreased in conditions with an increase in CNT content and a fixed amount of Triton X-100 at 1 g due to an increase in surface tension resulting from CNT adsorption within the suspension.
- (4) Dispersion of CNTs within the cement composite was observed and characterized by SEM images. It was demonstrated that Triton X-100 helped in the dispersion of CNTs within the composite. However, the dispersion of CNTs decreased with the addition of 3 g and 4 g of CNTs

with 1 g of Triton X-100 due to insufficient Triton X-100 to aid in dispersion. The highest dispersion ratio in this study was observed in the CX-2,1 condition, which was attributed to effective dispersion resulting from the addition of Triton X-100.

- (5) Density of the cement composite tended to decrease with the addition of Triton X-100 from 1 g to 2 g while maintaining CNTs at 1 g. This decrease was attributed to the formation of porosity within the composite resulting from the addition of Triton X-100. However, in conditions with the addition of CNTs from 1 g to 4 g, while keeping Triton X-100 at 1 g, there was an increase in density.
- (6) Compressive strength decreased in the condition with the addition of Triton X-100, while keeping CNTs fixed at 1 g. This decrease was attributed to the presence of porosity. Similarly, in conditions with an increase in CNT content to 3 g and 4 g with fixed Triton X-100 at 1 g, there was a decrease in compressive value due to agglomeration of CNTs within the composite, leading to the initiation of cracks at agglomeration points. However, the highest compressive strength was observed in the CX-2,1 condition, at 63.59 ± 1.48 MPa at a curing time of 28 days, which was higher than the control condition by 21.77%. This was attributed to the good dispersion of CNTs, which helped in receiving strength force and resulted in low porosity within the composite.
- (7) The electrical conductivity reduced in conditions with varied Triton X-100 and fixed CNTs at 1 g due to the presence of pores within the composite, hindering the conductive pathway of electron transport. However, in conditions with varied CNTs from 1 g to 4 g and fixed Triton X-100 at 1 g, there was an increase in electrical conductivity resulting from an expanded conductive pathway, facilitating electron transport within the composite. The highest value of electrical conductivity was observed in the CX-4,1 condition at 763.56 ± 17.60 $\mu\text{S}/\text{m}$ at a curing time of 28 days, which was 44.30% higher than the control condition. This demonstrated the enhancing effect of CNTs on the electrical properties of the cement composite.

5.2 Remaining issues and recommendations for further investigation

In this work, Triton X-100 proved to be suitable for the dispersion of CNTs in suspension and cement composite. However, the issue of bubble formation resulting from the addition of Triton X-100 is crucial for the compressive strength and electrical conductivity properties of the composite. Therefore, future research should be conducted to address the bubble formation problem. Some research suggests the use of a defoamer to mitigate bubble formation in cement composite paste [66], leading to a decrease in porosity and an improvement in compressive and electrical conductivity properties. Additionally, a cement vibrator machine is a useful tool for achieving a homogeneous mixture of cement paste with water and other additives, helping to reduce the presence of air bubbles in the cement paste after the mixing process. In addition, a compressometer or extensometer is utilized to characterize stress and strain graph during the deformation of CNT/cement composite samples. This equipment helps determine the effect of CNT on the strength properties received within the cement composite.

APPENDIX A

Size distribution of CNT

Size distribution of CNTs was collected from SEM images of CNTs and analyzed by using Image J program. 200 tube diameters of CNTs were collected from 4 SEM images for analysis, as shown in **Figs. A1-A4** and **Table A1**.

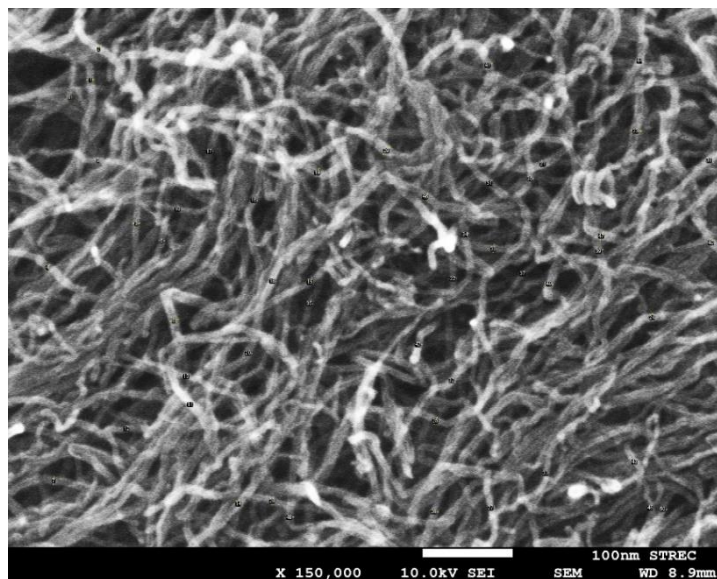


Fig. A1 1st SEM image of CNTs in 150,000 x (50 tube diameters were collected for size distribution using the ImageJ program)

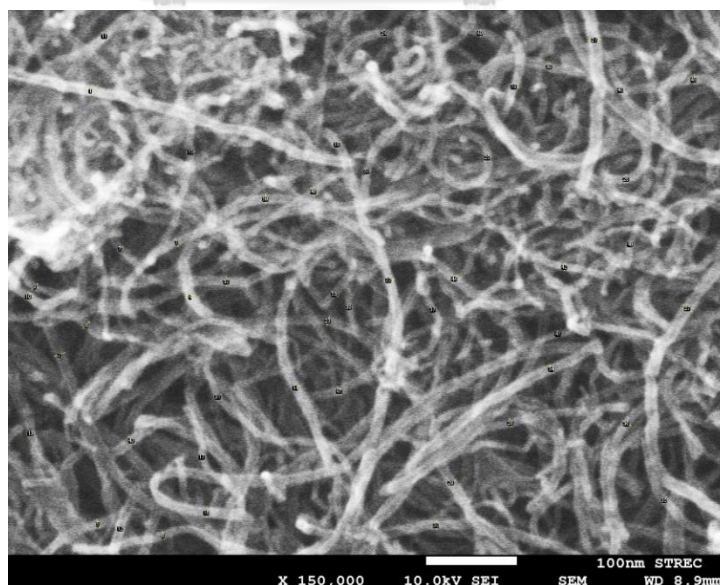


Fig. A2 2nd SEM image of CNTs in 150,000 x (50 tube diameters were collected for size distribution using the ImageJ program)

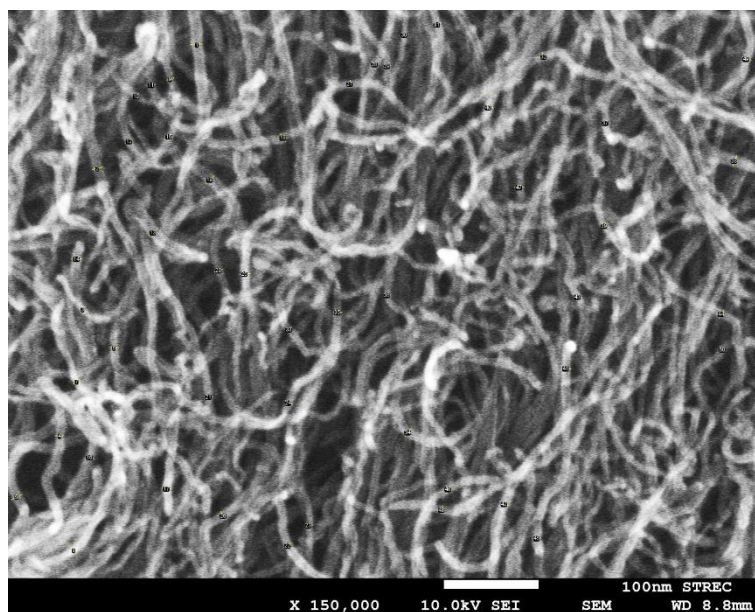


Fig. A3 3rd SEM image of CNTs in 150,000 x (50 tube diameters were collected for size distribution using the ImageJ program)

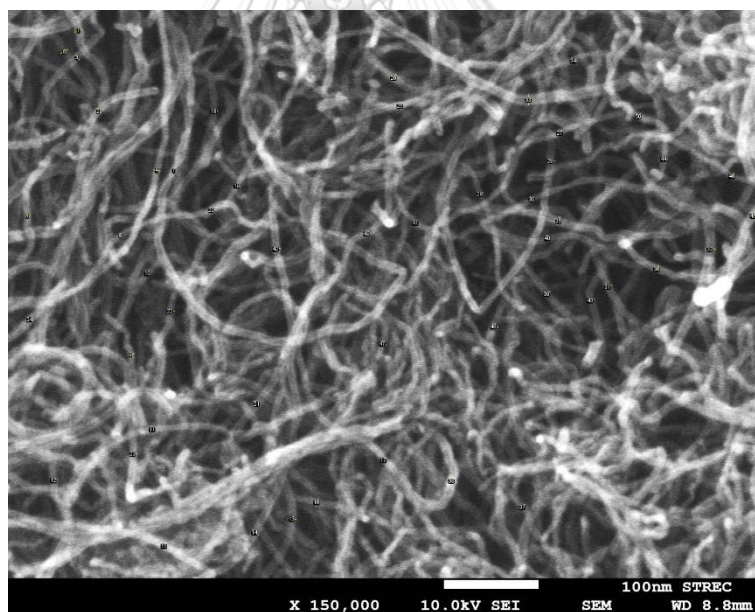


Fig. A4 4th SEM image of CNTs in 150,000 x (50 tube diameters were collected for size distribution using the ImageJ program)

Table A1 Size distribution of commercial CNTs

Counts	Diameter of CNTs (nm)			
	1 st image	2 nd image	3 rd image	4 th image
1	8.7	12.0	13.5	8.5
2	9.0	12.8	11.5	7.7
3	8.3	9.8	7.3	7.5
4	7.7	12.1	9.5	7.2
5	6.7	10.8	12.5	7.0
6	10.9	9.1	9.7	8.5
7	9.0	8.0	7.7	6.5
8	6.0	11.1	9.7	5.2
9	6.6	8.7	8.1	6.9
10	6.5	9.4	7.7	7.1
11	9.3	10.5	9.7	8.1
12	6.7	11.0	9.7	7.6
13	6.4	10.2	12.2	8.8
14	9.1	11.5	11.1	8.5
15	8.1	9.3	8.4	8.6
16	8.2	12.2	9.3	8.0
17	7.9	8.9	10.6	7.5
18	8.9	11.3	10.1	7.4
19	9.3	10.2	12.4	6.6
20	9.1	9.7	8.9	7.4

Counts	Diameter of CNTs (nm)			
	1 st image	2 nd image	3 rd image	4 th image
21	9.6	14.9	9.3	8.8
22	7.9	12.2	9.5	8.1
23	13.5	10.2	8.2	8.0
24	8.4	8.7	9.1	8.4
25	8.3	9.4	11.1	7.1
26	9.7	9.2	10.2	9.2
27	8.1	13.9	7.9	6.5
28	8.8	9.9	8.5	8.1
29	12.4	12.1	8.3	6.0
30	9.3	10.8	7.0	6.6
31	8.4	9.6	9.3	8.7
32	8.2	11.2	9.2	11.4
33	7.0	9.2	7.0	11.7
34	7.7	10.7	10.7	7.1
35	7.8	9.4	8.8	9.7
36	7.2	10.7	7.5	8.2
37	6.1	7.8	8.7	6.5
38	9.4	8.1	12.3	11.1
39	9.9	8.8	8.4	8.1
40	9.8	9.9	10.3	6.8
41	9.8	6.8	10.2	6.2

Counts	Diameter of CNTs (nm)			
	1 st image	2 nd image	3 rd image	4 th image
42	8.5	8.3	10.9	8.5
43	8.1	10.9	7.8	7.6
44	9.7	12.0	9.2	7.3
45	6.1	11.0	9.3	9.8
46	9.2	11.1	9.0	7.0
47	11.5	11.5	9.7	7.2
48	10.2	8.5	8.4	8.9
49	9.7	8.0	10.1	7.3
50	8.9	11.1	8.7	6.7

APPENDIX B

Flowability of CNT/Cement composite paste

Flowability of CNT/Cement composite paste was measured from average diameter of cement paste from 4 values, which were spread on flow table. The measured diameters were recorded for each diameter and used in calculation method as follows in **equation 15**. The diameter and flowability results of each condition are shown in **Table B1-B2**.

Flowability of CNT/Cement composite paste calculation :

$$\text{Flowability} = \frac{D_{avg} - D_0}{D_0} \times 100 \quad (15)$$

Whereas,

D_{avg} : Average diameter of cement paste (mm)

D_0 : Original base diameter (101.50 mm)

Table B1 Diameter and flowability of CNT/Cement composite paste with varied TX-100 concentrations.

Conditions	Diameter (mm)				Flowability (%)
	Diameter 1	Diameter 2	Diameter 3	Diameter 4	
Control	207.75	203.30	209.15	215.40	106.12
CX-1,0	188.20	194.10	199.20	191.00	90.55
CX-1,1	219.20	210.50	215.20	217.00	112.60
CX-1,1.5	223.50	223.80	223.90	224.80	121.02
CX-1,2	228.10	225.10	225.00	229.50	123.90

Table B2 Diameter and flowability of CNT/Cement composite paste with varied ratios of CNTs: TX-100

Conditions	Diameter (mm)				Flowability (%)
	Diameter 1	Diameter 2	Diameter 3	Diameter 4	
Control	207.75	203.30	209.15	215.40	106.12
CX-1,1	219.20	210.50	215.20	217.00	112.60
CX-2,1	211.30	210.30	212.90	215.10	109.57
CX-3,1	197.15	197.06	201.67	199.48	96.19
CX-4,1	194.15	191.35	189.10	190.40	88.70

APPENDIX C

Porosity and water absorption of CNT/Cement composite

The standard test method for density, absorption, and voids in hardened concrete, as outlined in ASTM C642 [46], was calculated from weight of sample after drying (**mass A**), weight of samples after immersing in water for 2 days (**mass B**), weight of samples after boiling (**mass C**) and weight of samples after suspending with wire in water or apparent mass (**mass D**) which detail of method was described in **Chapter 3**. The apparent density, porosity, and water absorption after immersion and boiling of CNT/Cement composite samples were calculated as follows in **equations 16 and 17**. The apparent density, porosity, and water absorption of each composite sample are shown in **Table C1-C2**.

Porosity of CNT/Cement composite calculation equation:

$$\text{Porosity (volume of permeable pore space), (\%)} = \frac{\text{Mass C} - \text{Mass A}}{\text{Mass C} - \text{Mass D}} \times 100 \quad (16)$$

Water absorption of CNT/Cement composite calculation equation:

$$\text{Water absorption after immersion and boiling, (\%)} = \frac{\text{Mass C} - \text{Mass A}}{\text{Mass A}} \times 100 \quad (17)$$

Where,

Mass A : Mass of oven-dried sample in air (g)

Mass C : Mass of surface-dry sample in air after immersion and boiling (g)

Mass D : Apparent mass of sample in water after immersion and boiling (g)

Table C1 Weight of each mass, apparent density, porosity, and water absorption of CNT/Cement composite samples with varied TX-100 concentrations

Conditions	Sample	Mass A (g)	Mass B (g)	Mass C (g)	Mass D (g)	Porosity (%)	Water absorption (%)
Control	1	206.55	244.33	244.95	125.70	32.20	18.59
	2	208.28	245.86	246.30	126.40	31.71	18.25
	3	219.71	260.20	261.07	133.50	32.42	18.82
CX-1,0	1	213.59	253.71	254.19	127.00	31.92	19.01
	2	219.38	261.19	261.79	130.80	32.38	19.33
	3	216.63	259.71	259.37	130.30	33.11	19.73
CX-0,1	1	190.11	227.60	231.73	108.40	33.75	21.89
	2	190.70	228.90	232.59	108.90	33.87	21.97
	3	200.87	240.16	243.15	115.10	33.02	21.05
CX-1,1	1	202.60	242.97	244.52	116.10	32.64	20.69
	2	210.90	253.10	254.65	121.20	32.78	20.74
	3	206.00	247.11	249.66	117.40	33.01	21.19
CX-1,1.5	1	187.12	225.11	227.95	103.50	32.81	21.82
	2	187.28	225.40	228.99	104.00	33.37	22.27
	3	202.72	244.38	245.86	116.50	33.35	21.28
CX-1,2	1	187.77	226.77	230.07	103.20	33.34	22.53
	2	178.19	215.34	218.33	98.00	33.36	22.53
	3	205.73	248.29	249.66	118.70	33.54	21.35

Table C2 Weight of each mass, apparent density, porosity, and water absorption of CNT/Cement composite samples with varied CNTs: TX-100 concentrations

Conditions	Sample	Mass A (g)	Mass B (g)	Mass C (g)	Mass D (g)	Porosity (%)	Water absorption (%)
Control	1	206.55	244.33	244.95	125.70	32.20	18.59
	2	208.28	245.86	246.30	126.40	31.71	18.25
	3	219.71	260.20	261.07	133.50	32.42	18.82
CX-1,1	1	202.60	242.97	244.52	116.10	32.64	20.69
	2	210.90	253.10	254.65	121.20	32.78	20.74
	3	206.00	247.11	249.66	117.40	33.01	21.19
CX-2,1	1	212.13	253.14	253.90	126.60	32.81	19.69
	2	222.78	264.46	265.78	133.50	32.51	19.30
	3	213.75	253.57	254.80	128.00	32.37	19.20
CX-3,1	1	218.07	258.70	259.63	131.50	32.44	19.06
	2	221.51	263.15	264.18	133.50	32.65	19.26
	3	216.94	257.45	258.34	130.50	32.38	19.08
CX-4,1	1	220.25	263.15	263.89	132.70	33.26	19.81
	2	222.68	263.79	264.19	134.10	31.91	18.64
	3	212.89	252.43	252.86	128.50	32.14	18.77



APPENDIX D

Compressive strength of CNT/Cement composite

The compressive strength and density of CNT/Cement composite samples were measured and calculated using the following **equations 18 and 19**. The compressive strength and bulk density of each composite sample are shown in **Table D1-D9**.

Equation for compressive strength of cement sample:

$$\text{Compressive strength (Pa)} = \frac{\text{Maximum load (N)}}{\text{Cross sectional area of cement sample (m}^2\text{)}} \quad (18)$$

Whereas,

Maximum load: maximum load value of sample from a compressive machine at failure (N)

Cross-sectional area of cement sample: area of sample that was perpendicular to direction of the applied load (m²)

Equation for bulk density of cement sample:

$$\text{Density} \left(\frac{\text{g}}{\text{cm}^3} \right) = \frac{\text{Mass of cement sample (g)}}{\text{Volume of cement sample (cm}^3\text{)}} \quad (19)$$

Whereas,

Mass of cement sample: weight of each cement sample (g)

Volume of cement sample: multiplying each dimension of cement sample (cm³)

1. Weight, dimension, compressive strength, and density of CNT/Cement composite samples with varied TX-100 concentration

Table D1 Weight, dimensions, compressive strength, and density of CNT/Cement composite samples with control conditions

Curing time (days)	Sample	Weight (g)	Width (mm)	Length (mm)	Depth (mm)	Max load (KN)	Compressive strength (MPa)	Density (g/cm ³)
3	1	257.41	50.90	53.30	48.30	105.10	38.74	1.96
	2	249.97	50.30	50.80	50.10	91.90	35.97	1.95
	3	251.47	51.00	50.60	50.25	95.70	37.08	1.94
7	1	240.52	51.00	50.75	48.85	111.90	43.23	1.90
	2	239.78	50.55	50.35	49.10	107.40	42.20	1.92
	3	244.38	51.15	50.75	48.70	121.90	46.96	1.93
14	1	242.63	51.15	50.85	48.75	135.40	52.06	1.91
	2	247.34	50.75	50.75	49.40	120.70	46.86	1.94
	3	240.20	51.20	49.35	49.70	132.50	52.44	1.91
28	1	243.35	50.25	50.70	49.70	127.50	50.05	1.92
	2	240.98	51.00	50.35	48.10	129.80	50.55	1.95
	3	254.28	52.50	50.80	49.60	150.20	56.32	1.92

Table D2 Weight, dimensions, compressive strength, and density of CNT/Cement composite samples with CX-1,0 condition.

Curing time (days)	Sample	Weight (g)	Width (mm)	Length (mm)	Depth (mm)	Max load (KN)	Compressive strength (MPa)	Density (g/cm ³)
3	1	257.22	52.65	50.90	50.25	93.30	34.81	1.91
	2	248.44	51.00	50.95	49.30	95.50	36.75	1.94
	3	245.93	50.75	51.40	49.40	101.70	38.99	1.91
7	1	252.29	50.80	51.00	49.70	123.10	47.51	1.96
	2	246.18	50.80	50.30	49.55	121.90	47.71	1.94
	3	247.08	50.50	50.60	50.05	91.80	35.93	1.93
14	1	247.52	51.00	50.70	49.40	133.50	51.63	1.94
	2	253.19	51.00	50.75	50.60	111.60	43.12	1.93
	3	258.82	50.70	52.45	49.55	140.10	52.68	1.96
28	1	244.07	50.75	50.55	50.30	147.50	57.50	1.89
	2	256.1	52.70	50.70	50.55	141.70	53.03	1.90
	3	244.1	50.35	50.65	50.00	115.40	45.25	1.91

Table D3 Weight, dimensions, compressive strength, and density of CNT/Cement composite samples with CX-0,1 condition.

Curing time (days)	Sample	Weight (g)	Width (mm)	Length (mm)	Depth (mm)	Max load (KN)	Compressive strength (MPa)	Density (g/cm ³)
7	1	215.83	50.70	50.90	48.00	94.20	36.50	1.74
	2	219.38	50.80	50.60	51.10	77.20	30.03	1.67
	3	232.65	50.80	53.00	49.65	100.90	37.48	1.74

Table D4 Weight, dimensions, compressive strength, and density of CNT/Cement composite samples with CX-1,1 condition.

Curing time (days)	Sample	Weight (g)	Width (mm)	Length (mm)	Depth (mm)	Max load (KN)	Compressive strength (MPa)	Density (g/cm ³)
3	1	222.81	50.70	51.20	48.40	83.80	32.28	1.77
	2	231.29	51.90	50.00	49.00	82.00	31.60	1.82
	3	227.90	50.75	50.75	49.40	87.60	34.01	1.79
7	1	223.26	50.55	50.40	49.65	99.50	39.05	1.76
	2	233.78	50.70	50.90	50.00	98.00	37.98	1.81
	3	239.30	50.80	51.90	50.50	105.00	39.83	1.80
14	1	238.73	52.15	50.70	50.25	125.30	47.39	1.80
	2	233.18	51.00	50.80	50.75	127.60	49.25	1.77
	3	242.23	52.40	50.75	51.55	122.80	46.18	1.77
28	1	213.56	50.75	50.50	49.10	128.30	50.06	1.70
	2	227.11	50.75	52.75	48.90	133.30	49.79	1.73
	3	231.07	50.90	51.75	50.20	138.50	52.58	1.75

Table D5 Weight, dimensions, compressive strength, and density of CNT/Cement composite samples with CX-1,1.5 condition

Curing time (days)	Sample	Weight (g)	Width (mm)	Length (mm)	Depth (mm)	Max load (KN)	Compressive strength (MPa)	Density (g/cm ³)
7	1	228.24	50.70	52.70	49.50	88.40	33.09	1.73
	2	212.19	50.50	50.50	49.70	86.10	33.76	1.67
	3	219.38	50.80	50.90	49.85	89.20	34.50	1.70

Table D6 Weight, dimensions, compressive strength, and density of CNT/Cement composite samples with CX-1,2 condition.

Curing time (days)	Sample	Weight (g)	Width (mm)	Length (mm)	Depth (mm)	Max load (KN)	Compressive strength (MPa)	Density (g/cm ³)
7	1	212.43	50.80	50.75	49.30	98.80	38.32	1.67
	2	217.32	52.90	50.70	50.35	64.10	23.90	1.61
	3	206.51	50.55	50.70	50.25	57.90	22.59	1.60

2. Weight, dimension, compressive strength, and density of CNT/Cement composite samples with varied CNTs: TX-100 concentrations

Table D7 Weight, dimensions, compressive strength, and density of CNT/Cement composite samples with CX-2,1 condition.

Curing time (days)	Sample	Weight (g)	Width (mm)	Length (mm)	Depth (mm)	Max load (KN)	Compressive strength (MPa)	Density (g/cm ³)
3	1	258.75	52.65	51.05	49.85	106.60	39.66	1.93
	2	251.30	51.10	50.65	49.70	98.90	38.21	1.95
	3	260.34	51.00	52.55	50.50	104.80	39.10	1.92
7	1	255.92	52.55	51.10	51.20	126.30	47.03	1.86
	2	247.43	51.10	50.90	49.80	124.10	47.71	1.91
	3	246.84	50.80	52.60	49.40	118.40	44.31	1.87
14	1	239.43	50.80	50.55	49.00	133.20	51.87	1.90
	2	251.81	50.60	50.80	50.70	144.30	56.14	1.93
	3	250.65	50.45	50.65	50.50	153.00	59.88	1.94
28	1	251.75	52.50	50.70	50.25	173.20	65.07	1.88
	2	245.00	50.95	50.45	49.90	164.20	63.88	1.91
	3	254.03	52.55	51.00	49.85	166.50	62.13	1.90

Table D8 Weight, dimensions, compressive strength, and density of CNT/Cement composite samples with CX-3,1 condition.

Curing time (days)	Sample	Weight (g)	Width (mm)	Length (mm)	Depth (mm)	Max load (KN)	Compressive strength (MPa)	Density (g/cm ³)
7	1	260.01	50.90	51.90	50.10	116.60	44.14	1.96
	2	249.84	50.80	50.60	49.80	111.40	43.34	1.95
	3	250.05	50.85	51.10	50.50	107.40	41.33	1.91

Table D9 Weight, dimensions, compressive strength, and density of CNT/Cement composite samples with CX-4,1 condition.

Curing time (days)	Sample	Weight (g)	Width (mm)	Length (mm)	Depth (mm)	Max load (KN)	Compressive strength (MPa)	Density (g/cm ³)
7	1	247.22	51.00	50.65	49.90	103.60	40.41	1.92
	2	264.44	51.20	53.20	50.75	104.50	38.36	1.91
	3	256.15	51.05	51.85	49.65	105.40	39.82	1.95

APPENDIX E

Electrical conductivity of CNT/Cement composite

Electrical conductivity of CNT/Cement composite was calculated from resistivity, which was measured from a digital multimeter using the following **equation 20**. The electrical resistance and electrical conductivity of each composite sample are shown in **Table E1-E9**.

Equation for electrical conductivity of CNT/Cement composite:

$$\sigma = \frac{L}{R \times A} \quad (20)$$

Where,

σ : Electrical conductivity (S/m)

L: Length between the electrode (2×10^{-2} m)

R: Electrical resistance (Ω)

A: Contact area between the electrode and cement sample (7.5×10^{-4} m²)

1. Electrical resistance and electrical conductivity of CNT/Cement composite samples with varied TX-100 concentrations

Table E1 Electrical resistance and electrical conductivity of CNT/Cement composite samples with control condition.

Curing time (days)	Sample	Electrical resistance (K Ω)	Electrical conductivity (μ S/m)
3	1	2.85	9,356.72
	2	4.00	6,663.33
	3	2.51	10,624.41
7	1	39.67	672.21
	2	37.30	714.92
	3	35.64	748.22
14	1	45.81	582.11
	2	43.91	607.30
	3	44.67	596.97
28	1	51.80	514.80
	2	49.18	542.22
	3	50.28	530.36

Table E2 Electrical resistance and electrical conductivity of CNT/Cement composite samples with CX-1,0 condition.

Curing time (days)	Sample	Electrical resistance (K Ω)	Electrical conductivity (μ S/m)
3	1	1.28	20,803.33
	2	1.53	17,395.09
	3	1.42	18,792.58
7	1	31.23	853.88
	2	28.75	927.54
	3	31.82	838.05
14	1	32.25	826.87
	2	32.42	822.53
	3	32.30	825.59
28	1	37.07	719.36
	2	39.86	822.54
	3	39.56	674.08

Table E3 Electrical resistance and electrical conductivity of CNT/Cement composite samples with CX-0,1 condition.

Curing time (days)	Sample	Electrical resistance (K Ω)	Electrical conductivity (μ S/m)
3	1	4.95	5,385.02
	2	5.18	5,145.02
	3	6.20	4,301.76
7	1	38.07	700.46
	2	37.96	702.50
	3	45.65	584.15
14	1	47.61	560.11
	2	46.40	574.71
	3	47.38	562.83
28	1	54.70	487.51
	2	50.48	528.26
	3	50.23	530.89

Table E4 Electrical resistance and electrical conductivity of CNT/Cement composite samples with CX-1,1 condition.

Curing time (days)	Sample	Electrical resistance (K Ω)	Electrical conductivity (μ S/m)
3	1	4.98	5,360.13
	2	4.71	5,659.31
	3	5.06	5,266.97
7	1	30.85	864.40
	2	30.82	865.24
	3	31.60	843.88
14	1	33.70	791.30
	2	33.05	806.86
	3	33.07	806.37
28	1	39.86	669.01
	2	41.96	635.53
	3	37.71	707.15

Table E5 Electrical resistance and electrical conductivity of CNT/Cement composite samples with CX-1,1.5 condition

Curing time (days)	Sample	Electrical resistance (K Ω)	Electrical conductivity (μ S/m)
3	1	5.46	4,882.22
	2	4.97	5,369.85
	3	4.57	5,838.99
7	1	32.45	821.78
	2	33.11	805.40
	3	31.78	839.10
14	1	34.89	764.31
	2	35.52	750.75
	3	35.60	749.06
28	1	42.80	623.05
	2	40.22	663.02
	3	38.92	685.17

Table E6 Electrical resistance and electrical conductivity of CNT/Cement composite samples with CX-1,2 condition.

Curing time (days)	Sample	Electrical resistance (K Ω)	Electrical conductivity (μ S/m)
3	1	5.84	4,568.56
	2	6.20	4,303.16
	3	5.93	4,496.91
7	1	33.68	791.77
	2	34.16	780.64
	3	33.95	785.47
14	1	36.66	727.40
	2	39.14	681.31
	3	37.92	703.23
28	1	39.73	671.20
	2	44.02	605.79
	3	44.14	604.14

2. Electrical resistance and electrical conductivity of CNT/Cement composite samples with varied CNTs: TX-100 concentrations.

Table E7 Electrical resistance and electrical conductivity of CNT/Cement composite samples with CX-2,1 condition.

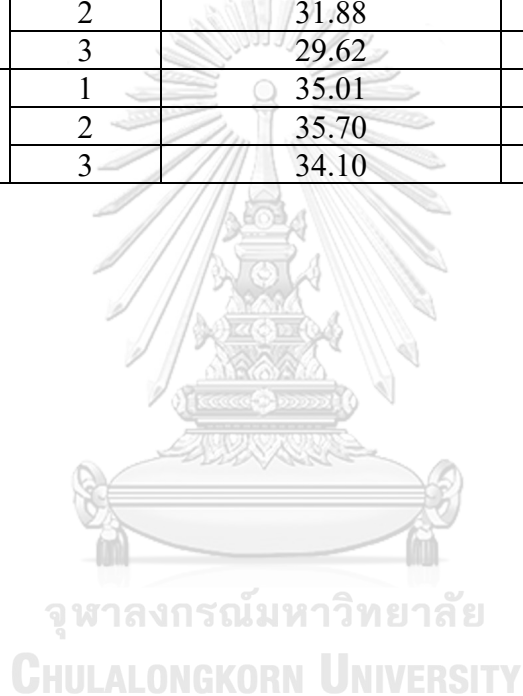
Curing time (days)	Sample	Electrical resistance (K Ω)	Electrical conductivity (μ S/m)
3	1	2.28	11,701.03
	2	2.58	10,355.99
	3	2.20	12,121.21
7	1	28.95	921.13
	2	31.20	854.70
	3	30.61	871.17
14	1	30.50	874.32
	2	31.98	833.85
	3	31.90	835.95
28	1	38.34	695.53
	2	36.31	734.41
	3	36.14	737.87

Table E8 Electrical resistance and electrical conductivity of CNT/Cement composite samples with CX-3,1 condition.

Curing time (days)	Sample	Electrical resistance (K Ω)	Electrical conductivity (μ S/m)
3	1	1.88	14,214.64
	2	2.97	8,975.65
	3	2.11	12,662.23
7	1	29.20	913.24
	2	30.31	879.80
	3	30.38	877.77
14	1	30.95	861.60
	2	31.02	859.66
	3	31.27	852.79
28	1	36.16	737.46
	2	35.80	744.88
	3	35.09	759.95

Table E9 Electrical resistance and electrical conductivity of CNT/Cement composite samples with CX-4,1 condition.

Curing time (days)	Sample	Electrical resistance (K Ω)	Electrical conductivity (μ S/m)
3	1	2.26	11,778.56
	2	2.19	12,204.42
	3	2.15	12,403.10
7	1	29.36	908.26
	2	27.27	977.88
	3	29.62	900.29
14	1	31.39	849.52
	2	31.88	836.47
	3	29.62	900.29
28	1	35.01	761.69
	2	35.70	746.97
	3	34.10	782.01



APPENDIX F

SEM image of CNT dispersion in composite

Dispersion of CNTs in the CNT/Cement composite samples was characterized using SEM in different areas: top area, two side areas, middle area, and bottom area. SEM images, which are shown in **Figs. F1-F7**, were obtained to investigate dispersion of CNTs in each condition and in different areas of composite samples.

1.1 Dispersion of CNTs in CNT/Cement composite with varied Triton X-100 conditions

1. Dispersion of CNTs with CX-1,0 condition.

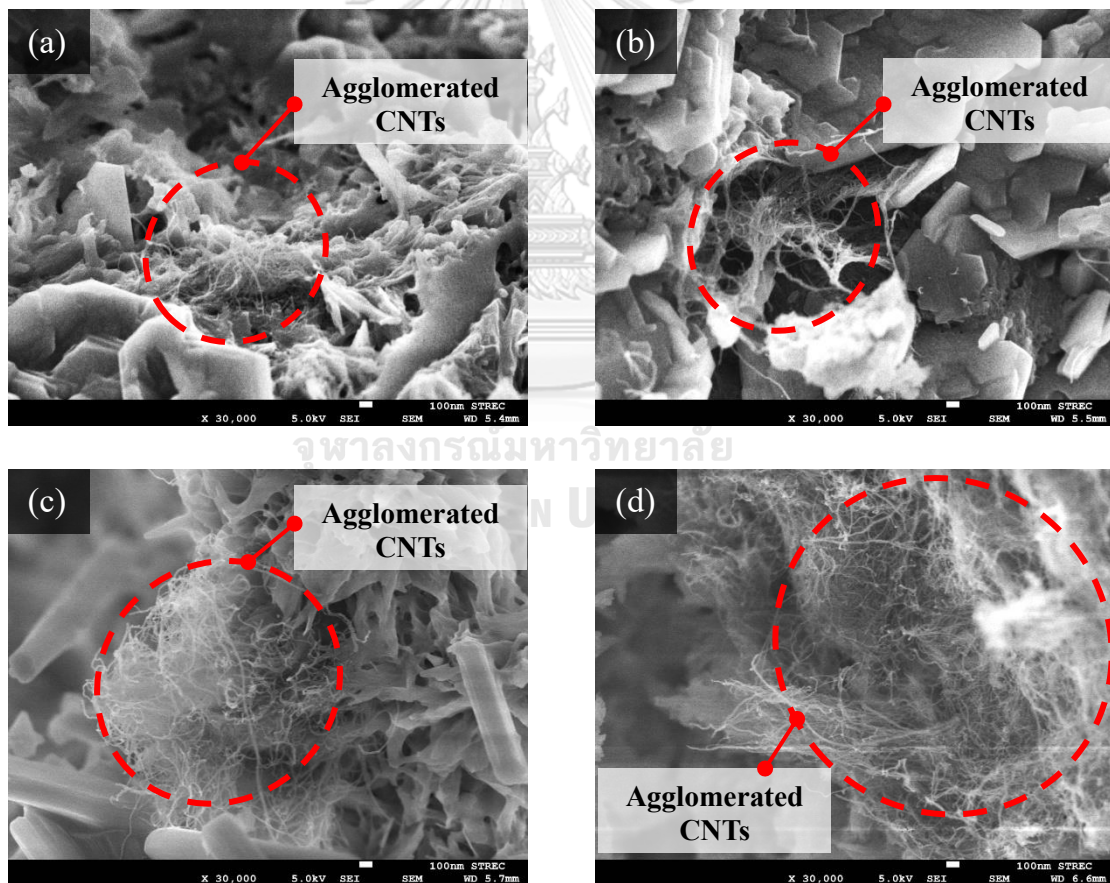


Figure F1. Dispersion of CNTs in composite with CX-1,0 condition in 5 different area (a) top area, (b) left area, (c) right area, (d) middle area, and (e) bottom area

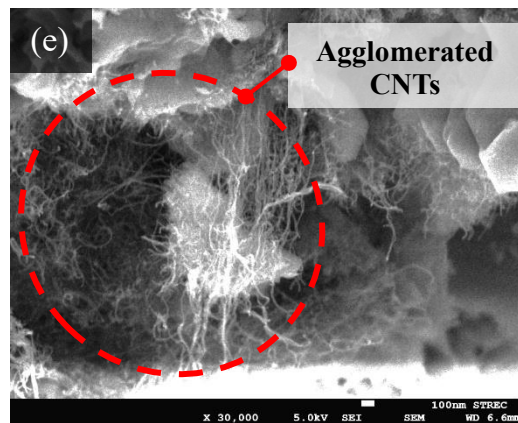


Figure F1. Dispersion of CNTs in composite with CX-1,0 condition in 5 different area (a) top area, (b) left area, (c) right area, (d) middle area, and (e) bottom area (continued)

2. Dispersion of CNTs with CX-1,1 condition

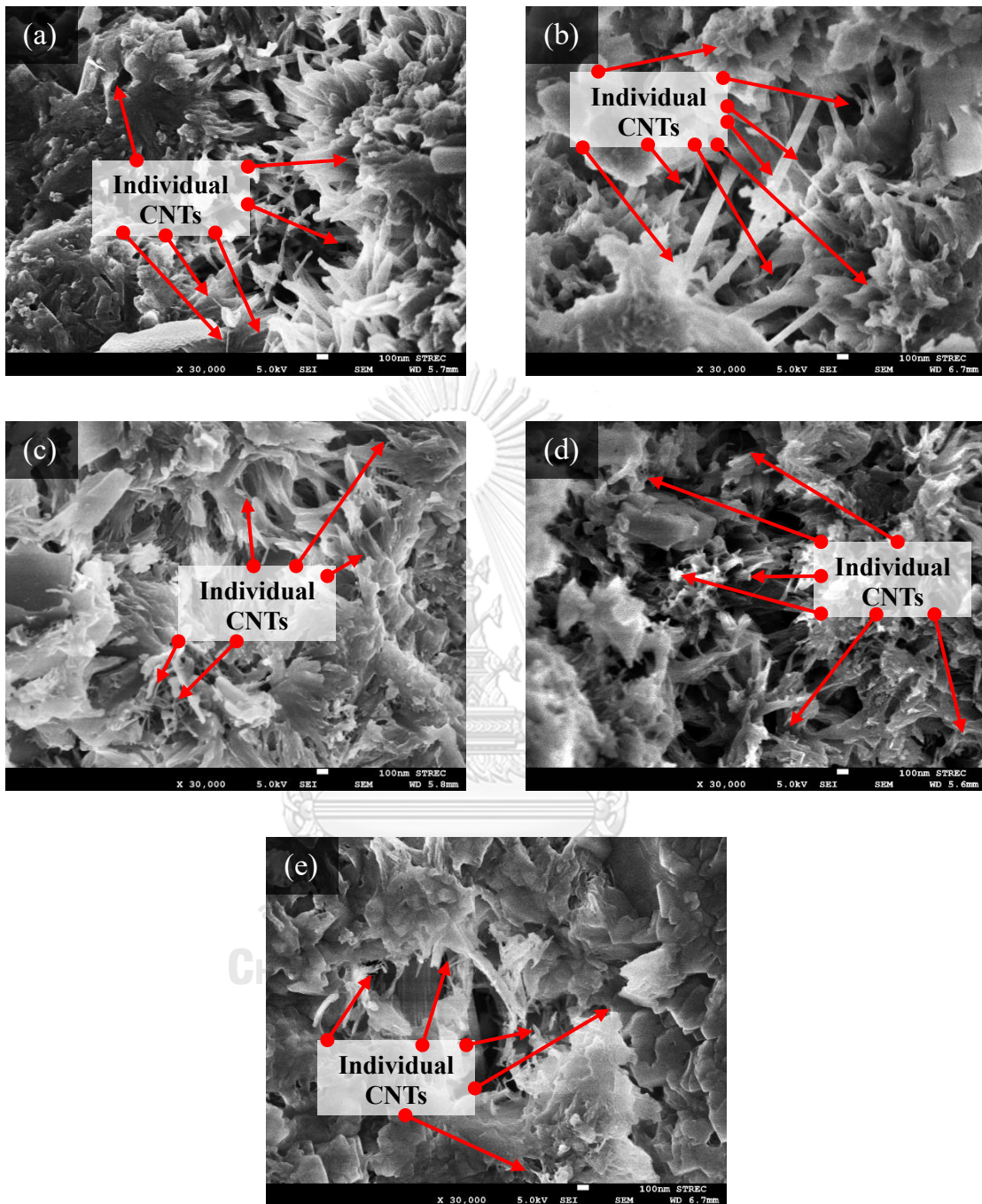


Figure F2. Dispersion of CNTs in composite with CX-1,1 condition in 5 different areas (a) top area, (b) left area, (c) right area, (d) middle area, and (e) bottom area

3. Dispersion of CNTs with CX-1,1.5 condition

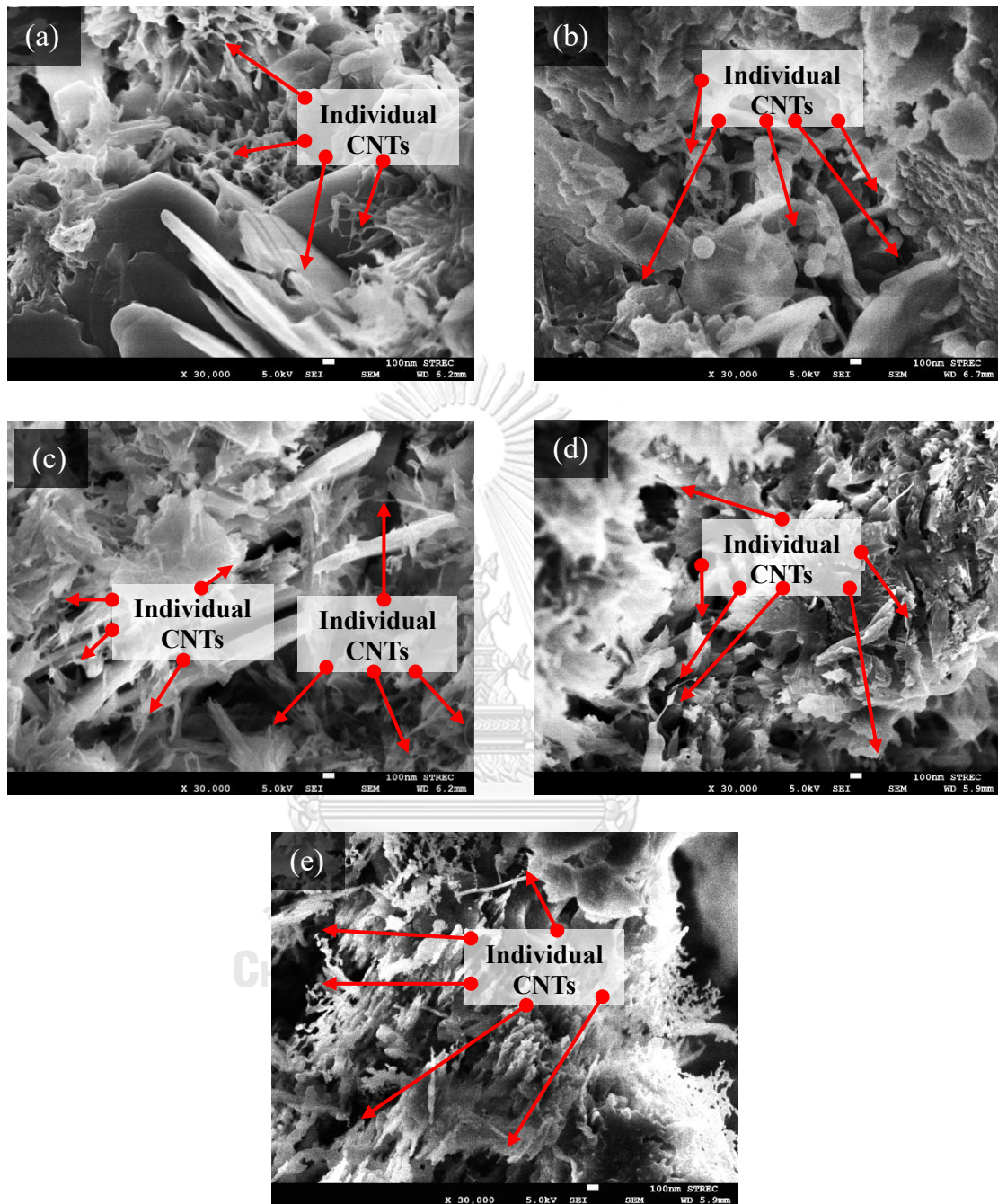


Figure F3 Dispersion of CNTs in composite with CX-1,1.5 condition in 4 different areas (a) top area, (b) left area, (c) right area, (d) middle area, and (e) bottom area

4. Dispersion of CNTs with CX-1,2 condition

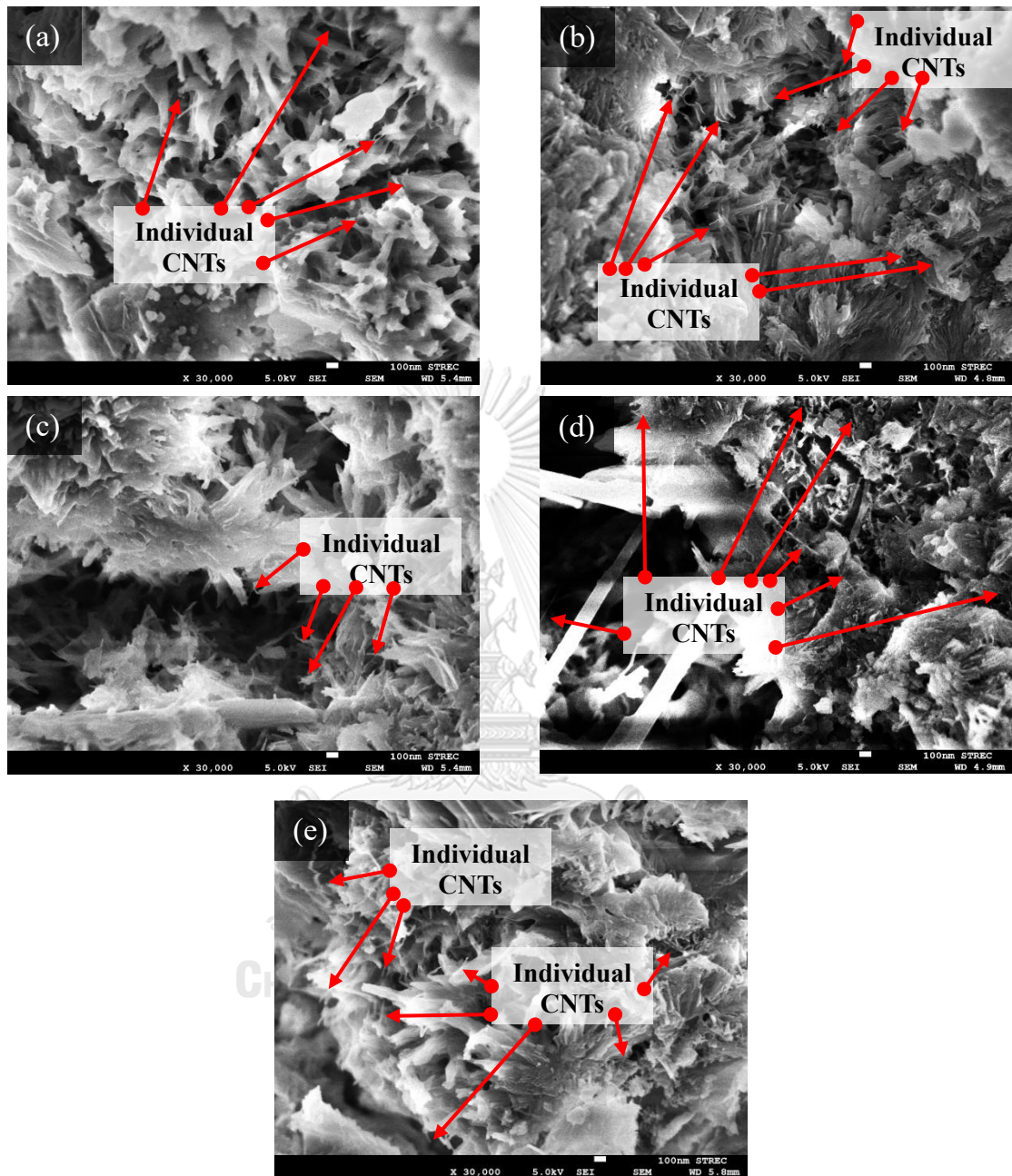


Figure F4. Dispersion of CNTs in composite with CX-1,2 condition in 5 different areas (a) top area, (b) left area, (c) right area, (d) middle area, and (e) bottom area

1.2 Dispersion of CNTs in CNT/Cement composite with varied CNT to Triton X-100

1. Dispersion of CNTs with CX-2,1 condition

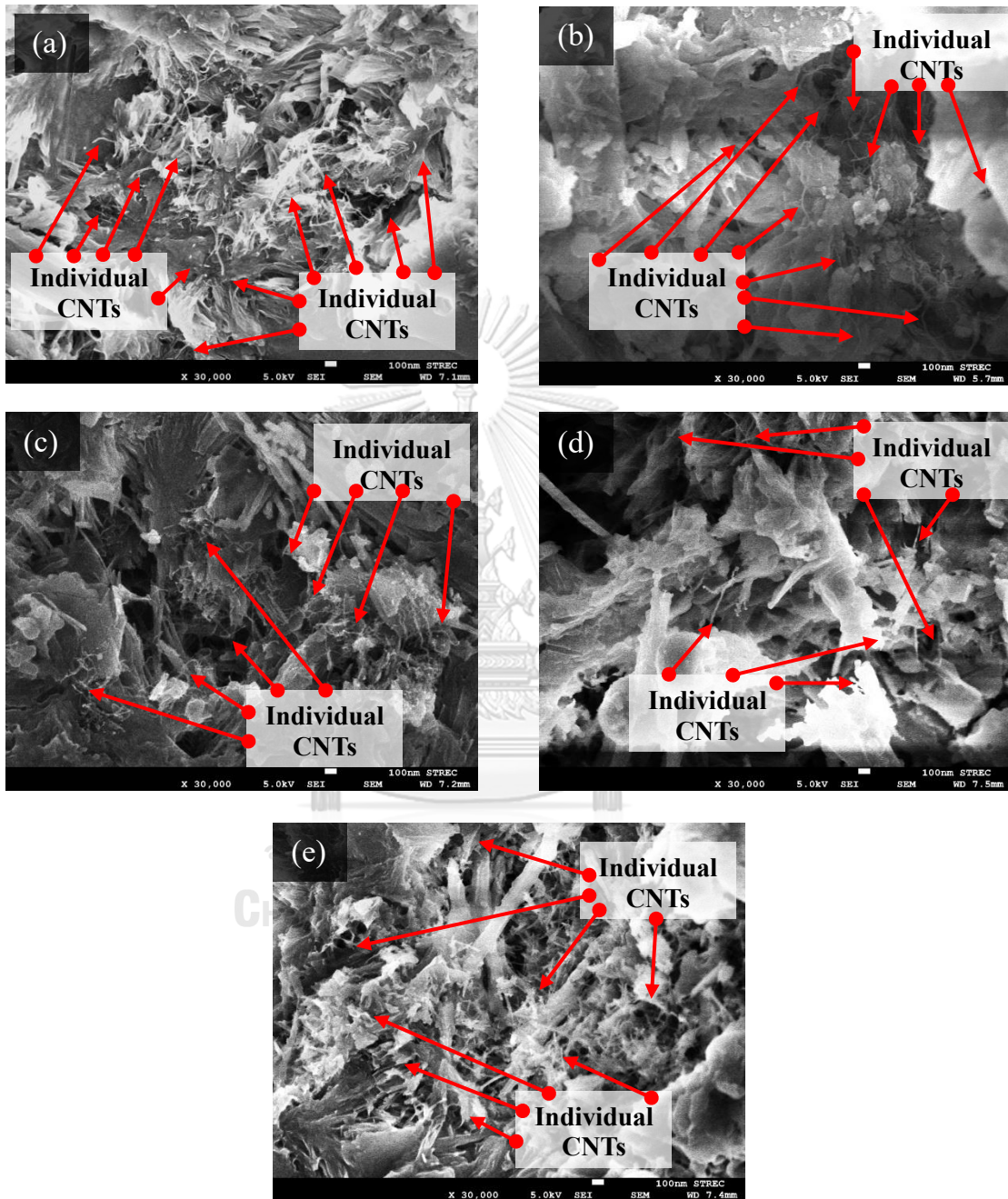


Figure F5. Dispersion of CNTs in composite with CX-2,1 condition in 5 different areas (a) top area, (b) left area, (c) right area, (d) middle area, and (e) bottom area

2. Dispersion of CNTs with CX-3,1 condition

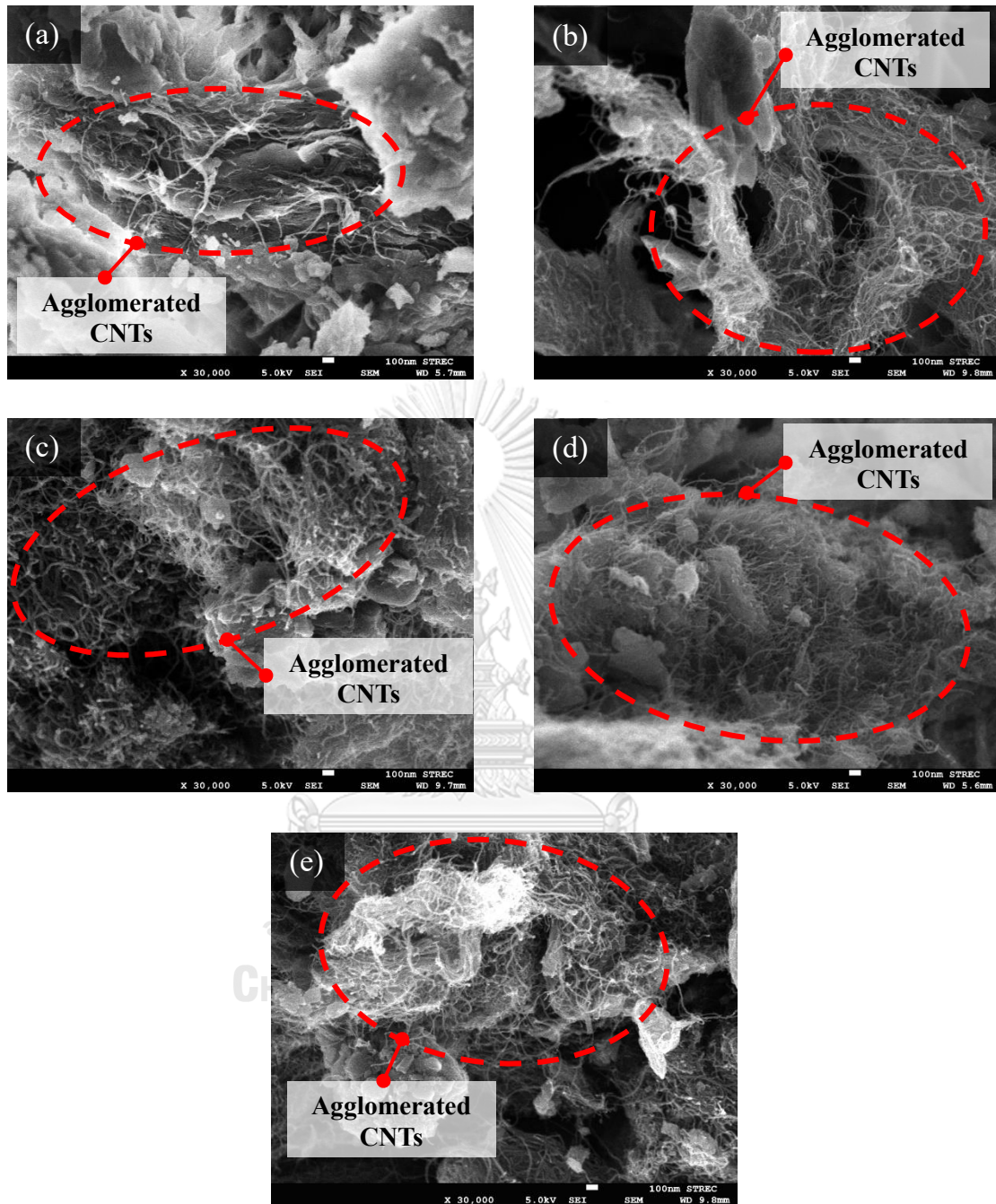


Figure F6. Dispersion of CNTs in composite with CX-3,1 condition in 5 different areas (a) top area, (b) left area, (c) right area, (d) middle area, and (e) bottom area

3. Dispersion of CNTs with CX-4,1 condition

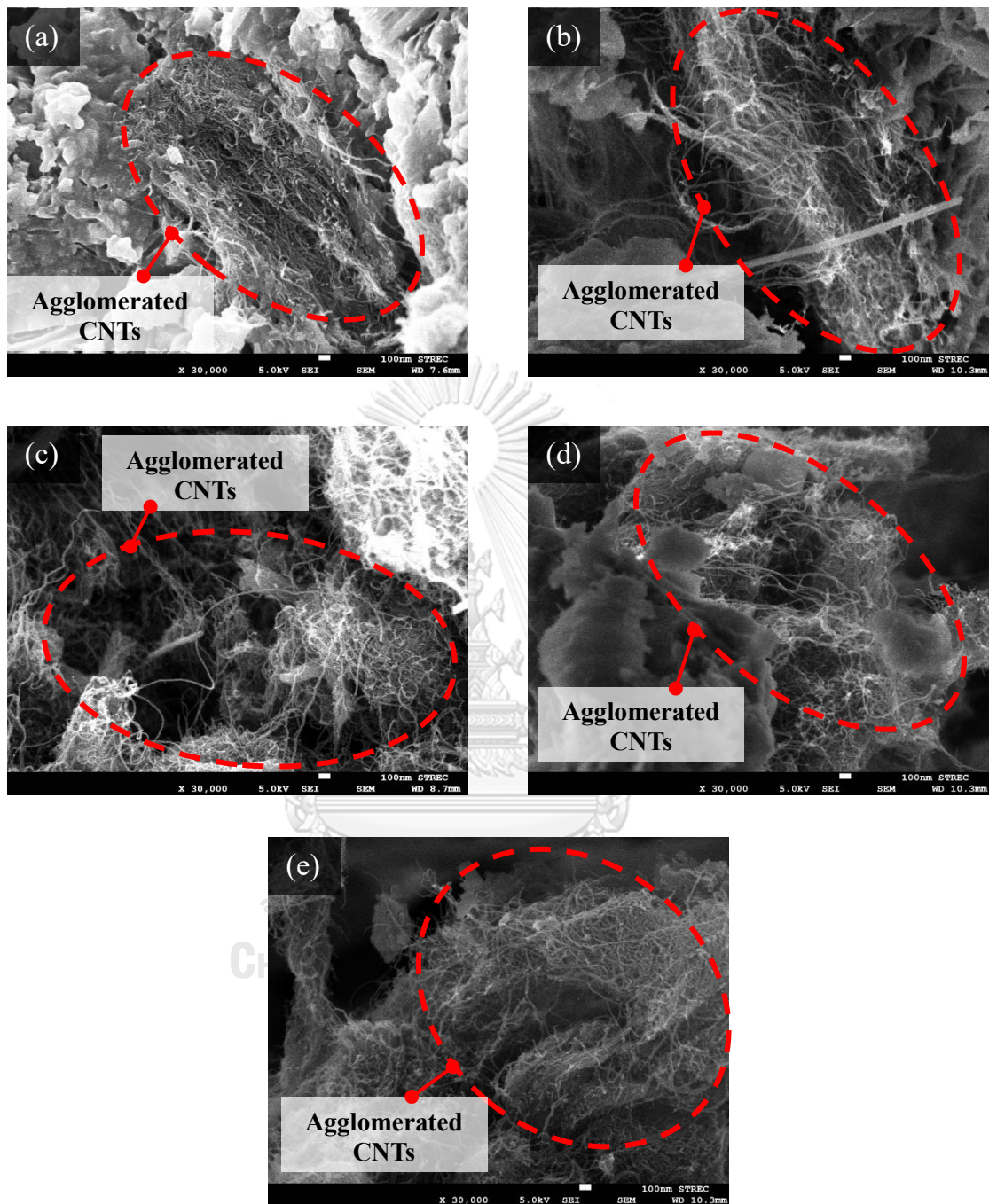


Figure F7. Dispersion of CNTs in composite with CX-4,1 condition in different areas (a) top area, (b) left area, (c) right area, (d) middle area, and (e) bottom area

APPENDIX G

CNT dispersion analysis

CNT dispersion analysis was calculated from SEM images of CNT dispersion within composite using grid cells to distinguish between cells with only one tube of CNTs (individual cells) and cells with more than one tube of CNTs (agglomerated cells). Analysis was performed following **equation 21** and CNT dispersion ratio are shown in **Table G1-G9**.

CNT dispersion analysis calculation equation:

$$CNT \text{ dispersion ratio} = \frac{\text{Individual CNT} - \text{Agglomerated CNTs}}{\text{Total cells}} \quad (21)$$

Whereas,

Individual CNT: Cells containing one CNT tube each.

Agglomerated CNTs: Cells containing more than one tube of CNTs each.

Total cells: Total number of cells in the picture.

1. CNT dispersion ratio with different amounts of grid line conditions.

Table G1 CNT dispersion ratio with CX-2,1 condition picture 1 different amount of grid line conditions.

Grid line condition	Number of cells (cell)		CNT dispersion ratio
	Individual CNT	Agglomerated CNTs	
6 × 6	5	17	-0.333
12 × 12	15	36	-0.146
18 × 18	44	49	-0.015
24 × 24	74	47	0.047
30 × 30	100	56	0.049
36 × 36	128	65	0.049

2. CNT dispersion ratio with varied Triton X-100 conditions

Table G2 CNT dispersion ratio within composite with CX-1,0 condition in 5 different area (24×24 cells)

Picture number	Area position	Number of cells (cell)		CNTs dispersion ratio
		Individual CNT	Agglomerated CNTs	
1	Top	5	44	-0.068
2	Left	7	74	-0.116
3	Right	20	183	-0.283
4	Middle	12	409	-0.689
5	Bottom	6	288	-0.490
Average				-0.329
SD				0.260

Table G3 CNT dispersion ratio within composite with CX-1,1 condition in 5 different area (24×24 cells)

Picture number	Area position	Number of cells (cell)		CNTs dispersion ratio
		Individual CNT	Agglomerated CNTs	
1	Top	9	0	0.016
2	Left	34	0	0.059
3	Right	15	2	0.023
4	Middle	14	1	0.023
5	Bottom	8	0	0.014
Average				0.027
SD				0.018

Table G4 CNT dispersion ratio within composite with CX-1,1.5 condition in 5 different area (24 × 24 cells)

Picture number	Area position	Number of cells (cell)		CNTs dispersion ratio
		Individual CNT	Agglomerated CNTs	
1	Top	14	1	0.023
2	Left	10	0	0.017
3	Right	24	0	0.042
4	Middle	13	0	0.023
5	Bottom	9	0	0.016
Average	0.024			
SD	0.010			

Table G5 CNT dispersion ratio within composite with CX-1,2 condition in 5 different area (24 × 24 cells)

Picture number	Area position	Number of cells (cell)		CNTs dispersion ratio
		Individual CNT	Agglomerated CNTs	
1	Top	15	1	0.024
2	Left	24	2	0.038
3	Right	10	0	0.017
4	Middle	22	0	0.038
5	Bottom	59	0	0.102
Average	0.044			
SD	0.034			

3. CNT dispersion ratio with varied CNT: TX-100

Table G6 CNT dispersion ratio within composite with CX-2,1 condition in 5 different area (24 × 24 cells)

Picture number	Area position	Number of cells (cell)		CNTs dispersion ratio
		Individual CNT	Agglomerated CNTs	
1	Top	75	47	0.049
2	Left	58	12	0.080
3	Right	86	29	0.099
4	Middle	28	3	0.043
5	Bottom	56	2	0.094
Average	0.073			
SD	0.026			

Table G8 CNT dispersion ratio within composite with CX-3,1 condition in 5 different area (24×24 cells)

Picture number	Area position	Number of cells (cell)		CNTs dispersion ratio
		Individual CNT	Agglomerated CNTs	
1	Top	7	148	-0.245
2	Left	8	422	-0.719
3	Right	9	417	-0.708
4	Middle	12	256	-0.424
5	Bottom	14	135	-0.210
Average		-0.461		
SD		0.244		

Table G9 CNT dispersion ratio within composite with CX-4,1 condition in 5 different area (24×24 cells)

Picture number	Area position	Number of cells (cell)		CNTs dispersion ratio
		Individual CNT	Agglomerated CNTs	
1	Top	8	187	-0.311
2	Left	23	264	-0.418
3	Right	11	474	-0.804
4	Middle	5	221	-0.375
5	Bottom	12	409	-0.689
Average		-0.519		
SD		0.215		

REFERENCES



จุฬาลงกรณ์มหาวิทยาลัย
CHULALONGKORN UNIVERSITY

1. Armenta, S., et al., *Carbon-Based Nanomaterials in Analytical Chemistry*, in *Handbook of Smart Materials in Analytical Chemistry*. 2019, John Wiley & Sons, Ltd Chichester, UK. p. 345-374.
2. Zhang, N., et al., *Dynamic properties of strain-hardening cementitious composite reinforced with basalt and steel fibers*. 2020. **14**(1): p. 1-14.
3. Kang, J., S. Al-Sabah, and R. Theo, *Effect of Single-walled Carbon Nanotubes on Strength Properties of Cement Composites*. *Materials (Basel)*, 2020. **13**(6): p. 1305.
4. Geng, Y., et al., *Effects of surfactant treatment on mechanical and electrical properties of CNT/epoxy nanocomposites*. 2008. **39**(12): p. 1876-1883.
5. Saifuddin, N., A. Raziah, and A.J.J.o.C. Junizah, *Carbon nanotubes: a review on structure and their interaction with proteins*. 2013. **2013**.
6. Eatemadi, A., et al., *Carbon nanotubes: properties, synthesis, purification, and medical applications*. *Nanoscale Res Lett*, 2014. **9**(1): p. 393.
7. Devi, R. and S.S.J.M.T. Gill, *A squared bossed diaphragm piezoresistive pressure sensor based on CNTs for low pressure range with enhanced sensitivity*. 2021: p. 1-9.
8. Qian, D., et al., *Mechanics of carbon nanotubes*. 2002. **55**(6): p. 495-533.
9. Mohamed Nacer, G., Z. Abdesselam, and H.J.O.J.o.C.E. Samia, *Investigating the local granulated blast furnace slag*. 2012. **2012**.
10. Maciel, M.H., et al., *Monitoring of Portland cement chemical reaction and quantification of the hydrated products by XRD and TG in function of the stoppage hydration technique*. 2019. **136**(3): p. 1269-1284.
11. Ayub, T., S.U. Khan, and F.A. Memon, *Mechanical characteristics of hardened concrete with different mineral admixtures: a review*. *ScientificWorldJournal*, 2014. **2014**: p. 875082.
12. Amhudo, R.L., T. Tavio, and I.G.P.J.C.E.J. Raka, *Comparison of Compressive and Tensile Strengths of Dry-Cast Concrete with Ordinary Portland and Portland Pozzolana Cements*. 2018. **4**(8): p. 1760-1771.
13. Harish, B., et al., *An experimental investigation on partial replacement of cement by glass powder in concrete*. 2016. **3**: p. 1218-1224.
14. Bediako, M., J.T.J.B.J.o.A.S. Kevern, and Technology, *Effects of Chemical Admixture on Flow and Strength Properties of Calcined Clay Used as a Supplementary Cementitious Material*. 2016. **13**(5): p. 1-6.
15. Madhavi, T.C. and S.J.A.J.E.A.S. Annamalai, *Electrical conductivity of concrete*. 2016. **11**(9): p. 5979-5982.
16. Lourie, O., D. Cox, and H.J.P.R.L. Wagner, *Buckling and collapse of embedded carbon nanotubes*. 1998. **81**(8): p. 1638.
17. Saez de Ibarra, Y., et al., *Atomic force microscopy and nanoindentation of cement pastes with nanotube dispersions*. 2006. **203**(6): p. 1076-1081.
18. Singh, A.P., et al., *Multiwalled carbon nanotube/cement composites with exceptional electromagnetic interference shielding properties*. 2013. **56**: p. 86-96.

19. Grossiord, N., et al., *Time-dependent study of the exfoliation process of carbon nanotubes in aqueous dispersions by using UV– Visible spectroscopy*. 2005. **77**(16): p. 5135-5139.
20. Ubertini, F., et al., *Natural frequencies identification of a reinforced concrete beam using carbon nanotube cement-based sensors*. 2014. **60**: p. 265-275.
21. Liew, K., et al., *Carbon nanotube reinforced cementitious composites: An overview*. 2016. **91**: p. 301-323.
22. de Almeida Carísio, P., et al., *Dispersion of Carbon Nanotubes with Different Types of Superplasticizer as a Dispersing Agent for Self-Sensing Cementitious Materials*. 2021. **11**(18): p. 8452.
23. Zou, B., et al., *Effect of ultrasonication energy on engineering properties of carbon nanotube reinforced cement pastes*. 2015. **85**: p. 212-220.
24. Krause, B., et al., *Dispersability and particle size distribution of CNTs in an aqueous surfactant dispersion as a function of ultrasonic treatment time*. 2010. **48**(10): p. 2746-2754.
25. Nochaiya, T. and A.J.A.S.S. Chaipanich, *Behavior of multi-walled carbon nanotubes on the porosity and microstructure of cement-based materials*. 2011. **257**(6): p. 1941-1945.
26. Li, G.Y., P.M. Wang, and X.J.C. Zhao, *Mechanical behavior and microstructure of cement composites incorporating surface-treated multi-walled carbon nanotubes*. 2005. **43**(6): p. 1239-1245.
27. Gay, C. and F.J.T.R.R. Sanchez, *Performance of carbon nanofiber–cement composites with a high-range water reducer*. 2010. **2142**(1): p. 109-113.
28. Mendoza, O., et al., *Influence of super plasticizer and Ca (OH) 2 on the stability of functionalized multi-walled carbon nanotubes dispersions for cement composites applications*. 2013. **47**: p. 771-778.
29. Han, B., et al., *Fabrication of piezoresistive CNT/CNF cementitious composites with superplasticizer as dispersant*. 2012. **24**(6): p. 658-665.
30. Dave, N. and T.J.I.J.A.C. Joshi, *A concise review on surfactants and its significance*. 2017. **13**(3): p. 663-672.
31. Robson, R.J. and E.A. Dennis, *The size, shape, and hydration of nonionic surfactant micelles. Triton X-100*. *The Journal of Physical Chemistry*, 1977. **81**(11): p. 1075-1078.
32. Rastogi, R., et al., *Comparative study of carbon nanotube dispersion using surfactants*. *Journal of colloid and interface science*, 2008. **328**(2): p. 421-428.
33. Ramírez-Arias, A.M., J.C. Moreno-Piraján, and L. Giraldo, *Adsorption of Triton X-100 in aqueous solution on activated carbon obtained from waste tires for wastewater decontamination*. *Adsorption*, 2020. **26**: p. 303-316.
34. Rennhofer, H. and B. Zanghellini, *Dispersion state and damage of carbon nanotubes and carbon nanofibers by ultrasonic dispersion: a review*. *Nanomaterials*, 2021. **11**(6): p. 1469.
35. Wang, H.J.C.O.i.C. and I. Science, *Dispersing carbon nanotubes using surfactants*. 2009. **14**(5): p. 364-371.
36. Tortorich, R.P. and J.W. Choi, *Inkjet Printing of Carbon Nanotubes*. *Nanomaterials (Basel)*, 2013. **3**(3): p. 453-468.

37. Huang, Y., et al. *Assessing the Dispersion Quality of Carbon Nanotubes Suspensions by Low Field Nuclear Magnetic Resonance*. in *IOP Conference Series: Materials Science and Engineering*. 2019. IOP Publishing.
38. Walters, D., et al., *Elastic strain of freely suspended single-wall carbon nanotube ropes*. 1999. **74**(25): p. 3803-3805.
39. Jang, S.H., S. Kawashima, and H. Yin, *Influence of Carbon Nanotube Clustering on Mechanical and Electrical Properties of Cement Pastes*. *Materials (Basel)*, 2016. **9**(4): p. 220.
40. ElKashef, M. and M.N. Abou-Zeid, *Performance of carbon nanotubes/cement composites using different surfactants*.
41. Echeverry-Cardona, L.M., et al., *Time-Stability Dispersion of MWCNTs for the Improvement of Mechanical Properties of Portland Cement Specimens*. *Materials (Basel)*, 2020. **13**(18): p. 4149.
42. ASTM, A., *305-14 Standard practice for mechanical mixing of hydraulic cement pastes and mortars of plastic consistency ASTM C305-14*. ASTM Int. West Conshohocken PA. Search in, 2014.
43. C, A., *Standard test method for flow of hydraulic cement mortar*. Philadelphia, PA, 2001.
44. Committee, A., *ASTM C109/C109M-02 Standard Test Method for Compressive Strength of Hydraulic Cement Mortars, Annu. B. ASTM Stand. 04 (2002) 1-6*.
45. Lim, K.M. and J.H. Lee, *Electrical conductivity and compressive strength of cement paste with multiwalled carbon nanotubes and graphene nanoplatelets*. *Applied Sciences*, 2022. **12**(3): p. 1160.
46. ASTM C642, A., *Standard test method for density, absorption, and voids in hardened concrete*. ASTM, ASTM International, 2013.
47. Bai, Y., et al., *Adsorption of Triton X-series surfactants and its role in stabilizing multi-walled carbon nanotube suspensions*. *Chemosphere*, 2010. **79**(4): p. 362-367.
48. Silvestro, L., et al., *Stability of carboxyl-functionalized carbon nanotubes in simulated cement pore solution and its effect on the compressive strength and porosity of cement-based nanocomposites*. *C*, 2022. **8**(3): p. 39.
49. Elkashef, M. and M.N. Abou-Zeid, *Performance of carbon nanotubes in mortar using different surfactants*. *Canadian Journal of Civil Engineering*, 2017. **44**(8): p. 619-625.
50. Reales, O.A.M., et al., *Influence of MWCNT/surfactant dispersions on the rheology of Portland cement pastes*. *Cement and Concrete Research*, 2018. **107**: p. 101-109.
51. Adhikary, S.K., et al., *Effects of carbon nanotubes on expanded glass and silica aerogel based lightweight concrete*. *Scientific reports*, 2021. **11**(1): p. 2104.
52. Bediako, M. and J.T. Kevern, *Effects of Chemical Admixture on Flow and Strength Properties of Calcined Clay Used as a Supplementary Cementitious Material*. *British Journal of Applied Science & Technology*, 2015. **13**(5): p. 1-6.
53. Cilla, M.S., P. Colombo, and M.R. Morelli, *Geopolymer foams by gelcasting*. *Ceramics International*, 2014. **40**(4): p. 5723-5730.

54. Nuaklong, P., et al., *Hybrid effect of carbon nanotubes and polypropylene fibers on mechanical properties and fire resistance of cement mortar*. Construction and Building Materials, 2021. **275**: p. 122189.
55. Franus, W., R. Panek, and M. Wdowin. *SEM investigation of microstructures in hydration products of portland cement*. in *2nd International Multidisciplinary Microscopy and Microanalysis Congress: Proceedings of InterM, October 16-19, 2014*. 2015. Springer.
56. Konsta-Gdoutos, M.S., Z.S. Metaxa, and S.P. Shah, *Highly dispersed carbon nanotube reinforced cement based materials*. Cement and Concrete Research, 2010. **40**(7): p. 1052-1059.
57. Tyson, B.M., et al., *A quantitative method for analyzing the dispersion and agglomeration of nano-particles in composite materials*. Composites Part B: Engineering, 2011. **42**(6): p. 1395-1403.
58. Güler, Ö., et al., *The synergistic effect of CNTs-polymeric surfactant on the properties of concrete nanocomposites: Comparative study*. Journal of Composite Materials, 2021. **55**(10): p. 1371-1384.
59. Kang, J., S. Al-Sabah, and R. Théo, *Effect of single-walled carbon nanotubes on strength properties of cement composites*. Materials, 2020. **13**(6): p. 1305.
60. Rodriguez, B., et al. *Carbonation study in a cement matrix with carbon nanotubes*. in *Journal of Physics: Conference Series*. 2019. IOP Publishing.
61. Muradyan, N.G., et al., *The Effect of Multi-Walled Carbon Nanotubes on the Compressive Strength of Cement Mortars*. Coatings, 2022. **12**(12): p. 1933.
62. Park, B. and Y.C. Choi, *Investigating the Effect of CNTs on Early Age Hydration and Autogenous Shrinkage of Cement Composite*. Applied Sciences, 2021. **11**(12): p. 5545.
63. Mishra, G., *Co-effect of carbon nanotube and nano-sized silica on dispersion and mechanical performance in cementitious system*. Diamond and Related Materials, 2022. **127**: p. 109162.
64. Uddin, M.A., et al., *The effect of curing time on compressive strength of composite cement concrete*. Applied Mechanics and Materials, 2012. **204**: p. 4105-4109.
65. Yun, H.-D., et al., *Microstructure and mechanical properties of cement mortar containing phase change materials*. Applied Sciences, 2019. **9**(5): p. 943.
66. Choi, K., et al., *Effects of dispersants and defoamers on the enhanced electrical performance by carbon nanotube networks embedded in cement-matrix composites*. Composite Structures, 2020. **243**: p. 112193.
67. Jang, S.-H., et al., *Experiments and micromechanical modeling of electrical conductivity of carbon nanotube/cement composites with moisture*. Cement and Concrete Composites, 2017. **77**: p. 49-59.
68. Jung, M., Y.-S. Lee, and S.-G. Hong, *Effect of incident area size on estimation of EMI shielding effectiveness for ultra-high performance concrete with carbon nanotubes*. IEEE Access, 2019. **7**: p. 183105-183117.
69. Jang, S.-H., S. Kawashima, and H. Yin, *Influence of carbon nanotube clustering on mechanical and electrical properties of cement pastes*. Materials, 2016. **9**(4): p. 220.

70. Liu, K., et al., *Effects of microstructure and pore water on electrical conductivity of cement slurry during early hydration*. *Composites Part B: Engineering*, 2019. **177**: p. 107435.
71. Yoo, D.-Y., I. You, and S.-J. Lee, *Electrical properties of cement-based composites with carbon nanotubes, graphene, and graphite nanofibers*. *Sensors*, 2017. **17**(5): p. 1064.
72. Sasmal, S., et al., *Electrical conductivity and piezo-resistive characteristics of CNT and CNF incorporated cementitious nanocomposites under static and dynamic loading*. *Composites Part A: Applied Science and Manufacturing*, 2017. **100**: p. 227-243.



VITA

NAME Rittikiat Wandaw

DATE OF BIRTH 3 November 1996

PLACE OF BIRTH Nakhon Si Thammarat

INSTITUTIONS ATTENDED M.Eng.
August 2019- Present
Major: Chemical Engineering
Chulalongkorn University, Bangkok, Thailand

B.Eng.
August 2015-May 2019
Major: Nanomaterial Engineering
King Mongkut's Institute of Technology Ladkrabang,
Bangkok, Thailand

HOME ADDRESS Nakhon Si Thammarat

PUBLICATION Rittikiat Wandaw, Rittanupap Thavorn, Voravut Ridmud,
Nathanon Noonanant, Ketsarin Ariya, Rachpisek
Jirasupangkoon, Jirapat Laiyangkul, Pitcha
Jongvivatsakul,
and Tawatchai Charinpanitkul, "Effect of Dispersing Agent
and Weight Ratio of Carbon nanotubes to Cement on
Electrical and Mechanical Properties of Their
Composites"Proceeding of the 9th Joint Conference on
Renewable Energy and Nanotechnology (JCREN2020),
Khon Kaen, Thailand, October 29th, 2020.